CENTRE NATIONAL DE LA RECHERCHE SCIENTIFIQUE UMR 5564

INSTITUT NATIONAL POLYTECHNIQUE DE GRENOBLE

INSTITUT DE RECHERCHE ET DEVELOPPEMENT

UNIVERSITE JOSEPH FOURIER GRENOBLE I

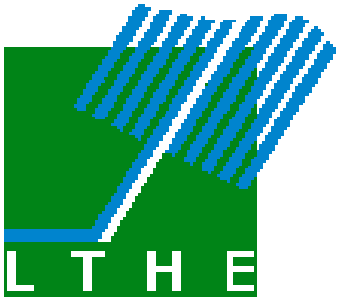


**LABORATOIRE D'ETUDE DES TRANSFERTS EN HYDROLOGIE ET ENVIRONNEMENT**

# SiSPAT USER'S MANUAL

**Si**mple
**S**oil
**P**lant
**A**tmosphere
**T**ransfer
Model

*SiSPAT, a numerical model of water and energy fluxes in the soil-plant-atmosphere continuum*

Version 3.0

Isabelle BRAUD, CNRS
LTHE, September 2000

LTHE, BP 53, 38041 Grenoble Cédex 9, France

Tel: 33 4 76 82 52 85, Fax: 33 4 76 82 52 86, E-mail: Isabelle.Braud@hmg.inpg.fr

## ACKNOWLEDGMENTS

We would like to thank Michel Vauclin who initiated the modelling effort of heat and water transfer into the soil-vegetation-atmosphere continuum. This led to a first version (without rainfall) of the current SiSPAT model, in the framework of the Doctoral thesis of Antonio-Celsio Dantas-Antonino. The current version of the SiSPAT model has retained the structure of this early model, but additional processes, especially rainfall and all its consequences, were included.

Because they used the model for their applications, several persons contributed to the improvement of the SiSPAT model: Gilles Boulet (Ph D Thesis LTHE-Grenoble, 1999), Patrick Bertuzzi (INRA-Avignon), Sophie Fouché-Roguiez (Ph D Thesis CEREG-Strasbourg, 1998), Christophe François (CETP, Vélizy), Enrique Gonzalez-Sosa (Ph D Thesis LTHE-Grenoble, 1999), Jérôme Demarty (Ph D Thesis CETP-Vélizy).

We also greatly appreciated the collaboration of Pierre Bessemoulin (CNRM-Toulouse), Jean-Christophe Calvet (CNRM-Toulouse), André Chanzy (INRA-Avignon), Bruno Monteny (IRD-Montpellier), Joël Noilhan (CNRM-Toulouse), Albert Olioso (INRA-Avignon), Pierre Ruelle (CEMAGREF-Montpellier). The LTHE team (Rafaël Angulo-Jaramillo, Stéphane Boubkraoui, Hervé Denis, Jean-Paul Gaudet, Randel Haverkamp, Robert Laty, Jean-Paul Laurent, Jean-Louis Thony, Jean-Pierre Vandervaere and Michel Vauclin) contributed to field campaigns providing most of the data used in the applications and validation of the SiSPAT model. Without their contribution, SiSPAT and all the similar models would remain intellectual games of academic interest but could not be used as tools contributing to a better understanding of physical phenomena. Only the confrontation of model results with data can ensure that the models have captured the main physical processes involved and can be used as reference tools contributing to the improvement of more simple parameterizations of land-surface processes.

All this research has been funded by the European Union in the framework of the Spatial Variability of Land Surface Processes (SLAPS II) project (contract EPOC-CT 90-0016) and the Echievald Field Experiment in a Threatened Desertification Area (EFEDA) projects (contract EPOCH-CT 90-0030 and EV5V-CT93-0272) and the French Institut des Sciences de l'Univers (INSU) (Programme Atmosphère et Océan à Moyenne Echelle (PATOM), Programme National de Télédétection Spatiale (PNTS), Programme de National de Recherche en Hydrologie (PNRH)).

## TABLE OF CONTENTS

LIST OF SYMBOLS AND THEIR UNITS

---

| | |
|---|---|
| $a_{bl}$ | Extinction coefficient of incoming radiation by the vegetation (-) |
| $a_j$, $b_j$, $c_j$, $d_j$, $e_j$ | Coefficients of the Laurent and Guerre-Chaley (1995) formula for thermal conductivity (-) |
| $C_{ch}$ | Isothermal volumetric heat capacity at constant matric potential (J $m^{-3}$ $K^{-1}$) |
| $C_h$=$C_{mh}$ | Capillary capacity ($m^{-1}$) |
| $c_l$ | Specific heat of water (J $kg^{-1}$ $K^{-1}$) |
| *coef1,coef2,coef3*: Coefficients of the bare soil albedo function of surface soil moisture (-) | |
| $c_p$ | Specific heat at constant pressure (J $kg^{-1}$ $K^{-1}$) |
| $C_m$, $C_o$, $C_{dry}$ | Volumetric heat capacity for mineral, organic matter and dry soil respectively (J $m^{-3}K^{-1}$) |
| *crack* | Cracks surface fraction (-) |
| $C_T$=$C_{hT}$ | Volumetric heat capacity (J $m^{-3}$ $K^{-1}$) |
| $C_{mT}$ | Capillary capacity at constant matric potential (m $s^{-1}$) |
| $d$ | Displacement height (m) |
| $d_g$ | Soil particle diameter characteristic scale (m) |
| $d_i$ | Soil particle diameter (m) |
| $dz_j$ | Thickness between nodes $j$ and $j+1$ (m) |
| $D_{ch}$ | Isothermal vapor conductivity (W $m^{-2}$) |
| $D_{cT}$ | Apparent thermal conductivity (W $m^{-1}$ $K^{-1}$) |
| $D_{mh}$ | Isothermal moisture conductivity (m $s^{-1}$) |
| $D_{mT}$ | Thermal vapor diffusivity ($m^2$ $s^{-1}$ $K^{-1}$) |
| $D_{va}$ | Molecular diffusivity of water vapour into the air ($m^{-2}$ $s^{-1}$) |
| $D_{vh}$ | Isothermal vapor diffusivity (kg $m^{-2}$ $s^{-1}$) |
| $D_{vT}$ | Vapor diffusivity associated with temperature gradients (kg $m^{-1}$ $s^{-1}$ $K^{-1}$) |
| $e_a$ | Air vapor pressure at level $z_a$ (Pa) |
| $e_{sat}(T)$ | Saturated vapor pressure at temperature $T$ (Pa) |
| $e_v$ | Partial pressure of water vapor (Pa) |
| $E$, $E_g$, $E_v$, $E_w$ | Evapotranspiration above the canopy, evaporation from the ground, total evapotranspiration from the vegetation and evaporation from the wet fraction of the canopy respectively (kg $m^{-2}$ $s^{-1}$) |
| $F(d_i)$ | Soil particle size distribution (-) |
| $g$ | Acceleration of gravity (m $s^{-2}$) |
| $G$ | Surface soil heat flux (W $m^{-2}$) |
| $h$ | Soil matric potential of water (m) |
| $h_{ae}$ | Air entry pressure in the Brooks and Corey retention model (main drying curve) (m) |
| $h_c$ | Soil matric potential of water separating the two Van Genuchten model portions when the retention curve model in extended in the dry domain (m) |
| $h_f$ | Leaf water potential (m) |
| $h_{fc}$ | Critical leaf water potential (m) |
| $h_j$ | Soil matric potential of water of layer $j$ (m) |
| $h_{1min}$ | Minimum value of the surface matrix potential allowed in the model (m) |
| $h_g$ | Scale factor in the Van Genuchten formula for the retention curve (m) |
| $h_{g1}$,$h_{g2}$ | Scale factor in the Van Genuchten formula for the retention curve (wet and dry domains) (m) |
| $h_o$ | Soil matric potential of water at which soil moisture is zero (m) |
| $h_u$ | Relative humidity (-) |

| | |
|---|---|
| $h_{we}$ | Water entry pressure in the Brooks and Corey retention model (main wetting curve) (m) |
| $H$, $H_g$, $H_v$ | Sensible heat flux above the canopy, from the ground and the canopy, respectively ($Wm^{-2}$) |
| $k$ | Von Karman constant (0.4) |
| $K$ | Liquid hydraulic conductivity ($m\ s^{-1}$) |
| $K_{sat}$ | Saturated liquid hydraulic conductivity ($m\ s^{-1}$) |
| $K_{smat}$ | Saturated liquid hydraulic conductivity for the soil matric ($m\ s^{-1}$) |
| $L$ | Monin-Obukhov length (m) |
| $L_v$ | Latent heat of vaporisation ($J\ kg^{-1}$) |
| $LAI$ | Leaf area index |
| $m$ | Shape parameter in the Van Genuchten retention model (-) |
| $M$ | Shape parameter of the particle size distribution curve (-) |
| $M_{rd}$ | Maximum root length density (m root/ $m^3$ soil) |
| $n$ | Shape parameter in the Van Genuchten retention model (-) |
| $n_1$, $n_2$ | Shape parameter in the Van Genuchten retention model (wet and dry domains) (-) |
| $n_{SW}$ | Parameter used in the Shuttleworth and Wallace (1985) resistances (-) |
| $p$ | Tortuosity factor (-) |
| $p_{atm}$ | Atmospheric surface pressure (Pa) |
| $p_d$ | Empirical aerodynamic shelter factor (-) |
| $phase(z_N)$ | Phase of the sinusoidal temperature function at the bottom of the soil profile (-) |
| $por$ | Soil porosity (-) |
| $p_{mr}$ | Parameter of the root density profile (-) |
| $P$ | Precipitation above the canopy ($ms^{-1}$) |
| $P_g$ | Precipitation reaching the ground or throughfall ($m\ s^{-1}$) |
| $q$ | Specific humidity ($kg\ kg^{-1}$) |
| $q_a$, $q_{av}$ | Specific humidity of air at level $z_a$ and $z_{av}$, respectively ($kg\ kg^{-1}$) |
| $q_{crack}$ | Flux per unit distance along the cracks ($s^{-1}$) |
| $Q_N$ | Mass flux at the bottom of the soil column ($kg\ m^{-2}\ s^{-1}$) |
| $Q_m$ | Mass flux within the soil ($kg\ m^{-2}\ s^{-1}$) |
| $Q_{mg}$ | Darcian non isothermal flow crossing the soil surface ($kg\ m^{-2}\ s^{-1}$) |
| $Q_r$ | Total plant root uptake ($kg\ m^{-2}\ s^{-1}$) |
| $q_{sat}(T)$ | Saturated specific humidity at temperature $T$ ($kg\ kg^{-1}$) |
| $r_{rac}$ | Root radius (m) |
| $R$ | Perfect gas constant for vapour ($461.5\ J\ kg^{-1}$) |
| $R_{aM}$, $R_{aH}$, $R_{aV}$ | Aerodynamic resistance between level $z_a$ and $z_{av}$ for momentum, heat and vapor, respectively ($s\ m^{-1}$) |
| $R_{aH}^{\ n}$ | Aerodynamic resistance under neutral conditions ($s\ m^{-1}$) |
| $R_{gM}$, $R_{gH}$, $R_{gV}$ | Aerodynamic resistance between the soil surface and level $z_{av}$ for momentum, heat and vapour, respectively ($s\ m^{-1}$) |
| $R_r$ | Total plant resistance ($s\ m^{-1}$) |
| $R_{rj}$ | Plant resistance of layer $j$ (s) |
| $R_{sj}$ | Soil resistance of layer $j$ (s) |
| $R_{stmax}$ | Maximum stomatal resistance ($s\ m^{-1}$) |
| $R_{stmin}$ | Minimal stomatal resistance ($s\ m^{-1}$) |
| $R_{sto}$ | Stomatal resistance ($s\ m^{-1}$) |

$R_{vM}$, $R_{vH}$, $R_{vV}$ Aerodynamic resistance between the canopy and level $z_{av}$ for momentum, heat and vapor, respectively (s $m^{-1}$)

$RA$, $RA_g$, $RA_v$ Incoming long wave radiation, net long wave radiation for the bare soil and canopy, respectively (W $m^{-2}$)

$RDF_j$ Root density function of layer $j$ ($m^{-1}$)

$RG$, $RG_g$, $RG_v$ Incoming solar radiation, net solar radiation for the bare soil and canopy, respectively (W $m^{-2}$)

$RG_r$ Reflected solar radiation (W $m^{-2}$)

$Rn$, $Rn_g$, $Rn_v$ Total net radiation, net radiation for the bare soil and canopy, respectively (W $m^{-2}$)

$S$ Plant root uptake (kg $m^{-3}$ $s^{-1}$)

$S_j$ Plant root uptake of layer $j$ (kg $m^{-3}$ $s^{-1}$)

$Stab$ Stability factor (-)

$t$ Time (s)

$T$ Soil temperature (K)

$T_j$ Toil temperature of layer $j$ (K)

$T_a$, $T_{av}$ Air temperature at level $z_a$ and $z_{av}$ respectively (K)

$T_{amp}(z_N)$ Semi-amplitude of the sinusoidal temperature function at the bottom of the soil profile (K)

$T_o$ Reference temperature (K)

$T_{mean}(z_N)$ Average of the sinusoidal temperature function at the bottom of the soil profile (K)

$T_{rad}$ Radiative surface temperature (K)

$T_r$ Vegetation transpiration (kg $m^{-2}$ $s^{-1}$)

$T_v$ Leaf temperature (K)

$u^*$ Friction velocity ($ms^{-1}$)

$U_a$, $U_{av}$ Wind speed at level $z_a$ and $z_{av}$, respectively (m $s^{-1}$)

$VPD$ $e_{sat}(T_a)$-$e_a$= Vapour Pressure Deficit (Pa)

$w$ Leaf width (m)

$W_r$ Amount of intercepted water (m)

$W_{rmax}$ Maximum amount of water of the interception reservoir (m)

$z$ Vertical coordinate (m)

$z_a$, $z_{av}$ Height of the atmosphere reference level and canopy artificial level (m)

$z_{om}$, $z_{oh}$, $z_{ov}$ Roughness length for momentum, heat and vapour, respectively (m)

$z_{rm1}$, $z_{rm2}$, $z_{rpm}$,$z_{rt}$: Characteristic lengths of the root density profile (m)

$z_v$ Mean canopy height (m)

$Z_{crack}$ Depth of the cracks (m)

*Greek letters.*

$\alpha_o$ Parameter used in the Shuttleworth and Wallace (1985) resistances (-)

$\alpha$ Parameter of the Gardner model ($m^{-1}$)

$\alpha_g$, $\alpha_v$ Bare soil and vegetation albedo respectively (-)

$\alpha_{tot}$ Total albedo (-)

$\beta$ Coefficient allowing for the participation of non foliage elements to transfer (1.1) (-)

$\delta$ Wet fraction of the canopy (-)

$\Delta z_j$ Thickness of layer $j$ (m)

$\varepsilon$ Soil porosity (-)

$\varepsilon_g$, $\varepsilon_v$ Bare soil and vegetation emissivity, respectively (-)

| | |
|---|---|
| $\gamma$ | Shape parameter of the Brooks and Corey retention curve (-) |
| $\eta$ | Exponent in the Brooks and Corey model for hydraulic conductivity (-) |
| $\lambda$ | Apparent thermal conductivity (W $m^{-1}K^{-1}$) |
| $\Lambda$ | Thermal inertia (J $m^{-2}$ $K^{-1}$ $s^{-1/2}$) |
| $\Lambda_s$ | Thermal inertia at saturation (J $m^{-2}$ $K^{-1}$ $s^{-1/2}$) |
| $\mu$ | Parameter of the *VPD* stress function of the stomatal resistance ($Pa^{-1}$) |
| $\nu$ | Kinematic viscosity ($m^2$ $s^{-1}$) |
| $\theta$ | Volumetric water content ($cm^3$ $cm^{-3}$) |
| $\theta*$ | Characteristic turbulent temperature scale (K) |
| $\theta_{ae}$ | Volumetric water content at the air entry pressure in the Brooks and Corey model (main drying curve) ($cm^3$ $cm^{-3}$) |
| $\theta_{lim}$, $\theta_{limo}$, | Characteristic volumetric water content of the soil albedo function of surface soil moisture ($cm^3$ $cm^{-3}$) |
| $\theta_k$ | Volumetric water content at which the liquid phase is no more continuous ($cm^3$ $cm^{-3}$) |
| $\theta_o$, $\theta_m$ | Volumetric organic matter and mineral soil content, respectively ($cm^3$ $cm^{-3}$) |
| $\theta_r$ | Residual volumetric water content ($cm^3$ $cm^{-3}$) |
| $\theta_{macro}$ | Macropore content ($cm^3$ $cm^{-3}$) |
| $\theta_{sat}$ | Saturated volumetric water content ($cm^3 cm^{-3}$) |
| $\theta_{wilt}$ | Wilting point volumetric water content (correponds to -150 m of water) ($cm^3 cm^{-3}$) |
| $\rho_a$ | Air density ($kgm^{-3}$) |
| $\rho_d$ | Dry bulk density of soil ($kgm^{-3}$) |
| $\rho_v$ | Water vapor density ($kgm^{-3}$) |
| $\rho_{vsat}$ | Saturated water vapor density ($kgm^{-3}$) |
| $\rho_w$ | Liquid water density ($kgm^{-3}$) |
| $\sigma$ | Stefan-Boltzman constant ($5.67\ 10^{-8}$ $Wm^{-2}K^{-4}$) |
| $\sigma_a$ | Coefficient for the partition of momentum between bare soil and vegetation (-) |
| $\sigma_f$ | Shielding factor (-) |
| $\tau$, $\tau_g$, $\tau_v$ | Momentum flux above the canopy, from the ground and the canopy, respectively ($kgm^{-1}s^{-2}$) |
| $\psi_m$, $\psi_h$, $\psi_v$ | Integrated stability functions for momentum, heat and vapor, respectively |
| $\zeta$ | Ratio of the average temperature gradient in the air to the macroscopic temperature gradient (-) |
| $\xi$ | Tortuosity factor (-) |

## 1. INTRODUCTION

The partition of rainfall reaching the ground into evaporation, transpiration, infiltration or runoff is mainly controlled by the soil-biosphere-atmosphere interface. The processes involved in these heat and water exchanges are numerous and complex: transfer in the non-saturated zone, infiltration, plant root uptake, plant growth, turbulent exchanges above and within the canopy, and encompass sciences such as soil physics, hydrology, meteorology and plant physiology. For applications in agronomy, meteorology, climatology or remote sensing, numerous models have been developed to simulate turbulent fluxes at the soil-plant-atmosphere interface and heat and/or water movement into the soil. According to the domain of applications or the speciality of their authors, one or several compartments of the model are sometimes very sophisticated as compared to the others. The soil can be divided into numerous layers and/or horizons (Sasamori, 1970; Belmans et al., 1983; Camillo et al., 1983; Lascano et al., 1987; Abramopoulos et al., 1988; Entekhabi and Eagleson, 1989; Passerat et al., 1989; Van de Griend and Van Boxel, 1989; Witono and Bruckler, 1989), or parameterized into one or several reservoirs (Deardorff, 1977, 1978; Dickinson, 1984; Sellers et al., 1986; Taconet et al., 1986; Noilhan and Planton, 1989; Lynn and Carlson, 1990; Inclán, 1993; Noilhan and Mahfouf, 1996). The role of vegetation can be parameterized and the actual evapotranspiration expressed as a function of potential one (Belmans et al., 1983; Entekhabi and Eagleson, 1989). More sophisticated models include one vegetation layer (Deardorff, 1978; Dickinson, 1984; Shuttleworth and Wallace, 1985; Taconet et al., 1986; Lascano et al., 1987; Abramopoulos et al., 1988; Noilhan and Planton, 1989; Lynn and Carlson, 1990), two vegetation layers (Sellers et al., 1986; Van de Griend and Van Boxel, 1989; Inclán, 1993), or even, up to ten layers (Flerchinger and Pierson, 1991).

The model of heat and water transfer in the soil-plant-atmosphere system described here was designed to reach at least two goals:

i) to give as physical as possible a representation of the main processes involved: coupled heat and water movement in the non-saturated zone, plant root uptake, turbulent transfer above and within the canopy, interception, infiltration and surface runoff,

ii) to achieve a balanced degree of simplification between the various compartments of the model.

The model, called SiSPAT, is a unidirectional model theoretically suited for studies at the field scale, although it has tentatively been applied at much larger scales (see section 7).

In the soil, coupled heat and water transfer equations are solved with a sink term corresponding to plant root uptake. The model is able to deal with non homogeneous soils, made of several horizons. Both liquid and vapour transfer are considered. Vegetation is assimilated to one layer, but two energy budgets are considered: one for the partially bare soil and one for the vegetation. The case of a bare soil can also be treated. The model is forced at a reference level by atmospheric variables (wind speed, air temperature and

humidity, incoming solar and long-wave radiation and rainfall). The model was first developed by Dantas-Antonino (1992). Its description with further developments has been published in Braud et al. (1995b) and in the User's Manual Braud (1996). Additional options in the choice of soil hydrodynamic and thermal properties, boundary layers conditions, outputs have been added and are described in this updated version of the manual.

The description of the model will be divided into four chapters describing sucessively the soil module (chapter 2), the soil-plant-atmosphere interface module (chapter 3), the soil-plant module (root extraction) (chapter 4). The coupling between the various modules is described in chapter 5. The practical implementation of the model with a complete description of input and output files is given in chapter 6. Finally chapter 7 summarises the various applications of the model and provides some information on additional versions of the model which have been developed.

The code is written in standard FORTRAN 77. Its structure is modular so that it is quite easy to modify one of the modules. For each routine, input and output arguments are described into the code.

# 2. DESCRIPTION OF THE SOIL MODULE.

## 2.1. Introduction.

SiSPAT is a unidimensional model, assuming that horizontal heat and water transfer in the soil-plant-atmosphere continuum can be neglected and that movements can be considered as vertical. In the soil, coupled heat and water transfer are considered. They include liquid and vapour phase transfer. A sink term accounting for water extraction by roots is also considered. The model can deal with soils made of several horizons, characterised by different hydrodynamic and thermal properties.

## 2.2. Basic equations.

The approach of Philip and De Vries (1957), modified by Milly (1982), forms the basis of the model of coupled moisture and heat flows in a partially saturated porous medium used in the SiSPAT model. The dependent variables are the temperature $T$ and the soil matric potential of water $h$. With the choice of matric potential, the model is able to deal with nonhomogeneous soils, made up of several horizons, because the matric potential is continuous at the interface of these horizons. This is not the case for the volumetric water content $\theta$ (Vauclin et al., 1979). The corresponding one dimensional equations for vertical movement (axis $z$ orientated positively downward) read (see also Passerat et al., 1989; Witono and Bruckler, 1989):

$$C_h \frac{\partial h}{\partial t} = \frac{\partial}{\partial z}\left( D_{mh} \frac{\partial h}{\partial z} + D_{mT} \frac{\partial T}{\partial z} - K \right) - \frac{S}{\rho_w} \tag{2.1a}$$

$$C_T \frac{\partial T}{\partial t} = \frac{\partial}{\partial z}\left( D_{ch} \frac{\partial h}{\partial z} + D_{cT} \frac{\partial T}{\partial z} \right) \tag{2.1b}$$

$S$ is the plant root uptake and is described in section 4.

The storage coefficents are the capillary capacity $C_h = \left( \frac{\partial \theta}{\partial h} \right)_T$ and the volumetric heat capacity $C_T$. The transport coefficients are the isothermal moisture conductivity $D_{mh} = K + D_{vh}/\rho_w$, the thermal vapor diffusivity $D_{mT} = D_{vT}/\rho_w$, the isothermal vapor conductivity $D_{ch} = L_v D_{vh}$, the apparent thermal conductivity $D_{cT} = \lambda$ where $K$ is the liquid hydraulic conductivity, $D_{vh}$ is the isothermal vapor diffusivity, $D_{vT}$ is the vapor diffusivity associated with temperature gradients and $L_v$ is the latent heat of vaporization. These various coefficients are functions of water content and/or temperature and are described below.

## 2.3. Determination of transfer and storage coefficients.

*2.3.1. Retention and hydraulic conductivity curves.*

The determination of the coefficients defined above requires first the specification, for each horizon, of two functionals relating matric potential to volumetric water content (retention curve $h(\theta)$) and hydraulic conductivity to water content (hydraulic conductivity $K(\theta)$).

i) Four options are available in SiSPAT for the retention curve choice.

* If *imodh=1*, the Brooks and Corey (1964) model modified by Haverkamp et al. (1996) can be used. The main drying curve (MDC) or the main wetting curve (MWC) can be chosen (Eq. 2.2), but the model does not include the secondary branches, allowing to pass from the drying to the wetting curve or vice versa. This would require to know all the history of the soil and keep it in memory, which would be computationally tedious. Therefore, the MWC or the MDC is chosen at the beginning of the simulation and is kept identical during all the simulation.

$$\begin{cases} \dfrac{\theta}{\theta_{ae}} = \left( \dfrac{h_{ae}}{h} \right)^{\gamma} & h \le h_{ae} \\ \dfrac{\theta}{\theta_{ae}} = 1 + \gamma - \gamma \dfrac{h}{h_{we}} & h_{ae} \le h \le h_{we} \\ \theta = \theta_{sat} & h_{we} \le h \le 0 \end{cases}$$ Main Wetting Curve (*icurve=0*)(2.2a)

$$\begin{cases} \dfrac{\theta}{\theta_{ae}} = \left( \dfrac{h_{ae}}{h} \right)^{\gamma} \left( 1 + \gamma - \gamma \dfrac{h_{we}}{h} \right) & h \le h_{ae} \\ \theta = \theta_{sat} & h_{ae} \le h \le 0 \end{cases}$$ Main Drying Curve (*icurve=1*) (2.2b)

where $$h_{we} = h_{ae} \left( \frac{1+\gamma}{\gamma} \right) \left( 1 - \frac{\theta_{sat}}{\varepsilon} \right)$$ (2.2c)

(Haverkamp and Parlange, 1986) and

$$\theta_{ae} = \frac{\theta_{sat}}{1 + \gamma - \gamma \dfrac{h_{we}}{h_{ae}}}$$ (2.2d)

* The second and third model available are two options for the Van Genuchten (1980) model (Eq. 2.3).

$$\frac{\theta - \theta_r}{\theta_{sat} - \theta_r} = \left[ 1 + \left( \frac{h}{h_g} \right)^n \right]^{-m}$$ (2.3a)

with $n = \frac{2}{1-m}$ (Burdine, 1953) (*imodh=0*) (2.3b)

or $n = \frac{1}{1-m}$ (Mualem, 1976) (*imodh=3*) (2.3c)

* The fourth model (*imodh=2*) is a Van Genuchten model, modified into the dry domain to ensure that the volumetric water content is zero at a finite soil water pressure $h_o$. The idea was first proposed by Ross et al. (1991) who gave the detailed calculations for the Brooks and Corey model. A threshold pressure $h_c$ is prescribed such that a "classical" Van Genuchten model is used for pressure higher than $h_c$ and the modified model is used for pressure lower than $h_c$ . Parameters $h_{g2}$ and $n_2$ must be determined such that the function and its first derivative are continuous for $h = h_c$ (details are provided in Appendix 1). The procedure is iterative but converges rapidly. This option is only available with the Burdine (1953) hypothesis (Eq. 2.3b) and a residual water content equal to zero.

$$\begin{cases} \frac{\theta}{\theta_s} = \left[1 + \left(\frac{h}{h_{g1}}\right)^{n1}\right]^{-1+\frac{2}{n1}} & h \geq h_c \\ \frac{\theta}{\theta_s} = \left[1 + \left(\frac{h}{h_{g2}}\right)^{n2}\right]^{-1+\frac{2}{n2}} - \left[1 + \left(\frac{h_o}{h_{g2}}\right)^{n2}\right]^{-1+\frac{2}{n2}} & h \leq h_c \end{cases} \quad (2.4)$$

Practically, a value $h_o$= -60000 m ensures that the relative humidity is close to zero when the volumetric water content is zero. Ross et al. (1991) used a value $h_c$=-10 m, but a value $h_c$=-100 m proved to be more suited for clay soils (Braud and Chanzy, 2000).

ii) <u>For the hydraulic conductivity curve, two options can be chosen.</u>

* If *ikh=0*, the Brooks and Corey (1964) model can be chosen

$$K(\theta) = K_{sat}\left(\frac{\theta}{\theta_{sat}}\right)^{\eta} \quad (2.5a)$$

with $\eta = \frac{2}{mn} + 2 + 2p$ (2.5b)

where $p$ is the tortuosity factor related to the shape parameter of the Van Genuchten retention model (Burdine hypothesis) and the particle size distribution curve $F(d_i)$ parameter $M$ by:

$$M = m(1+p) \quad (2.5c)$$

where $F(d_i) = \left[1 + \left(\frac{d_g}{d_i}\right)^{\frac{2}{1-M}}\right]^{M}$ (2.5d)

with $d_i$ the particle diameter and $d_g$ the scale for the diameters (Haverkamp et al., 1997; Zammit, 1999).

* The second option (*ikh=1*) is the Van Genuchten (1980) model for the hydraulic conductivity:

$$K(\theta)=K_{sat}\left(\frac{\theta-\theta_r}{\theta_s-\theta_r}\right)^{1/2}\left[1-\left(1-\left(\frac{\theta-\theta_r}{\theta_s-\theta_r}\right)^{1/m}\right)^{m}\right]^2 \qquad (2.6)$$

* The possibility to take into account the presence of macropores was included for the Brooks and Corey model using the following modified model (*ikh=1* and $\theta_{macro}\neq 0$):

$$K(\theta) = K_{smat}\left(\frac{\theta}{\theta_{sat}}\right)^{\eta} \qquad \theta \le \theta_{sat}-\theta_{macro} \quad (2.7a)$$

$$K(\theta)=10^{\frac{\theta-\theta_{sat}}{\theta_{macro}}[log10(K_{sat})-log10(K(\theta_{sat}-\theta_{macro}))]+log10(K_{sat})} \qquad \theta_{sat}-\theta_{macro} \le \theta \le \theta_{sat} \quad (2.7b)$$

where $K_{smat}$ (m $s^{-1}$) is the saturated hydraulic conductivity of the soil matric, $\theta_{macro}$ ($m^3$ $m^{-3}$) is the macropores content and $K(\theta_{sat}-\theta_{macro})$ (m $s^{-1}$) the hydraulic conductivity at water content $(\theta_{sat}-\theta_{macro})$.

Although all the choices are acceptable for the retention and hydraulic conductivity curves, Fuentes et al. (1992) showed that the combination of the Van Genuchten model (Burdine hypothesis) for the retention curve and of the Brooks and Corey model for the hydraulic conductivity curve was better fulfilling mathematical constraints imposed by static and dynamical considerations.

2.3.2. *Capillary capacity*.

The capillary capacity $C_h=\left(\frac{\partial\theta}{\partial h}\right)$ can then easily be calculated.

* For the Brooks and Corey model, it is given by:

$$\begin{cases} C_h = -\dfrac{\gamma\theta_{ae}}{h}\left(\dfrac{h_{ae}}{h}\right)^{\gamma} & h \le h_{ae} \\ C_h = -\dfrac{\gamma\theta_{ae}}{h_{we}} & h_{ae} \le h \le h_{we} \quad \text{Main Wetting curve} \\ C_h = 0 & h_{we} \le h \le 0 \end{cases} \qquad (2.8a)$$

$$\begin{cases} C_h = -\dfrac{\gamma\theta_{ae}}{h}\left(\dfrac{h_{ae}}{h}\right)^{\gamma}(1+\gamma)\left(1-\dfrac{h_{we}}{h}\right) & h \le h_{ae} \text{ Main Drying Curve (2.8b)} \\ C_h = 0 \quad h_{ae} \le h \le 0 \end{cases}$$

* For the Van Genuchten model, the capillary capacity is given by:

$$C_h = (\theta_{sat} - \theta_r)\left(-\frac{mn}{h_g}\right)\left(\frac{h}{h_g}\right)^{n-1}\left[1+\left(\frac{h}{h_g}\right)^{n}\right]^{-m-1} \qquad (2.9)$$

* For the modified Van Genuchten model (Burdine hypothesis), the capillary capacity reads:

$$C_h = \theta_{sat}\left(-\frac{m_1 n_1}{h_{g1}}\right)\left(\frac{h}{h_{g1}}\right)^{n_1-1}\left[1+\left(\frac{h}{h_{g1}}\right)^{n1}\right]^{-m1-1} \qquad h \ge h_c \qquad (2.10a)$$

$$C_h = \theta_{sat}\left(-\frac{m_2 n_2}{h_{g2}}\right)\left(\frac{h}{h_{g2}}\right)^{n2-1}\left[1+\left(\frac{h}{h_{g2}}\right)^{n2}\right]^{-m2-1} \qquad h \le h_c \qquad (2.10b)$$

2.3.3. *Computation of diffusivities*.

i) The isothermal diffusivity $D_{vh}$ is defined by (Philips and De Vries, 1957):

$$D_{vh} = \xi D_{va} F(\varepsilon-\theta)\frac{p_{atm}}{p_{atm}-e_v}\frac{\partial \rho_v}{\partial h} \qquad (2.11)$$

where $\xi$ is the tortuosity factor.

$F(\varepsilon-\theta)$ is a function of the air content given by:

$$\begin{cases} F(\varepsilon-\theta) = (\varepsilon-\theta)\left(1+\theta/\theta_k\right) & \theta \le \theta_k \\ F(\varepsilon-\theta) = \varepsilon \quad \theta > \theta_k \end{cases} \qquad (2.12)$$

where $\theta_k$ is the water content at which the liquid phase is no more continuous.

$D_{va}$ ($m^2\ s^{-1}$) is the water vapor diffusivity into the air and is expressed as:

$$D_{va} = 2.17\,10^{-7}\left(\frac{T}{273.15}\right)^{1.88} \qquad \text{(De Vries, 1975)} \qquad (2.13)$$

with the temperature $T$ in Kelvin.

Finally, the density of water vapor is given by:

$$\rho_v = h_u \rho_{vsat}(T) = \frac{h_u e_{sat}(T)}{RT} \qquad (2.14)$$

where the relative humidity is obtained by the Kelvin law:

$$h_u = \exp\left(\frac{gh}{RT}\right) \tag{2.15}$$

The derivative of the density of water vapor with respect to pressure is given by:

$$\left(\frac{\partial \rho_v}{\partial h}\right) = \frac{g\rho_v}{RT} = \frac{ge_v}{R^2T^2} \tag{2.16}$$

ii) The vapor diffusivity at constant matrix potential $D_{vt}$ is given by:

$$D_{vT} = \zeta D_{va} F(\varepsilon - \theta) \frac{p_{atm}}{p_{atm} - e_v} \frac{\partial \rho_v}{\partial T} \tag{2.17}$$

where $\zeta$ is the ratio of the average temperature gradient in the air to the macroscopic temperature gradient. The derivative of the density of water vapour with respect to temperature is given by:

$$\left(\frac{\partial \rho_v}{\partial T}\right) = -\frac{\rho_v gh}{RT^2} - \frac{\rho_v}{T} + h_u \frac{\rho_{vsat}(T)}{e_{sat}(T)} \frac{\partial e_{sat}(T)}{\partial T} \tag{2.18a}$$

and can be rewritten as:

$$\left(\frac{\partial \rho_v}{\partial T}\right) = -\frac{\rho_v}{T}\left(\frac{L_v(T)}{RT} - Log(h_u) - 1\right) + h_u \frac{\rho_{vsat}(T)}{e_{sat}(T)} \frac{\partial e_{sat}(T)}{\partial T} \tag{2.18b}$$

by using the Clapeyron law:

$$\frac{L_v(T)}{RT^2} = \frac{1}{e_{sat}(T)} \frac{\partial e_{sat}(T)}{\partial T} \tag{2.19}$$

2.3.4. *Thermal properties*.

i) The volumetric heat capacity $C_T$ is calculated by summing the contributions of organic matter, minerals and water using the De Vries (1975) model (the contribution of air is neglected).

$$C_T = C_o\theta_o + C_m\theta_m + C_{dry}\theta \tag{2.20}$$

The volumetric heat capacity of minerals (J m$^{-3}$ K$^{-1}$) can be approximated by:

$$C_{dry} = 2\ 10^6(1 - por) \tag{2.21}$$

ii) For the apparent thermal conductivity $\lambda$, four options are possible in the SiSPAT model.

* If *icth=0*, the De Vries (1963) model, which allows a dependence of $\lambda$ with temperature and water content, can be used. The description of the De Vries (1963) model given below is adapted from Passerat de Silans (1986). The apparent thermal conductivity of the medium is obtained as a combination of the contributions of all its constituents: quartz, other minerals, organic matter and air denoted by subscripts $_q$, $_m$, $_o$, and $_a$ and water (no subscript for water). $\theta_i$ will denote the

volumetric content for constituent *i*, $\lambda_i$ its thermal conductivity and $k_i$ a shape factor associated with the constituent *i*.

$$\lambda = \frac{\sum_i k_i \lambda_i \theta_i}{\sum_i k_i \theta_i} \tag{2.22}$$

The shape factors were calculated by De Vries by assuming ellipsoidal particles:

$$k_i = \frac{1}{3\sum_{v=a,b,c} \frac{1}{1+\left(\frac{\lambda_i}{\lambda_o}-1\right)g_v}} \tag{2.23}$$

where a,b,c represents the axes of the ellipsoids. The $g_v$ coefficients were empirically adjusted by De Vries and are such that $g_a + g_b + g_c = 1$. $\lambda_o$ is the thermal conductivity of the continuous phase (either water or air when the soil is dry) for which $k_o=1$. $k_i$ represents then the ratio of temperature gradients of phase *i* and of the continuous phase and $\zeta$ is defined as:

$$\varsigma = \frac{k_a}{\sum_i k_i \theta_i} \tag{2.24}$$

Table 1 summarises the values of the thermal conductivity of the various constituents.

*Table 1: Thermal conductivity of some media.*

| Constituants | Thermal conductivity ($Wm^{-1} K^{-1}$) |
|---|---|
| Water | 0.6 |
| Dry air | 0.025 |
| Quartz | -0.02714 *T* +16.462 (*T* in K) |
| Other minerals | 2.93 |
| Organic matter | 0.25 |

Practically, the value of the thermal conductivity depends on the water content of the medium:

i) The medium is dry ($\theta \le \theta_k$) and the continuous phase is the air.

$$\lambda = \lambda_{dry} + \frac{\theta}{\theta_k}\left(\lambda_k - \lambda_{dry}\right) \tag{2.25a}$$

$$\lambda_{dry} = 1.25\frac{\varepsilon\lambda_{adry} + \sum_{i=q,m,o} k_i \theta_i \lambda_i}{\varepsilon + \sum_{i=q,m,o} k_i \theta_i} \tag{2.25b}$$

where $\lambda_{adry}$ is the conductivity of dry air, considered here as the conductivity of the continuous medium and $\lambda_k = \lambda(\theta_k)$.

ii) The medium is wet ($\theta > \theta_k$) and the continuous phase is the water.

* if $\theta_{wilt} \le \theta \le \theta_{sat}$

$$g_a = g_b = 0.333 - \left(\frac{\theta_{sat} - \theta}{\theta_{sat} - \theta_{wilt}}\right)(0.333 - 0.035) \qquad (2.26a)$$

$$\lambda_a = \lambda_{adry}\left(1 + 0.08T \sin\left(\frac{\varepsilon - \theta}{\varepsilon}\pi\right)\right) \qquad (2.26b)$$

(Cary, 1979).

* if $\theta_k \le \theta \le \theta_{wilt}$

$$g_a = g_b = 0.013 + \left(\frac{\theta - \theta_k}{\theta_{wilt} - \theta_k}\right)(g_{awilt} - 0.013) \qquad (2.27)$$

where $g_{awilt} = g_a(\theta_{wilt})$

When measurements of the thermal conductivity are available, Passerat de Silans (1986) has shown that the numerical coefficients in the formulae given above could be adjusted to match the observations.

* The second option (*icth=1*) represents the use of a constant value for the thermal conductivity.

* If *icth=2*, $\lambda$ can be specified using the model of Laurent and Guerre-Chaley (1995) adapted from Mac Innes cited by Campbell (1985) (*icth=2*):

$$\lambda = e_j + a_j \frac{\theta}{por} + b_j\left(1 - exp\left(-c_j \frac{\theta}{por}\right)\right)^{d_j} \qquad (2.28)$$

* If *icth=3*, the model proposed by Van de Griend and O'Neill (1986) can be chosen. It is most adapted to situations where only the soil texture is known and no soil thermal properties measurements are available. The thermal inertia $\Lambda(\theta)$ is expressed as a function of the soil water content $\theta$:

$$\Lambda(\theta) = \sqrt{\lambda(\theta) C_h(\theta)} = \frac{1}{0.654}\left[\Lambda_s + 2300\theta - 1890\right] \qquad (2.29)$$

where $\Lambda_s$ is a texture dependent coefficient, tabulated by Van de Griend and O'Neill (1986) and given in Table 2. The thermal conductivity is therefore given by:

$$\lambda(\theta) = \frac{1}{C_{dry} + 4.18 \quad 10^6\theta}\left[\frac{1}{0.654}\left(\Lambda_s + 2300\theta - 1890\right)\right]^2 \qquad (2.30)$$

| Class Number | Class | Thermal inertia at saturation $\Lambda_s$ ($J\ m^{-2}\ K^{-1}\ s^{-1/2}$) |
|---|---|---|
| 1 | Sand | 2830 |
| 2 | Loamy Sand | 2765 |
| 3 | Sandy Loam | 2700 |
| 4 | Silt Loam | 2635 |
| 5 | Loam | 2570 |
| 6 | Sandy Clay Loam | 2505 |
| 7 | Silty Clay Loam | 2440 |
| 8 | Clay Loam | 2375 |
| 9 | Sandy Loam | 2310 |
| 10 | Silty Clay | 2245 |
| 11 | Clay | 2180 |

*Table 2: Values of the thermal inertia at saturation for different soil textural classes (from Van de Griend and O'Neill, 1986)*

## 2.4. Initial and boundary conditions.

To run the model, initial profiles of *h* and *T* are needed as well as boundary conditions.

For the lower boundary condition, five options are available:

(i) *itypinf=1*: prescribed value of *h* and *T*. These values are constant in time.

(ii) *itypinf=2*: specified water flux value (for example, zero flux if the boundary is impervious). This values is constant in time. For soil temperature at depth $z_N$ corresponding to the bottom of the soil profile, a sinusoidal function of time (Day of the Year – DoY) is used:

$$T(z_N) = T_{mean}(z_N) + T_{amp}(z_N)\sin\left(2\pi\left(\frac{DoY - phase(z_N)}{365.25}\right)\right) \qquad (2.31)$$

This function requires three parameters: $T_{mean}(z_N)$ the average annual temperature at depth $z_N$; $T_{amp}(z_N)$ the semi-amplitude of the annual sinusoidal wave at depth $z_N$; $phase(z_N)$ the phase of the annual sinusoidal wave at depth $z_N$.

(iii) *itypinf=3*: gravitational water flux, i.e. the isothermal water flux is equal to the hydraulic conductivity corresponding to the water content at the bottom of the soil profile and sinusoidal function of time (Day of the Year – DoY) for the soil temperature at depth $z_N$, corresponding to the bottom of the soil profile (Eq. (2.31)

(iv) *itypinf=4*: values of the matric potential and of the temperature are prescribed, but they can evolve in time. Both time evolutions as a function of Doy of the Year are given in two separated files and are interpolated daily by the model.

(v) *itypinf=5*: values of the matric potential are prescribed, but they can evolve in time. The time evolution as a function of Day of the Year is given in a file and is interpolated daily by the model. The temperature at the bottom of the soil profile is a sinusoidal function of time as given by Eq. (2.31).

Note that options *itypinf=1, 4, 5* support positive values of the matric potential. Therefore, if the level of an aquifer is known as a function of time, the time evolution of the matric potential at the bottom of the soil profile can be deduced, assuming the hydrostatic hypothesis. However the SiSPAT model is presently not able to calculate the evolution of the depth of an aquifer, or a saturated zone by itself.

The upper boundary condition of the soil module is provided by the solution of the soil-plant-atmosphere interface (see chapter 3), which gives the surface soil heat and mass fluxes and the surface matric potential $h_1$ and temperature $T_1$. The soil module can thus be run by setting the fluxes (Neumann condition) or the values of temperature and matric potential (Dirichlet condition). The Dirichlet condition proved to be numerically more stable and efficient in most of the cases study, dealing with arid climate conditions and rainfall of high intensities. On the other hand, the Neumann condition led to better mass balance closure under wetter conditions. The latter option is therefore recommended for the simulations under wet and temperate climates.

Furthermore, if the soil surface becomes saturated, the upper boundary condition is automatically changed and a potential value: *h=0* is imposed (infiltration under a positive head is not allowed in SiSPAT). A minimum value of the surface matrix potential ($h_o$ equal to -60000 m of water) is also prescribed in order to avoid numerical divergence when the soil is very dry.

## 2.5. A crude way to handle cracks.

A very crude way to handle cracks was included into the SiSPAT model. Two parameters are needed as input: $Z_{crack}$, the depth (m) of the cracks and *crack*, the surface fraction of cracks. $P_g$ been the rainfall reaching the ground surface (after interception by the canopy), it is assumed that $(1-crack)P_g$ is infiltrating into the soil and $crack * P_g$ is entering the cracks. This fraction of rainfall is then assumed to be infiltrated uniformly along the crack, with a flux per unit distance ($s^{-1}$) given by:

$$q_{crack} = \frac{crack * P_g}{Z_{crack}} \qquad (2.32)$$

This representation of cracks is of course candidate to possible future improvement.

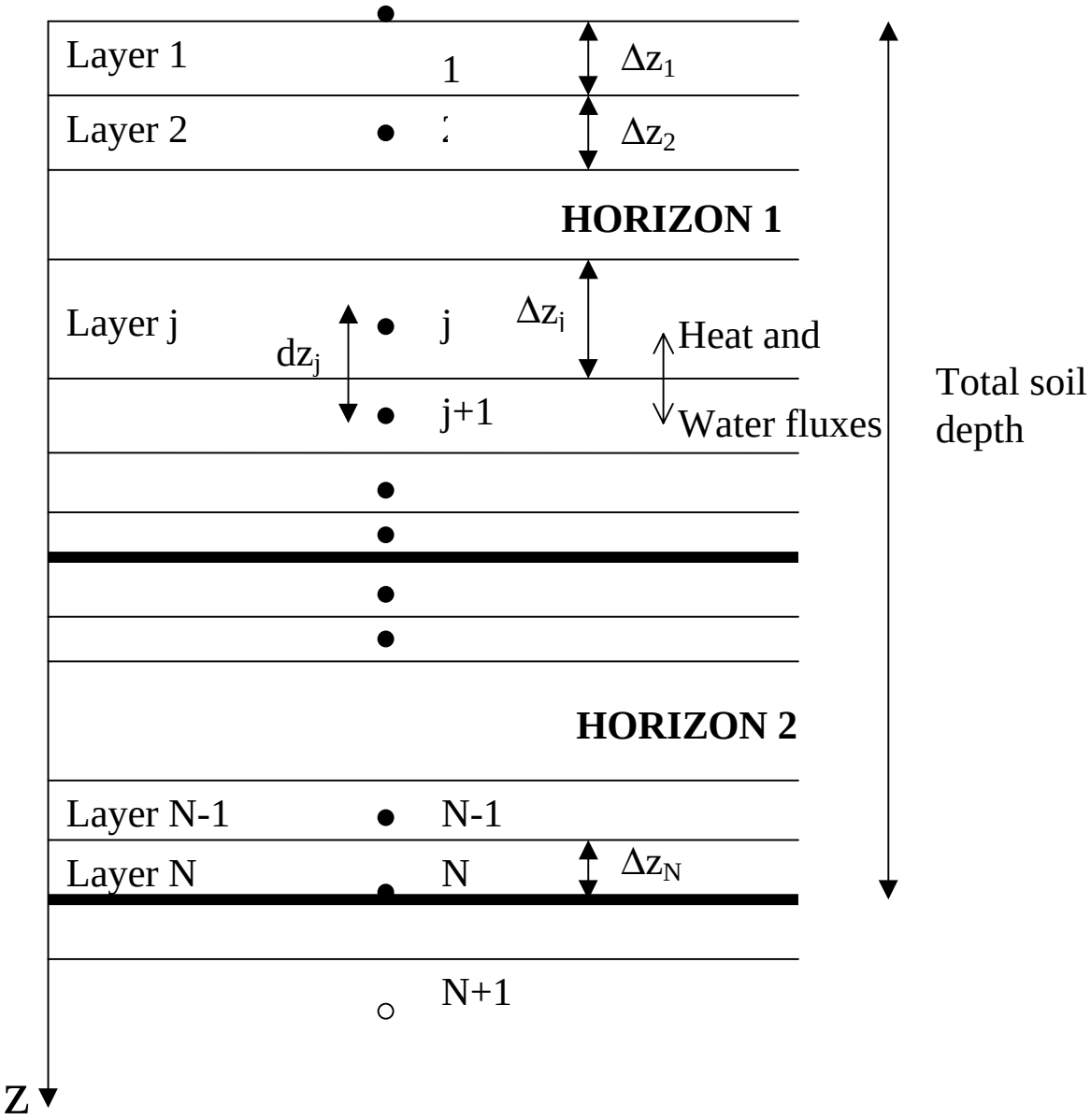


*Fig. 1: Scheme of the discretization of the soil, including the definition of nodes, layers and horizons*

## 2.6. Discretisation of the soil module.

As mentioned above, the model can deal with soils made of several horizons, with different soil properties. Numerically, each horizon is divided into layers with an increased resolution at the lower and upper boundaries of the horizon (see below*). Heat and water fluxes are calculated at the boundary between layers, whereas variables (temperature and matrix potential) are calculated at the nodes situated within these layers* (see Fig. 1). The first node is situated just at the soil surface (Fig. 1). When a flux condition is defined at the lower boundary of the soil column, an artificial node is defined

The discretisation procedure (subroutine **maillagecouche**) enables to calculate the thickness *between nodes* (internode thickness) and not the thickness of the layers. For each horizon, the total thickness is $e_{tot}$. Then, the user defines the thicknesses $e_u$ and $e_b$ of the upper and lower interfaces where the resolution must be increased In between, the internode thickness is constant and defined by the number of nodes $N_{bet}$ specified by the user ( $dz(i) = \left(e_{tot} - e_u - e_b\right) \Big/ N_{bet}$ . For each interface, the minimum values of the internode thickness $dz_{u\ min}$ of the upper interface (resp. $dz_{b\ min}$ of the bottom interface) are also defined by the user (see Fig. 2). A logarithmic increase of the internode thickness is then used. The total number of nodes in the upper $N_u$ (resp. bottom $N_b$) interface are therefore given by:

$$N_u = \frac{Log\left(1 - \frac{e_u\left(1-\varpi_u\right)}{dz_{u\min}}\right)}{Log(\varpi_u)} \qquad (2.33a)$$

$$N_b = \frac{Log\left(1 - \frac{e_b\left(1-\varpi_b\right)}{dz_{b\min}}\right)}{Log(\varpi_b)} \qquad (2.33b)$$

where $\varpi_u$=1.25 and $\varpi_b$=0.8.

The internode thicknesses within each interface are then calculated by:

$$dz_u(i) = dz_{u\min}\varpi_u^{i-1} \qquad i = 1,..,N_u \qquad (2.34a)$$

$$dz_b(i) = dz_{b\min}\varpi_b^{i-1} \qquad i = 1,..,N_b \qquad (2.34b)$$

An utility program called *maillage.f* is available to perform the discretization of the soil profile.

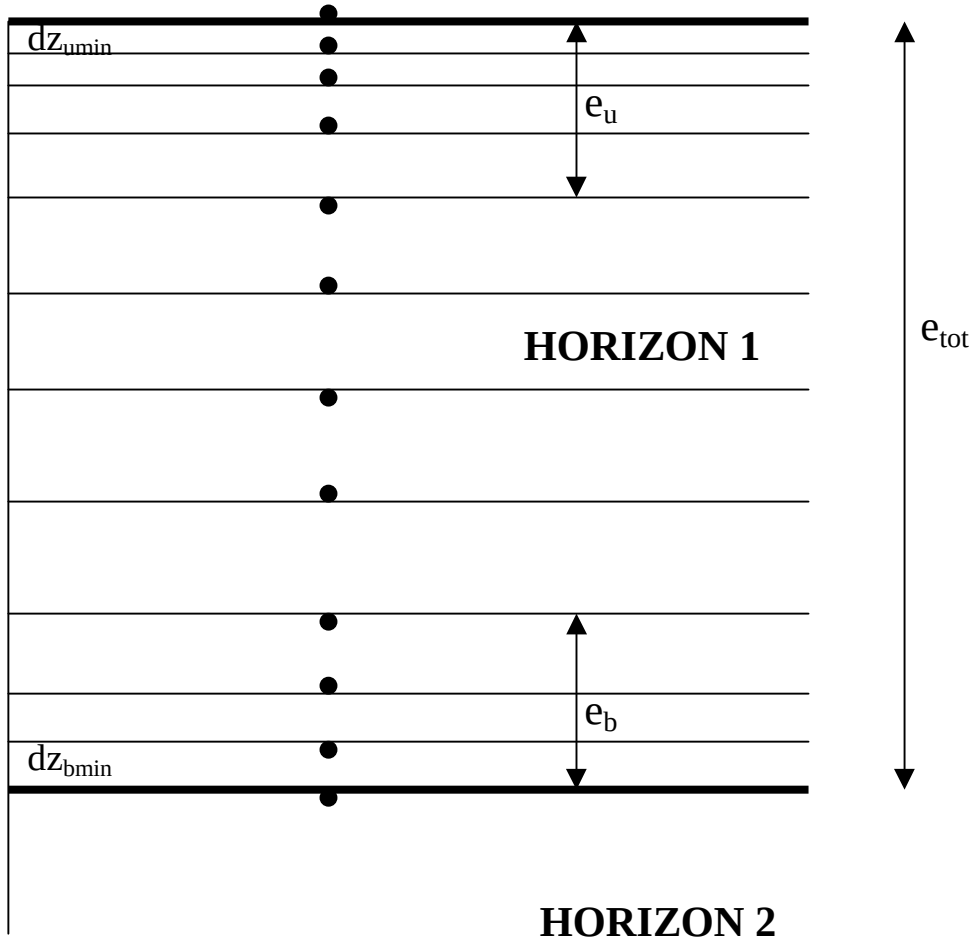


*Fig. 2: Definition of the thicknesses used in the discretization of the soil profile*

## 2.7. Numerical discretisation of heat and water transfer flux equations.

Finite differences are used. The scheme is implicit but explicit linearisation of the transfer and storage coefficients (which depend on matrix potential and temperature) is used (Haverkamp et al., 1977). The latter are interpolated in space (at the boundary of the layers) using geometric mean between two nodes (Vauclin et al., 1979). Equations are discretised using the local mass balance method, where the mass balance of each layer *j* is evaluated (see Fig. 3). The details are given for the mass balance equation (2.1a), but the procedure is similar for the heat balance equation.

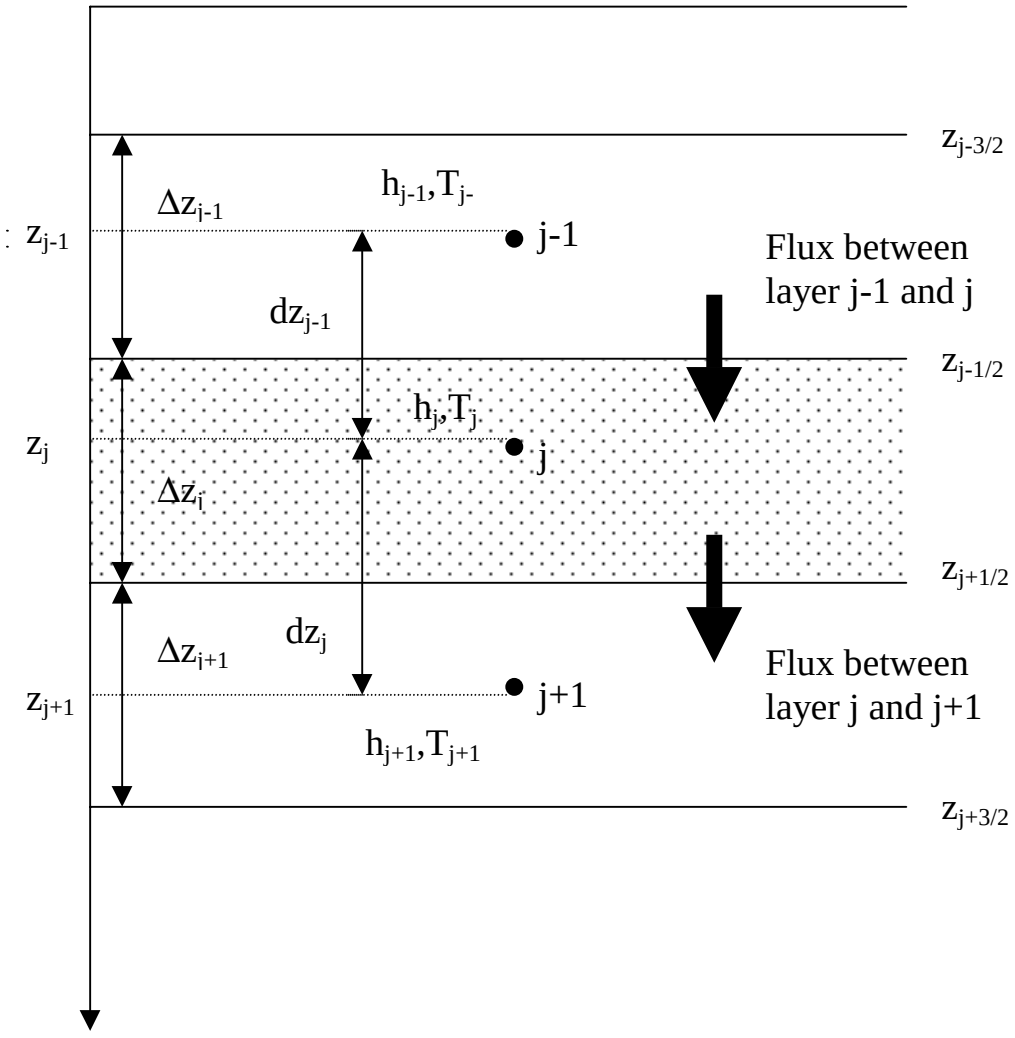


*Fig. 3: Definition of the layers used for the application of the mass balance method*

2.6.1 *Discretisation for layers* $2 \le j \le N-1$.

For layer *j*, the equation is integrated between depths $z_{j-1/2}$ and $z_{j+1/2}$ and time $t^i$ and $t^{i+1}$ ($\Delta t^{i+1}=t^{i+1}-t^i$).

$$\int_{\Delta t^{i+1}} \int_{z_{j-1/2}}^{z_{j+1/2}} C_h \frac{\partial h}{\partial t}\, dz\, dt = \int_{\Delta t^{i+1}} [\int_{z_{j-1/2}}^{z_{j+1/2}} \frac{\partial}{\partial z}\left( D_{mh} \frac{\partial h}{\partial z} + D_{mT} \frac{\partial T}{\partial z} - K \right) dz - \int_{z_{j-1/2}}^{z_{j+1/2}} \frac{S}{\rho_w} dz]\, dt \qquad (2.35)$$

Integrals on the left-hand side are inverted and by using the theorem of the mean and an implicit linearisation, (2.35) can be written:

$$\int_{z_{j-1/2}}^{z_{j+1/2}} C_{hj}^{i+1}\left(h^{i+1}-h^{i}\right) dz = \int_{\Delta t^{i+1}} \left[ D_{mh} \frac{\partial h}{\partial z} + D_{mT} \frac{\partial T}{\partial z} - K \right]_{z_{j-1/2}}^{z_{j+1/2}} - \int_{\Delta t^{i+1}} \frac{S_j}{\rho_w}\left(z_{j+1/2}-z_{j-1/2}\right) dt \qquad (2.36)$$

After a second implicit linearisation and with $\Delta z_j = \left(z_{j+1/2}-z_{j-1/2}\right)$ (thickness of layer j) and $dz_j = \left(z_{j+1}-z_j\right)$ (thickness between nodes *j* and *j+1*), the final discretised equation reads for $2 \le j \le N-1$ where *N* is the total number of nodes:

$$\begin{aligned} C_{hj}^{i+1} \frac{h_j^{i+1}-h_j^i}{\Delta t^{i+1}} \Delta z_j = & \left[ D_{mhj+1/2}^{i+1} \frac{h_{j+1}^{i+1}-h_j^{i+1}}{dz_j} + D_{mTj+1/2}^{i+1} \frac{T_{j+1}^{i+1}-T_j^{i+1}}{dz_j} - K_{j+1/2}^{i+1} \right] - \\ & - \left[ D_{mhj-1/2}^{i+1} \frac{h_j^{i+1}-h_{j-1}^{i+1}}{dz_{j-1}} + D_{mTj-1/2}^{i+1} \frac{T_j^{i+1}-T_{j-1}^{i+1}}{dz_{j-1}} - K_{j-1/2}^{i+1} \right] - \Delta z_j \frac{S_j^{i+1}}{\rho_w} \end{aligned} \qquad (2.37)$$

For the heat equation, the following is obtained:

$$\begin{aligned} C_{Tj}^{i+1} \frac{T_j^{i+1}-T_j^i}{\Delta t^{i+1}} \Delta z_j = & \left[ D_{chj+1/2}^{i+1} \frac{h_{j+1}^{i+1}-h_j^{i+1}}{dz_j} + D_{cTj+1/2}^{i+1} \frac{T_{j+1}^{i+1}-T_j^{i+1}}{dz_j} \right] - \\ & - \left[ D_{chj-1/2}^{i+1} \frac{h_j^{i+1}-h_{j-1}^{i+1}}{dz_{j-1}} + D_{cTj-1/2}^{i+1} \frac{T_j^{i+1}-T_{j-1}^{i+1}}{dz_{j-1}} \right] \end{aligned} \qquad (2.38)$$

The explicit linearisation of coefficients leads to:

$$C_{hj}^{i+1} = C_{hj}^i \qquad D_{mhj}^{i+1} = D_{mhj}^i \qquad D_{mTj}^{i+1} = D_{mTj}^i \qquad K_j^{i+1} = K_j^i \qquad (2.39a)$$

$$C_{Tj}^{i+1} = C_{Tj}^i \qquad D_{chj}^{i+1} = D_{chj}^i \qquad D_{cTj}^{i+1} = D_{cTj}^i \qquad (2.39b)$$

The root extraction terms are taken at time $t^{i+1}$ and their calculation is described in chapters 4 and 5. and the internodal values are calculated as the geometric mean of the values at the nodes (Vauclin et al., 1979):

$$D_{mhj-1/2}^{i+1} = \left[ D_{mhj-1}^{i} D_{mhj}^{i} \right]^{1/2} \qquad D_{mTj-1/2}^{i+1} = \left[ D_{mTj-1}^{i} D_{mTj}^{i} \right]^{1/2} \qquad K_{j-1/2}^{i+1} = \left[ K_{j-1}^{i} K_{j}^{i} \right]^{1/2} \qquad (2.40a)$$

$$D_{chj-1/2}^{i+1} = \left[ D_{chj-1}^{i} D_{chj}^{i} \right]^{1/2} \qquad D_{cTj-1/2}^{i+1} = \left[ D_{cTj-1}^{i} D_{cTj}^{i} \right]^{1/2} \qquad (2.40b)$$

Equations (2.37) and (2.38) are rearranged, leading to the following linear system for $2 \le j \le N-1$:

$$A1_{hj} h_{j-1}^{i+1} + A3_{hj} h_{j}^{i+1} + A5_{hj} h_{j+1}^{i+1} + A2_{hj} T_{j-1}^{i+1} + A4_{hj} T_{j}^{i+1} + A6_{hj} T_{j+1}^{i+1} = B_{hj} \qquad (2.41a)$$

$$A1_{Tj} h_{j-1}^{i+1} + A3_{Tj} h_{j}^{i+1} + A5_{Tj} h_{j+1}^{i+1} + A2_{Tj} T_{j-1}^{i+1} + A4_{Tj} T_{j}^{i+1} + A6_{Tj} T_{j+1}^{i+1} = B_{Tj} \qquad (2.41b)$$

where

$$A1_{hj} = -\frac{D_{mhj-1/2}^{i}}{dz_{j-1}} \qquad A1_{Tj} = -\frac{\Delta t^{i+1}}{\Delta z_j C_{Tj}^{i}} \frac{D_{chj-1/2}^{i}}{dz_{j-1}}$$

$$A2_{hj} = -\frac{D_{mTj-1/2}^{i}}{dz_{j-1}} \qquad A2_{Tj} = -\frac{\Delta t^{i+1}}{\Delta z_j C_{Tj}^{i}} \frac{D_{cTj-1/2}^{i}}{dz_{j-1}}$$

$$A3_{hj} = \frac{D_{mhj-1/2}^{i}}{dz_{j-1}} + \frac{D_{mhj+1/2}^{i}}{dz_{j}} + \frac{\Delta z_j C_{hj}^{i}}{\Delta t^{i+1}} \qquad A3_{Tj} = \frac{\Delta t^{i+1}}{\Delta z_j C_{Tj}^{i}} \left( \frac{D_{chj-1/2}^{i}}{dz_{j-1}} + \frac{D_{chj+1/2}^{i}}{dz_{j}} \right)$$

$$A4_{hj} = \frac{D_{mTj-1/2}^{i}}{dz_{j-1}} + \frac{D_{mTj+1/2}^{i}}{dz_{j}} \qquad A4_{Tj} = 1 + \frac{\Delta t^{i+1}}{\Delta z_j C_{Tj}^{i}} \left( \frac{D_{chj-1/2}^{i}}{dz_{j-1}} + \frac{D_{chj+1/2}^{i}}{dz_{j}} \right)$$

$$A5_{hj} = -\frac{D_{mhj+1/2}^{i}}{dz_{j}} \qquad A5_{Tj} = -\frac{\Delta t^{i+1}}{\Delta z_j C_{Tj}^{i}} \frac{D_{chj+1/2}^{i}}{dz_{j}}$$

$$A6_{hj} = -\frac{D_{mTj+1/2}^{i}}{dz_{j}} \qquad A6_{Tj} = -\frac{\Delta t^{i+1}}{\Delta z_j C_{Tj}^{i}} \frac{D_{cTj+1/2}^{i}}{dz_{j}}$$

$$B_{hj} = K_{j-1/2}^{i} - K_{j+1/2}^{i} - \Delta z_j \frac{S_j^{i+1}}{\rho_w} + \frac{\Delta z_j C_{hj}^{i}}{\Delta t^{i+1}} h_j^{i} \qquad B_{Tj} = T_j^{i} \qquad (2.42)$$

When cracks are present at depth $z_j$, the additional term $q_{crack}*\Delta z_j$ is added to $B_{hj}$.

2.6.2. *Discretisation for layer j=1.*

For the first layer, the value of the above coefficients depends on the choice of the boundary condition type.

If a Dirichlet condition is considered (known values of the temperature and/or matrix potential), coefficients read:

$$
\begin{aligned}
A1_{h1} &= 0 & A1_{T1} &= 0 \\
A2_{h1} &= 0 & A2_{T1} &= 0 \\
A3_{h1} &= 1 & A3_{T1} &= 0 \\
A4_{h1} &= 0 & A4_{T1} &= 1 \\
A5_{h1} &= 0 & A5_{T1} &= 0 \\
A6_{h1} &= 0 & A6_{T1} &= 0 \\
B_{h1} &= h_1^i & B_{T1} &= T_1^i
\end{aligned}
\qquad (2.43)
$$

If a Neumann condition is chosen (prescribed values of the heat flux $G$ and mass flux $Q_{mg}$ at the surface), coefficients read:

$$
\begin{aligned}
A1_{h1} &= 0 & A1_{T1} &= 0 \\
A2_{h1} &= 0 & A2_{T1} &= 0 \\
A3_{h1} &= \frac{D^i_{mh1+1/2}}{dz_1} + \frac{\Delta z_1 C^i_{h1}}{\Delta t^{i+1}} & A3_{T1} &= \frac{\Delta t^{i+1}}{\Delta z_1 C^i_{T1}}\left(\frac{D^i_{ch1+1/2}}{dz_1}\right) \\
A4_{h1} &= \frac{D^i_{mT1+1/2}}{dz_1} & A4_{T1} &= 1 + \frac{\Delta t^{i+1}}{\Delta z_1 C^i_{T1}}\left(\frac{D^i_{ch1+1/2}}{dz_1}\right) \\
A5_{h1} &= -\frac{D^i_{mh1+1/2}}{dz_1} & A5_{T1} &= -\frac{\Delta t^{i+1}}{\Delta z_1 C^i_{T1}}\frac{D^i_{ch1+1/2}}{dz_1} \\
A6_{h1} &= -\frac{D^i_{mT1+1/2}}{dz_1} & A6_{T1} &= -\frac{\Delta t^{i+1}}{\Delta z_1 C^i_{T1}}\frac{D^i_{cT1+1/2}}{dz_1} \\
B_{h1} &= \frac{Q_{mg}}{\rho_w} - K^i_{1+1/2} - \Delta z_1 \frac{S_1^{i+1}}{\rho_w} + \frac{\Delta z_1 C^i_{h1}}{\Delta t^{i+1}} h_1^i & B_{T1} &= T_1^i + G\frac{\Delta t^{i+1}}{\Delta z_1 C^i_{T1}}
\end{aligned}
\qquad (2.44)
$$

Combinations of Dirichlet and Neumann conditions for the heat and mass equations are of course possible.

### 2.6.3. *Discretisation for layer j=N.*

At the bottom of the soil profile a Dirichlet condition is imposed for the heat equation. It is up to the user to read the evolution of this temperature on a file or to impose a variation with time: the code can be modified adequately. This possibility can be interesting when long term simulations over the year are performed and the seasonal evolution of deep temperature is to be taken into account.

For the mass equation, a Dirichlet condition can also be used. In this case the coefficients for the last layer are given by:

$$
\begin{aligned}
A1_{hN} &= 0 & A1_{TN} &= 0 \\
A2_{hN} &= 0 & A2_{TN} &= 0 \\
A3_{hN} &= 1 & A3_{TN} &= 0 \\
A4_{hN} &= 0 & A4_{TN} &= 1 \\
A5_{hN} &= 0 & A5_{TN} &= 0 \\
A6_{hN} &= 0 & A6_{TN} &= 0 \\
B_{hN} &= h_N^i & B_{TN} &= T_N^i
\end{aligned}
\qquad (2.45)
$$

If a Neumann condition is chosen, an artificial node $h_{N+1}$ must be defined and the flux is calculated between nodes $N$ and $N+1$ with $dz_N = dz_{N-1} = 2\Delta z_N$ Let $Q_N$ be this flux. If we assume that this flux can be defined by the Darcy flux (i.e. vapor flux and water flux induced by temperature gradients can be neglected), we get:

$$
Q_N^i = -K_{N+1/2}^i \left( \frac{h_{N+1}^i - h_N^i}{dz_N} - 1 \right) \qquad (2.46)
$$

If the flux is the gravitational flow $h_{N+1}=h_N$. and $Q_N^i = K_{N+1/2}^i$.

Equation (2.46) allows to calculate $h_{N+1}$ as a function of $h_N$ and of the flux at the bottom of the column:

$$
h_{N+1}^i = h_N^i + 2\Delta z_N \left( 1 - \frac{Q_N^i}{K_{N+1/2}^i} \right) \qquad (2.47)
$$

When this is introduced into the mass flux equation, the resulting values of the coefficients are:

$$
\begin{aligned}
A1_{hN} &= -\frac{D_{mhN-1/2}^i}{dz_{N-1}} \\
A2_{hN} &= -\frac{D_{mTN-1/2}^i}{dz_{N-1}} \\
A3_{hN} &= \frac{D_{mhN-1/2}^i}{dz_{N-1}} + \frac{2\Delta z_N C_{hN}^i}{\Delta t^{i+1}} \\
A4_{hN} &= \frac{D_{mTN-1/2}^i}{dz_{N-1}} \\
A5_{hN} &= 0 \\
A6_{hN} &= 0 \\
B_{hN} &= K_{N-1/2}^i - K_{N+1/2}^i - 2\Delta z_N \frac{S_N^{i+1}}{\rho_w} + \frac{2\Delta z_N C_{hN}^i}{\Delta t^{i+1}} h_N^i + D_{mhN+1/2}^i \left( 1 - \frac{Q_N^i}{K_{N+1/2}^i} \right)
\end{aligned}
\qquad (2.48)
$$

2.6.4. *Final linear system to be solved.*

The above equations can finally be written in a matrix form:

$$[A][X]=[B] \tag{2.49}$$

where

$$[X]=\begin{bmatrix} h_1 \\ h_2 \\ . \\ h_j \\ . \\ h_N \\ T_1 \\ T_2 \\ . \\ T_j \\ . \\ T_N \end{bmatrix} \qquad [B]=\begin{bmatrix} B_{h1} \\ B_{h2} \\ . \\ B_{hj} \\ . \\ B_{hN} \\ B_{T1} \\ B_{T2} \\ . \\ B_{Tj} \\ . \\ B_{TN} \end{bmatrix}$$

and the matrix $[A]$ is a four blocks tridiagonal matrix:

$$[A]=\left[\begin{array}{ccccccc:ccccccc}
A3_{h1} & A5_{h1} & & & & & & A4_{h1} & A6_{h1} & & & & & \\
A1_{h2} & A3_{h2} & A5_{h2} & & & & & A2_{h2} & A4_{h2} & A6_{h2} & & & & \\
 & . & . & . & & & & & . & . & . & & & \\
 & & A1_{hj} & A3_{hj} & A5_{hj} & & & & & A2_{hj} & A4_{hj} & A6_{hj} & & \\
 & & & . & . & . & & & & & . & . & . & \\
 & & & & A1_{hN-1} & A3_{hN-1} & A5_{hN-1} & & & & & A2_{hN-1} & A4_{hN-1} & A6_{hN-1} \\
 & & & & & A1_{hN} & A3_{hN} & & & & & & A2_{hN} & A4_{hN} \\
\hdashline
A3_{T1} & A5_{T1} & & & & & & A4_{T1} & A6_{T1} & & & & & \\
A1_{T2} & A3_{T2} & A5_{T2} & & & & & A2_{T2} & A4_{T2} & A6_{T2} & & & & \\
 & . & . & . & & & & & . & . & . & & & \\
 & & A1_{Tj} & A3_{Tj} & A5_{Tj} & & & & & A2_{Tj} & A4_{Tj} & A6_{Tj} & & \\
 & & & . & . & . & & & & & . & . & . & \\
 & & & & A1_{TN-1} & A3_{TN-1} & A5_{TN-1} & & & & & A2_{TN-1} & A4_{TN-1} & A6_{TN-1} \\
 & & & & & A1_{TN} & A3_{TN} & & & & & & A2_{TN} & A4_{TN}
\end{array}\right]$$

This linear system is easily solved by using an algorithm derived from the Thomas algorithm proposed by Douglas et al. (1959) and given in details in Touma (1984). It provides the values of the temperature and matrix potential at all the nodes of the soil module.

## 2.8. List of subroutines used in the soil module.

The full description of the subroutines, including input and output arguments is given in the Fortran code (Fortran 77). Here are only listed the names of the subroutines and what they do.

| | |
|---|---|
| subroutine **calcwh** | : Computation of the water content at each node as a function of the matric potential using either the Brooks and Corey or the Van Genuchten retention model. |
| subroutine **caphyd** | : Computation of the hydraulic capacity $C_h = \left(\frac{\partial\theta}{\partial h}\right)$ for the Van Genuchten retention model. |
| subroutine **caphydbc** | : Computation of the hydraulic capacity for the Brooks and Corey retention model. |
| subroutine **coefhydther** | : Computation of the storage and transfer coefficients of the water and heat transfer equations. The routine includes the computation of those coefficients at the nodes of the soil module and also of the internodal values. |
| subroutine **coefmat** | : Computation of the coefficients of the $[A]$ and $[B]$ matrices. |
| function **conduc** | : Computation of the hydraulic conductivity as a function of the volumetric water content using the Brooks and Corey model. |
| function **conducvg** | : Computation of the hydraulic conductivity using the Van Genuchten model (Mualem hypothesis) |
| subroutine **devries** | : Computation of the thermal conductivity of the soil using the De Vries (1975) model. |
| subroutine **flux** | : Computation of the water (liquid and vapor) and heat fluxes between two soil layers. |
| subroutine **maillagecouche** | : Discretisation of the soil profile by computation of the depths of the nodes and the thicknesses of the layers. |
| subroutine **trib** | : Resolution of the linear system $[A][X] = [B]$ using the modified Thomas algorithm. |
| subroutine **xdvht** | : Computation of the $D_{vh}$ and $D_{vT}$ transfer coefficients. |
| function **wh** | : Computation of the volumetric water content as a function of the matric potential for the Van Genuchten retention model. |
| function **whbc** | : Computation of the volumetric water content as a function of the matric potential for the Brooks and Corey retention model. |
| subroutine **xhn** | : Daily interpolation of bottom boundary condition matrix potential or temperature |

# 3. DESCRIPTION OF THE SOIL-PLANT-ATMSOPHERE INTERFACE MODULE.

## 3.1. Introduction.

In this module, the interactions between the soil, the vegetation and the atmosphere are modelled using an electrical analogy and a resistance network, schematised in Fig. 4. The model is forced at a reference level with the following climatic variables: air temperature and specific humidity, wind speed, incoming solar and long-wave radiation and rainfall, given at a time step of 1 hour as a maximum. The atmospheric forcing (except rainfall) is linearly interpolated to match the time step of the model which is lower than 100-200s and of the order of 1s when it is raining. Rainfall input is given in mm per time step of the observations. The rainfall intensity is assumed to be constant over the observation time step and is converted into m $s^{-1}$. The time step of the model is adapted to match the observation time step of rainfall to ensure the conservation of the total rainfall amount. Vegetation characteristics such as Leaf Area Index, root density profile, vegetation height, vegetation albedo can also be interpolated linearly if several measurements are available (daily interpolation). If this is not the case, they are kept constant.

Two layers are considered at the surface: one for the vegetation and one for the underlying bare soil. One energy budget is written for each component. Interception of rainfall by the canopy is also taken into account using a reservoir approach.

The basic equations used in this module will be described first (section 3.2). It includes the radiative transfer through the canopy, the turbulent transfers above and through the canopy (expression of momentum, water and heat fluxes), the way the aerodynamic and canopy resistances are calculated and finally the model used for the stomatal resistance. These equations finally lead to a non-linear system of five equations with five unknowns, which has been linearised to increase the computational efficiency. The steps of this linearisation will be described in section 3.3. and section 3.4. will be dedicated to the brief description of the various subroutines related to this soil-plant-interface module.

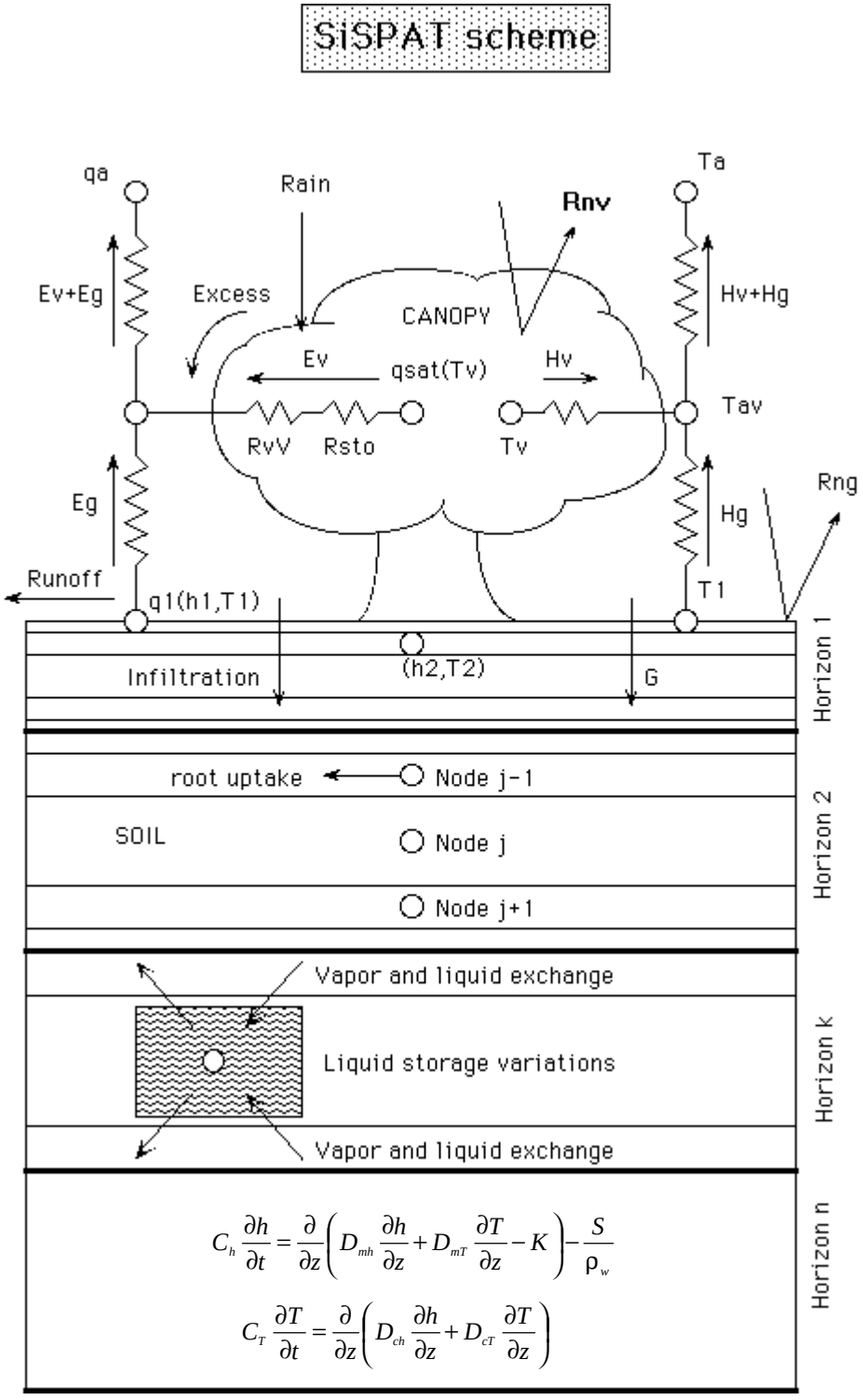


*Fig. 4: Scheme of the SiSPAT model*

## 3.2. Basic equations of the soil-plant-atmosphere interface module.

3.2.1. *Radiative transfers*.

Following Taconet et al. (1986), a two layer system is considered for the radiative transfer (vegetation above bare soil). The shielding factor $\sigma_f$, defined by Deardorff (1978), is used to partition the radiation between the vegetation and the bare soil and represents the radiation intercepted by the vegetation. A Beer-Lambert type law, function of the Leaf Area Index and of a parameter, $a_{bl}$ (-), controlling the exponential decrease, is used. Kanemasu et al. (1977) proposed a value of 0.4 for $a_{bl}$. A 0.4-0.8 range for this parameter is commonly admitted.

$$\sigma_f = 1 - exp(-a_{bl} LAI) \qquad (3.1)$$

The vegetation is considered as semi-transparent. For solar radiation *RG*, the following radiative properties can be defined::

- reflection factor for solar radiation $\sigma_f \alpha_v$
- absorption factor $\sigma_f (1 - \alpha_v)$
- transmissivity factor $(1 - \sigma_f)$

For long-wave radiation *RA*, they read:

- reflection factor for long-wave radiation $\sigma_f \varepsilon_v$
- absorption factor $\sigma_f (1 - \varepsilon_v)$
- transmissivity factor $(1 - \sigma_f)$

where $\alpha_v$ and $\varepsilon_v$ are the albedo and the emissivity of the vegetation respectively. In a similar way, $\alpha_g$ and $\varepsilon_g$ will denote the albedo and emissivity of the underlying soil. Multiple reflections between the soil and the canopy are allowed. Formulae for the net solar and longwave radiations for the vegetation and the bare soil ($RG_v$ and $RA_v$ and $RG_g$ and $RA_g$ respectively), as functions of the shielding factor, the vegetation and bare soil albedos and emissivities can be calculated as follows (positive terms correspond to a gain of energy and negative terms to a loss). Fig. 5 gives the scheme used for solar radiation and Fig. 6, the scheme retained for long-wave radiations.

i) <u>The net solar radiation for the vegetation</u> is the sum of the following terms: direct incoming solar radiation, reflected radiation at the top of the canopy, solar radiation transmitted to the bare soil, radiation coming from the solar radiation reflected on the bare soil surface, the same one reflected at the bottom of the canopy, and the same one transmitted to the atmosphere through the canopy.

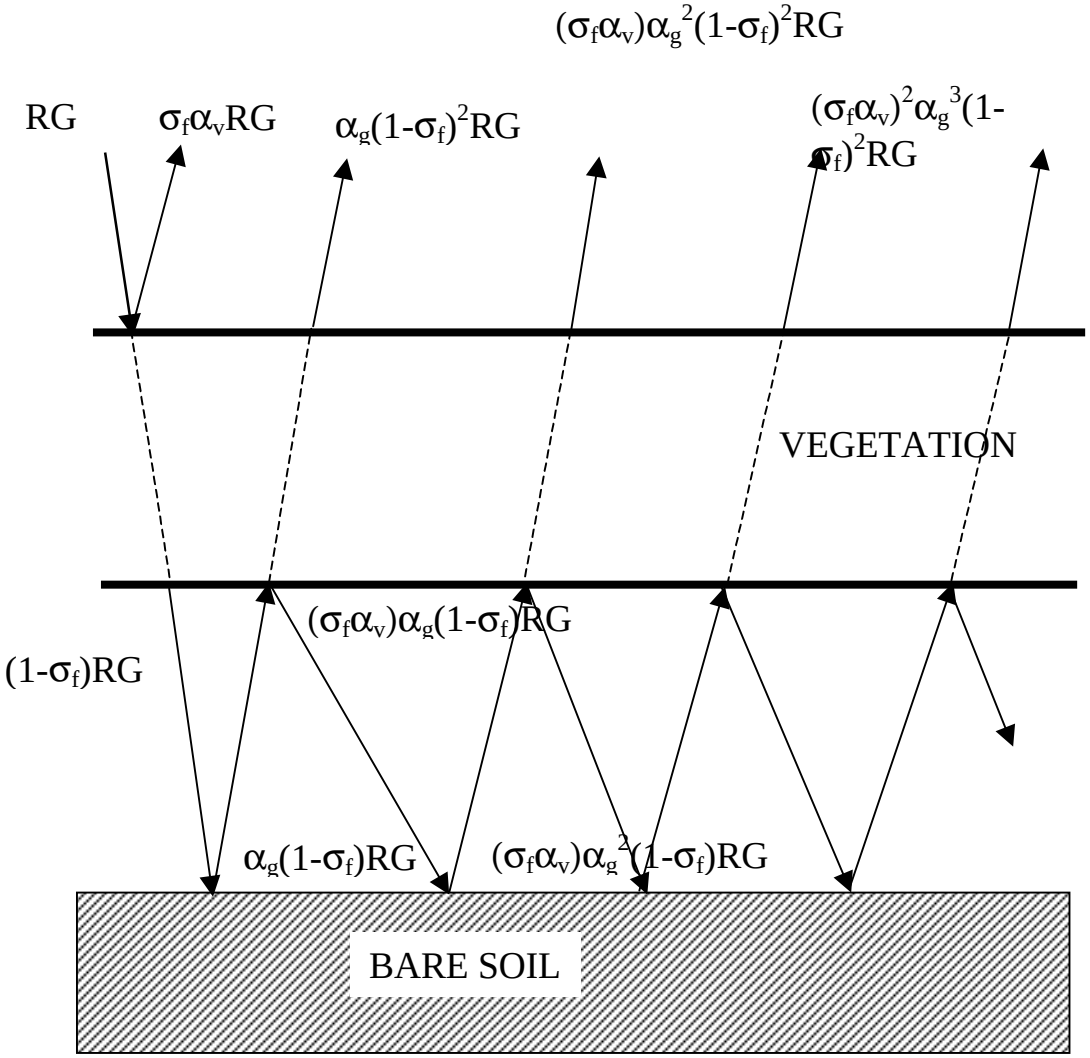


*<u>Fig. 5</u>: Scheme of the various components of the net solar radiation*

$$RG_v = RG - \sigma_f\alpha_v RG - (1-\sigma_f)RG + \sum_{n=1}^{\infty}(\alpha_g)^n(\sigma_f\alpha_f)^{n-1}(1-\sigma_f)RG - \sum_{n=1}^{\infty}(\alpha_g)^n(\sigma_f\alpha_f)^n(1-\sigma_f)RG - \sum_{n=1}^{\infty}(\alpha_g)^n(\sigma_f\alpha_f)^{n-1}(1-\sigma_f)^2 RG \quad (3.2a)$$

which can be simplified as:

$$RG_v = RG(1-\alpha_v)\sigma_f\left(1+\frac{\alpha_g(1-\sigma_f)}{1-\sigma_f\alpha_g\alpha_v}\right) \quad (3.2b)$$

by using the mathematical relationships for geometric series.

ii) The net solar radiation for the bare soil is the sum of the following terms: direct solar radiation transmitted by the canopy, the same one reflected by the soil surface. This component is then reflected at the bottom of the canopy and received by the bare soil and is further reflected.

$$RG_g = \left(1-\sigma_f\right)RG + \sum_{n=1}^{\infty}\left(\alpha_g\right)^n\left(\sigma_f\alpha_v\right)^n\left(1-\sigma_f\right)RG - \sum_{n=1}^{\infty}\left(\alpha_g\right)^n\left(\sigma_f\alpha_v\right)^{n-1}\left(1-\sigma_f\right)RG \quad (3.3a)$$

which is simplified as:

$$RG_g = \frac{RG\left(1-\alpha_g\right)\left(1-\sigma_f\right)}{1-\sigma_f\alpha_g\alpha_v} \quad (3.3b)$$

iii) For the long-wave radiation, the net contribution for the vegetation is the sum of the following terms (which includes terms linked to the incoming long-wave radiation coming form the atmosphere and the infra-red radiation emitted by the canopy and the bare soil respectively): direct incoming long-wave radiation, reflected radiation at the top of the canopy, long-wave radiation transmitted to the bare soil, radiation coming from the long-wave radiation reflected on the bare soil surface, the same one reflected at the bottom of the canopy, and the same one transmitted to the atmosphere through the canopy. The infra-red radiation emitted by the canopy itself must also be added. This radiation is emitted in two directions: the atmosphere and the bare soil surface where it can be reflected. This reflected radiation is then received by the canopy and one part is reflected towards the soil surface, the other one is transmitted to the atmosphere. The same process is observed for the radiation emitted by the bare soil surface. Therefore, the net long-wave radiation for the canopy reads:

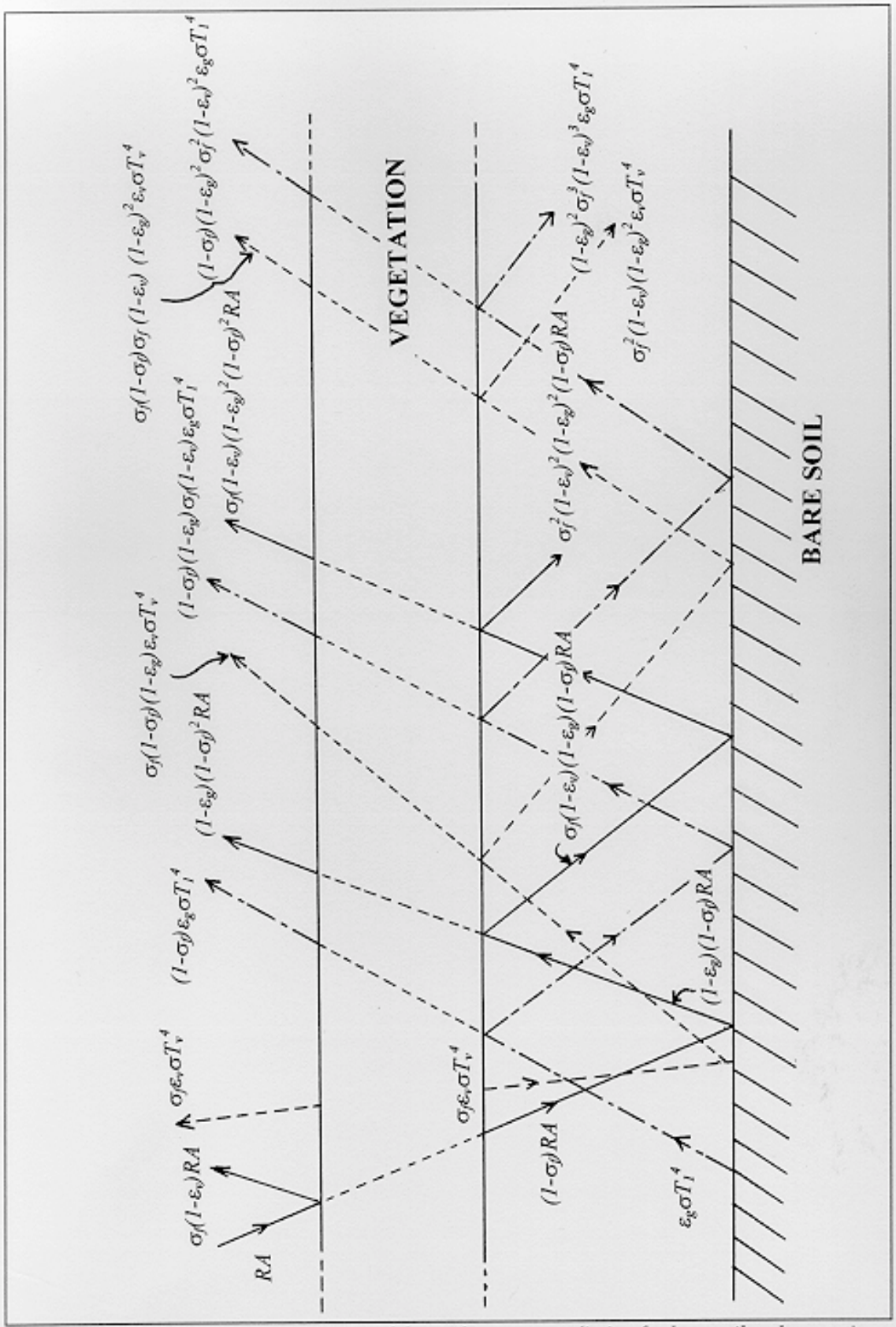


*Fig. 6: Scheme of the various components of the net long-wave radiation for bare soil and vegetation.*

$$
\begin{aligned}
RA_v = {} & RA - \sigma_f(1-\varepsilon_v)RA - (1-\sigma_f)RA + \sum_{n=1}^{\infty}(1-\sigma_f)RA(1-\varepsilon_g)^n(\sigma_f)^{n-1}(1-\varepsilon_v)^{n-1} \\
& - \sum_{n=1}^{\infty}(1-\sigma_f)RA(1-\varepsilon_g)^n(\sigma_f)^n(1-\varepsilon_v)^n - \sum_{n=1}^{\infty}(1-\sigma_f)^2 RA(1-\varepsilon_g)^n(\sigma_f)^{n-1}(1-\varepsilon_v)^{n-1} \\
& - \sigma_f\varepsilon_v\sigma T_v^4 - \sigma_f\varepsilon_v\sigma T_v^4 + \sum_{n=1}^{\infty}\sigma_f\varepsilon_v\sigma T_v^4(1-\varepsilon_g)^n(\sigma_f)^{n-1}(1-\varepsilon_v)^{n-1} \\
& - \sum_{n=1}^{\infty}\sigma_f\varepsilon_v\sigma T_v^4(1-\varepsilon_g)^n(\sigma_f)^n(1-\varepsilon_v)^n - \sum_{n=1}^{\infty}\sigma_f\varepsilon_v\sigma T_v^4(1-\sigma_f)(1-\varepsilon_g)^n(\sigma_f)^{n-1}(1-\varepsilon_v)^{n-1} \\
& + \varepsilon_g\sigma T_1^4 - \sum_{n=1}^{\infty}\varepsilon_g\sigma T_1^4(1-\varepsilon_g)^{n-1}(\sigma_f)^n(1-\varepsilon_v)^n - (1-\sigma_f)\varepsilon_g\sigma T_1^4 \\
& + \sum_{n=1}^{\infty}\varepsilon_g\sigma T_1^4(1-\varepsilon_g)^n(\sigma_f)^n(1-\varepsilon_v)^n - \sum_{n=1}^{\infty}\varepsilon_g\sigma T_1^4(1-\sigma_f)(1-\varepsilon_g)^n(\sigma_f)^n(1-\varepsilon_v)^n
\end{aligned}
\tag{3.4a}
$$

which leads to:

$$
RA_v = \sigma_f\left(\varepsilon_v\left(RA - \sigma T_v^4\right) + \frac{\varepsilon_v\varepsilon_g\sigma\left(T_1^4 - T_v^4\right) + (1-\sigma_f)(1-\varepsilon_g)\varepsilon_v\left(RA - \sigma T_v^4\right)}{1-\sigma_f(1-\varepsilon_v)(1-\varepsilon_g)}\right) \tag{3.4b}
$$

iv) <u>The net long-wave radiation for the bare soil</u> surface can be obtained in a similar way. It is the sum of the direct atmospheric long-wave radiation transmitted to the bare soil by the canopy, the same term reflected by the soil surface and once again this term reflected at the bottom of the canopy towards the soil surface. The long-wave radiation emitted at the bottom of the canopy is received and then reflected at the soil surface. The long-wave radiation emitted by the soil surface is reflected at the bottom of the canopy, then received by the soil surface and reflected again. The net long-wave for the bare soil surface can therefore be written:

$$
\begin{aligned}
RA_g = {} & (1-\sigma_f)RA - \sum_{n=1}^{\infty}(1-\sigma_f)RA(1-\varepsilon_g)^n(\sigma_f)^{n-1}(1-\varepsilon_v)^{n-1} \\
& + \sum_{n=1}^{\infty}(1-\sigma_f)RA(1-\varepsilon_g)^n(\sigma_f)^n(1-\varepsilon_v)^n \\
& + \sigma_f\varepsilon_v\sigma T_v^4 - \sum_{n=1}^{\infty}\sigma_f\varepsilon_v\sigma T_v^4(1-\varepsilon_g)^n(\sigma_f)^{n-1}(1-\varepsilon_v)^{n-1} \\
& + \sum_{n=1}^{\infty}\sigma_f\varepsilon_v\sigma T_v^4(1-\varepsilon_g)^n(\sigma_f)^n(1-\varepsilon_v)^n \\
& - \varepsilon_g\sigma T_1^4 + \sum_{n=1}^{\infty}\varepsilon_g\sigma T_1^4(1-\varepsilon_g)^{n-1}(\sigma_f)^n(1-\varepsilon_v)^n \\
& - \sum_{n=1}^{\infty}\varepsilon_g\sigma T_1^4(1-\varepsilon_g)^n(\sigma_f)^n(1-\varepsilon_v)^n
\end{aligned}
\tag{3.5a}
$$

which can be simplified as:

$$RA_g = \frac{\left(1-\sigma_f\right)\varepsilon_g\left(RA-\sigma T_1^4\right)-\varepsilon_g\varepsilon_v\sigma_f\sigma\left(T_1^4-T_v^4\right)}{1-\sigma_f\left(1-\varepsilon_v\right)\left(1-\varepsilon_g\right)} \quad (3.5b)$$

The net radiation for the vegetation and the bare soil surface respectively are given by:

$$Rn_v = RG_v + RA_v \quad (3.6a)$$

$$Rn_g = RG_g + RA_g \quad (3.6b)$$

and the net radiation for the whole system *Rn* is the sum of the contribution of the canopy and of the bare soil:

$$Rn = Rn_v + Rn_g \quad (3.7)$$

Net radiation is often measured and can serve as a validation variable for the model. Two additional variables can be calculated and compared to possible measurements: the total albedo, $\alpha_{tot}$ (-) of the system (or total reflected solar radiation $RG_r$ (W $m^{-2}$)) and the radiative surface temperature $T_{rad}$ (K).

The total reflected solar radiation is equal to :

$$RG_r = \sigma_f\alpha_v RG + \sum_{n=1}^{\infty}\left(\alpha_g\right)^n\left(\sigma_f\alpha_f\right)^{n-1}\left(1-\sigma_f\right)^2 RG \quad (3.8)$$

which can be simplified as follows:

$$RG_r = RG\left[\sigma_f\alpha_v + \frac{\alpha_g\left(1-\sigma_f\right)^2}{1-\sigma_f\alpha_v\alpha_g}\right] \quad (3.9)$$

The total simulated albedo is therefore given by:

$$\alpha_{tot} = \sigma_f\alpha_v + \frac{\alpha_g\left(1-\sigma_f\right)^2}{1-\sigma_f\alpha_v\alpha_g} \quad (3.10)$$

A global radiative surface temperature is calculated as:

$$T_{rad} = \left[\left(RA - RA_v - RA_g\right)/\sigma\right]^{0.25} \quad (3.11)$$

The vegetation albedo and emissivity are input parameters and are assumed to be constant in time.

For the bare soil albedo, three options are proposed into the model:

- *ialphas=0*: The bare soil albedo is constant in time.
- *ialphas=1*: The bare soil albedo depends on the surface soil moisture $\theta_1$ through a function derived from Passerat de Silans (1986).

$$\begin{cases} \alpha_g = \alpha_{g0} & \theta \geq \theta_{\lim 0} \\ \alpha_g = coef1\left(1-\frac{\theta_1}{\varepsilon}\right)+coef2\left(\frac{\theta_1}{\varepsilon}\right) & \theta \leq \theta_{\lim} \\ \alpha_g = coef3 & \theta_{\lim} \leq \theta \leq \theta_{sat} \end{cases} \quad (3.12a)$$

where $\theta_{\lim} = \varepsilon \frac{(coef1 - coef3)}{(coef1 - coef2)}$ (3.12b)

and $\alpha_{g0} = coef1\left(1-\frac{\theta_{lim0}}{\varepsilon}\right)+coef2\left(\frac{\theta_{lim0}}{\varepsilon}\right)$ (3.12c)

to ensure continuity of the function.

- *ialphas=2*: The bare soil albedo is calculated as a function of the total albedo, vegetation albedo and shielding factor. This ensures that the total reflected solar radiation is equal to the measured one. In this case, total measured albedo can be interpolated in time, like the vegetation height or the *LAI*.

$$\alpha_g = \frac{\alpha_{tot} - \sigma_f \alpha_v}{(1-\sigma_f)^2 + \sigma_f \alpha_v \alpha_g - (\sigma_f \alpha_v)^2} \quad (3.13)$$

Bare soil and vegetation albedos are corrected for the position of the solar angle (Dantas-Antonino, 1992). The solar angle is practically calculated using a package of astronomic routines borrowed from the ARPEGE mesoscale meteorological model of METEO-FRANCE.

For the bare soil emissivity, two options are proposed within the model:

- *iemiss=0*: The bare soil emissivity is constant in time.
- *iemiss=1*: The bare soil emissivity depends on soil surface humidity.

$$\varepsilon_g = 0.9 + 0.18\theta_1 \quad (3.14)$$

3.2.2. *Expression of turbulent fluxes of momentum, heat and water vapor*.

The interface allows for the coupling between the soil and the atmospheric compartments. It is similar to the model proposed by Taconet et al. (1986) and it follows Deardorff (1978) formalism, where the vegetation is also modelled as a single layer. The solution of the interface allows for the separate calculation of the soil and canopy temperature and of the heat and mass fluxes from the bare soil and the vegetation.

Characteristic atmospheric variables are defined at a reference level $z_a$, typically located at 2 m above the canopy. Vegetation is modelled as a single layer situated at an artificial level $z_{av}$ above the ground (Fig. 4), characterised by air temperature $T_{av}$, specific humidity $q_{av}$ and wind speed $U_{av}$. As

defined by Thom (1972), $U_{av}$ is the mean velocity within the canopy which leads to the same drag coefficient as the real profile.

Following Thom (1971, 1972) and Taconet et al. (1986), turbulent fluxes above the canopy are expressed as:

$$\tau = -\rho_a u^{*2} = -\rho_a (U_a - U_{av}) / R_{aM} \quad \text{for momentum transfer} \quad (3.15a)$$

$$E = -\rho_a (q_a - q_{av}) / R_{aV} \quad \text{for vapour transfer} \quad (3.15b)$$

$$H = -\rho_a c_p (T_a - T_{av}) / R_{aH} \quad \text{for heat transfer} \quad (3.15c)$$

The partition of the momentum flux between the ground $\tau_g$ and the canopy $\tau_v$, is made through a coefficient $\sigma_a$ expressed as a function of the leaf area index (Shaw and Pereira, 1981; Taconet et al., 1986):

$$\sigma_a = 1 - \frac{0.5}{0.5 + LAI} \exp\left(\frac{-LAI^2}{8}\right) \quad (3.16)$$

Thus, momentum fluxes expressed in terms of resistances take the following form:

$$\tau_v = \sigma_a \tau = -\rho_a U_{av} / R_{vM} \quad (3.17a)$$

$$\tau_g = (1 - \sigma_a)\tau = -\rho_a U_{av} / R_{gM} \quad (3.17b)$$

$$\tau = \tau_g + \tau_v = -\rho_a (U_a - U_{av}) / R_{aM} \quad (3.17c)$$

The sensible heat fluxes from the ground and the canopy $H_g$ and $H_v$ are expressed as:

$$H_g = -\rho_a c_p (T_{av} - T_1) / R_{gH} \quad (3.18a)$$

$$H_v = -\rho_a c_p (T_{av} - T_v) / R_{vH} \quad (3.18b)$$

For latent heat flux, the contributions of the bare soil and of the canopy are (kg $m^{-2}$ $s^{-1}$) respectively:

$$E_g = -\rho_a (q_{av} - q_1) / R_{gV} \quad (3.19a)$$

$$E_v = -\rho_a \left(\frac{\delta}{R_{vV}} + \frac{(1-\delta)}{R_{vV} + R_{sto}}\right)\left(q_{av} - q_{sat}(T_v)\right) \quad (3.19b)$$

where $\delta$ is the wet fraction of the canopy. Therefore, the term $E_v$ includes both evaporation from the wet canopy $E_w$ and the transpiration $T_r$ respectively given by:

$$E_w = -\rho_a \frac{\left(q_{av} - q_{sat}(T_v)\right)}{R_{vV}} \delta \quad (3.20a)$$

$$T_r = -\rho_a \frac{\left(q_{av} - q_{sat}(T_v)\right)}{R_{vV} + R_{sto}} (1 - \delta) \quad (3.20b)$$

with $$E_v = E_w + T_r \quad (3.20c)$$

The specific humidity at the surface $q_1$ (kg kg$^{-1}$) is related to the soil surface temperature $T_1$ (K) and the relative humidity at the surface $h_u$ (-) by:

$$q_1 = \frac{0.622\, e_{sat}(T_1)\, h_u}{p_{atm} - 0.378\, e_{sat}(T_1)\, h_u} \tag{3.21}$$

The use of Kelvin's law:

$$h_u = \exp\left(\frac{g h_1}{R T_1}\right) \tag{3.22}$$

partly realises the coupling between the soil compartment and the interface.

The wet fraction of the canopy $\delta$ is defined following Deardorff (1978) as:

$$\delta = \left(W_r / W_{r\max}\right)^{2/3} \qquad 0 \le \delta \le 1 \tag{3.23}$$

where $W_r$ is the actual amount of water intercepted by the foliage (m). Its time evolution is expressed (Noilhan and Planton, 1989) as:

$$\frac{\partial W_r}{\partial t} = \left(P - P_g\right) - \frac{E_w}{\rho_w} \qquad W_r \le W_{r\max} \tag{3.24}$$

where $P$ and $Pg$ are the rainfall intensity (m s$^{-1}$) above the canopy and reaching the ground (throughfall), respectively. The evaporation from the canopy $E_w$ accounts for evaporation from the wet canopy if positive and dew deposition if negative. In Eq. (3.23) and (3.24), $W_{rmax}$ is the maximum capacity of the interception reservoir (m) and is given by Noilhan and Planton (1989):

$$W_{r\max} = 2.10^{-4}\, \sigma_f\, LAI \tag{3.25}$$

Finally, the soil-plant-interface module can be summarised as a non-linear system of five equations with five unkowns: surface matric potential $h_1$ and surface temperature $T_1$, canopy specific humidity and temperature $q_{av}$ and $T_{av}$ and leaf temperature $T_v$. These five equations are the energy budget of the canopy, the energy budget of the underlying bare soil, the continuity of the heat and vapour fluxes through the canopy and the continuity equation for the water transfer through the soil surface:

$$Rn_g = H_g + L_v E_g + G \tag{3.26a}$$

$$Rn_v = H_v + L_v E_v \tag{3.26b}$$

$$H = H_g + H_v \tag{3.26c}$$

$$E = E_g + E_v \tag{3.26d}$$

$$E_g + Q_{mg} - P_g \rho_w = 0 \tag{3.26e}$$

In Eq. (3.26a), $G$ is the surface soil heat flux expressed as a function of $h_1$ and $T_1$, using the soil compartment equations:

$$G = -\left( D_{ch}(h_1, T_1)\left(\frac{\partial h}{\partial z}\right)_{z=0} + D_{cT}(h_1, T_1)\left(\frac{\partial T}{\partial z}\right)_{z=0} \right) \tag{3.27}$$

and in Eq. (3.26e), $Q_{mg}$ is the Darcian nonisothermal mass flow crossing the soil surface:

$$Q_{mg} = -\rho_w \left( D_{mh}(h_1, T_1)\left(\frac{\partial h}{\partial z}\right)_{z=0} + D_{mT}(h_1, T_1)\left(\frac{\partial T}{\partial z}\right)_{z=0} - K(h_1, T_1) \right) \tag{3.28}$$

This non-linear system was initially solved using a Gauss-Newton-Raphson algorithm, but computing times were quite large. All the equations have been linearised and the procedure will be described in section 3.3.

### 3.2.3. *Expression of aerodynamic and canopy resistances.*

In SiSPAT, two types of resistances can be used. The first set of resistances (*iresaero=0*) is derived from the ″empirical″ approach of Thom (1972) and Taconet et al. (1986). The second set of possible resistances (*iresaero=1*) is derived from the approach of Shuttleworth and Wallace (1985), and formulae are directly taken from the SWEAT (Soil Water and Energy and Transpiration) model described by Daamen and Simmonds (1994).

Both formulations require the definition of the displacement height $d$ (m) and the roughness length for momentum $z_{om}$ (m). Three options for this derivation are proposed into the model:

- *idzom=0*: Constant values are used for the whole simulation.
- *idzom=1*: Formulae proposed by Brutsaert (1982) are used:

$$d = 0.63 z_v \tag{3.29}$$

$$z_{om} = 0.13 z_v \tag{3.30}$$

- *idzom=2*: The displacement height $d$ and the roughness length for momentum $z_{om}$ are calculated using Shaw and Pereira (1981) formulae with a drag coefficient equal to 0.07.

$$d = 1.1 z_v Log\left[1 + (0.07 LAI)^{0.25}\right] \tag{3.31}$$

$$z_{om} = z_{om}^{g} + 0.3 z_v (0.07 LAI)^{0.5} \quad LAI \le 2.85$$
$$z_{om} = 0.3 z_v \left(1 - \frac{d}{z_v}\right) \qquad LAI > 2.85 \tag{3.32}$$

where $z_{om}^{g} = 0.001$ m is the roughness length for momentum associated with the bare soil.

#### 3.2.3.1. Resistances derived from Thom (1972) and Taconet el al. (1986) (*iresaero=0*).

For the determination of the aerodynamic resistances, it is assumed that both wind speed and temperature profiles above the canopy are logarithmic and given by:

$$U_a(z_a) = \frac{u*}{k}\left( Log\left( \frac{z_a - d}{z_{om}} \right) - \Psi_m\left( \frac{z_a - d}{L} \right) \right) \quad (3.33)$$

$$T_a(z_a) - T_{av} = \frac{\theta*}{k}\left( Log\left( \frac{z_a - d}{z_{oh}} \right) - \Psi_h\left( \frac{z_a - d}{L} \right) \right) \quad (3.34)$$

where $u*$ is the friction velocity, $\theta*$ a characteristic temperature, $d$ is the displacement heigth, $z_{om}$ the roughness length for momentum and $z_{oh}$ the roughness length for heat. It is assumed that roughness lengths for heat and vapour ($z_{oh}$ and $z_{ov}$ respectively) are equal, as well as the corresponding integrated stability functions $\Psi_h$ and $\Psi_v$. $L$ is the Monin-Obukhov (1954) length given by:

$$L = \frac{u*^3 \overline{T}}{gk\left( \frac{-H}{\rho c_p} \right)} = \frac{u*^2 \overline{T}}{gk\theta*} \quad (3.35)$$

where $\overline{T} = \left(T_a + T_{av}\right)/2$ is a mean temperature between levels $z_a$ and $z_{av}$.

From Thom (1972), levels $d+z_{om}$ and $d+z_{oh}$ can be seen as virtual source or sink for momentum and heat (or vapour) respectively. $d+z_{oh}$ is assumed to be equal to the canopy level $z_{av}$. Two options relating the roughness lengths for momentum $z_{om}$ and heat $z_{oh}$ are proposed within the model:

- *izoh=0*: A constant value of the ratio $z_{om}/z_{oh}$ is used.
- *izoh=1*: The roughness lengths for heat and momentum depend on the friction velocity $u*$ (m $s^{-1}$) and is given by (Brutsaert, 1982):

$$z_{oh} = z_{om} \exp\left[ -\left( 2.46\left( \frac{u* z_{om}}{\nu} \right)^{0.25} - 2 \right) \right] \quad \text{for a canopy} \quad (3.36)$$

and $$z_{oh} = 7.4 z_{om} \exp\left[ -\left( 2.46\left( \frac{u* z_{om}}{\nu} \right)^{0.25} \right) \right] \quad \text{for bare soil} \quad (3.37)$$

where $\nu$=1.46 $10^{-5}$ $m^2$ $s^{-1}$ is the kinematic velocity.
Eq. (3.36) was shown to give the best agreement between measurements and theory over several data set (Verhoef et al., 1997).

The functions $\Psi_m$ and $\Psi_h$ allow to take the thermal stratification of the atmosphere into account. Paulson (1970) stability functions are used, except for the stable case where Beljars and Holtstag (1991) modification was implemented

$$\Psi_m(y) = 2Log(a) + Log(b) - 2Arc\tan(x) + \frac{\pi}{2} \qquad y \le 0 \quad (3.38a)$$

where $\begin{cases} x = (1-16y)^{1/4} \\ a = \dfrac{1+x}{2} \\ b = \dfrac{1+x^2}{2} \end{cases}$

$$\psi_m(y) = -\left[0.7y + 0.75\left(y - \frac{5}{0.35}\right)exp(-0.35y) + \frac{3.75}{0.35}\right] \quad y \geq 0 \text{ (3.38b)}$$

and $$\Psi_h(y) = 2Log(a) \qquad y \leq 0 \qquad \text{(3.39a)}$$

where $\begin{cases} x = (1-16y)^{1/4} \\ a = \dfrac{1+x}{2} \end{cases}$

$$\psi_h(y) = -\left[\left(1+\frac{2}{3}y\right)^{1.5} + 0.667\left(y - \frac{5}{0.35}\right)exp(-0.35y) + \frac{3.335}{0.35} - 1\right] \quad y \geq 0 \text{ (3.39b)}$$

An iterative procedure derived from Itier (1980) is used to calculate $u^*$, $\theta^*$ and $L$ from (3.33), (3.34) and (3.35) using the wind speed and air temperature at the reference level (forcing variables) and canopy temperature $T_{av}$. A minimum value of the wind speed difference (resp. air temperature difference) are imposed and are equal to 0.01 m $s^{-1}$ for wind speed (resp. 0.05 °C for air temperature). Note that in standard meteorological network, temperature is measured at 2 m whereas wind speed is measured at 10 m. It is taken into account into the code, where the heights of measurements for the air temperature and wind speed must be specified and can be different. When there is no canopy (pure bare soil), $T_{av}$ is replaced by $T_1$ in (3.34) and the same iterative procedure is used.

When $u^*$, $\theta^*$ and $L$ have been calculated, the canopy wind speed is obtained through (Thom, 1972):

$$U_{av} = u^*\left(\frac{\sigma_a 9 p_d}{\beta LAI}\right)^{1/2} \qquad \text{(3.40)}$$

where $p_d = 2$ for $LAI \leq 2$ and $p_d = LAI/2+1$ otherwise, is an empirical aerodynamic shelter factor introduced by Thom (1971) and $\beta = 1.1$ allows for the participation of non-foliage elements such as stems.

The aerodynamic resistance for momentum between the atmosphere and the canopy is obtained from (3.15a):

$$R_{aM} = \frac{U_a - U_{av}}{u*^2} \tag{3.41}$$

The aerodynamic resistance for heat and water vapour are assumed to be the same and are deduced from (3.15c, 3.34 and 3.35):

$$R_{aH} = \frac{\left( Log\left( \frac{z_a - d}{z_{oh}} \right) - \Psi_h\left( \frac{z_a - d}{L} \right) \right)}{ku*} \tag{3.42}$$

The aerodynamic resistance $R_{vM}$ controls the exchanges between the canopy and the air within the canopy. From Taconet (1987), it can be expressed as a function of the wind speed within the canopy $U_{av}$, and *LAI*:

$$R_{vM} = \frac{9 p_d}{U_{av}\, \beta\, LAI} \tag{3.43}$$

The aerodynamic resistance $R_{gM}$, which controls momentum transfer between the soil surface and the air within the canopy, is deduced from (3.15) and (3.17):

$$R_{gM} = \frac{U_{av}}{(1 - \sigma_a)(u*)^2} \tag{3.44}$$

For the canopy resistances, $R_{gH}$ is assumed to be the same as $R_{gM}$. $R_{vH}$ is modelled as a function of $U_{av}$ and *LAI* by considering that heat and mass transfers within the canopy are less effective than momentum transfer. Following Taconet et al. (1986), it may be written:

$$R_{vH} = \frac{28 p_d}{U_{av}\, \beta\, LAI} \tag{3.45}$$

The aerodynamic resistance for vapour $R_{gV}$ is assumed to be equal to that for heat $R_{gH}$. In Eqs. (3.19b) and (3.20b), $R_{sto}$ is the stomatal resistance, which will be discussed below. In Eqs. (3.19) and (3.20), the aerodynamic resistance to vapour flow is related to the resistance to heat flow $R_{vH}$ by:

$$R_{vH} = \beta R_{vV} \tag{3.46}$$

3.2.3.2. Resistances derived from the Shuttleworth and Wallace (1985) approach (*iresaero=1*).

This option is only available in case of a vegetated surface, whereas the previous one also works in case of bare soil. Details can be found in Daamen and Simmonds (1994) from which this module was borrowed. The aerodynamic resistance is defined in neutral conditions by:

$$R_{aH}^{n} = \frac{\left( Log(\frac{z_a - d}{z_{om}}) \right)^2}{k^2 U_a} \tag{3.47}$$

A stability parameter which allows to take the stratification of the atmosphere into account is defined as follows:

$$Stab = 5g \frac{(z_a - d)(T_{av} - T_a)}{T_a U_a^2} \tag{3.48}$$

and the aerodynamic resistance for heat and vapour is corrected as follows:

$$\begin{aligned} R_{aH} &= R_{aV} = \frac{R_{aH}^{n}}{(1 + Stab)^2} \qquad Stab \le 0 \\ R_{aH} &= R_{aV} = R_{aH}^{n} (1 + Stab)^{-0.75} \qquad Stab \ge 0 \end{aligned} \tag{3.49}$$

canopy resistances are calculated following Shuttleworth and Wallace (1985). The aerodynamic resistance between the bare soil and the canopy level is defined as the integral of the eddy diffusion coefficient, which is assumed to exhibit an exponential decay within the canopy, between levels $z_{om}^{g}$ and $z_v+d$.

$$R_{gH} = R_{gV} = z_v \exp(n_{SW}) \frac{\exp\left( -\frac{n_{SW} z_{om}^{g}}{z_v} \right) - \exp\left( -\frac{n_{SW}(d + z_{om})}{z_v} \right)}{n_{SW} k^2 U_a \frac{z_v - d}{Log\left( \frac{z_a - d}{z_{om}} \right)}} \tag{3.50}$$

The canopy resistance between the vegetation and the canopy level is obtained as follows:

$$R_{vH} = R_{vV} = n_{SW} \left( \frac{w}{U_a(z_v)} \right)^{1/2} \frac{1}{4\alpha_o LAI\left(1 - \exp\left(-n_{SW} / 2\right)\right)} \tag{3.51}$$

where $U_a(z_v) = U_a \dfrac{Log\left( \frac{z_v - d}{z_{om}} \right)}{Log\left( \frac{z_a - d}{z_{om}} \right)}$ is the wind speed at the top of the canopy, $w$=0.01 m is the width of the leaves, $n_{SW}$=2.5, $\alpha_o$=0.005 and $z_{om}^{g}$=0.001m is the roughness length for momentum associated with the bare soil.

*3.2.4. Stomatal resistance model.*

To complete the description of the interface, the stomatal resistance, introduced in Eq. (3.20), must be defined. Environmental factors control the degree of stomatal opening. The activity of the stomata is summarized into the stomatal resistance which depends on three factors in the SiSPAT model: incoming solar radiation, vapor pressure deficit and available water at the root level. A dependence on temperature is sometimes taken into account (Jarvis, 1976; Sellers et al., 1986, for example), but is often neglected for small vegetation (Noilhan and Planton, 1989). Thus, the stomatal resistance for the canopy has been expressed as:

$$R_{sto} = R_{st\,\min} \frac{f_{RG}(RG) f_{h_f}(h_f) f_{VPD}(VPD)}{LAI} \tag{3.52}$$

In Eq. (3.52), $R_{stmin}$ is the minimum stomatal resistance corresponding to no radiative and soil water stress conditions. The factor $f_{RG}$ accounts for the influence of the photosynthetically active radiation (Sellers et al., 1986). Following Noilhan and Planton (1989), it has been taken as:

$$f_{RG}(RG) = \frac{1+f}{f + R_{st\,\min}/R_{st\,\max}} \qquad with \quad f = 0.55 \frac{RG}{RG_L} \frac{2}{LAI} \tag{3.53}$$

where $RG_L$=100Wm$^{-2}$ for crop.

Following Béguet et al. (1994), the function of the Vapour Pressure Deficit *VPD* reads:

$$f_{VPD}(VPD) = 1 + \mu VPD \tag{3.54}$$

where $\mu$ is a parameter which controls the increase of the stomatal resistance when the *VPD* increases. A typical value for $\mu$ is 2.5 10$^{-4}$ Pa$^{-1}$.

The $f_{hf}$ factor describes soil water stress influence. Some authors express it as a function of the soil water content (Deardorff, 1978; Taconet et al., 1986; Noilhan and Planton, 1989 for example). In this study, the leaf water potential $h_f$ (m), also used by Sellers et al. (1986), Van de Griend and Van Boxel (1989) or Lynn and Carlson (1990) has been retained. The main reason for this choice is that $h_f$ is an output of the soil-plant-interface modelling as will be shown in chapter 4. The general form proposed by Campbell (1985) and cited by Flerchinger and Pierson (1991) was used, with the value 5.5 fitted by Choudhury and Idso (1985) for the exponent:

$$f_{hf}(h_f) = 1 + \left( \frac{h_f}{h_{fc}} \right)^{5.5} \tag{3.55}$$

The $h_{fc}$ parameter is the critical leaf water potential. When $|h_f| > |h_{fc}|$, the stomatal resistance increases very rapidly, reducing considerably the transpiration. Typically $h_{fc}$ may vary between -100 m and -150 m of water.

## 3.3. Numerical solution.

In the initial version of the model, the non-linear system of five equations with five unknowns defined by (3.26) was solved iteratively using the Newton-Raphson algorithm. This solution was very much time consuming and was preventing the use of the model for long term studies. A more efficient solution, based on a linearisation of the system was thus proposed and is described below. Computing times were reduced by a factor of two and the accuracy of the numerical solution remains satisfactory, as long as the time step remains quite small (< 200s).

### *3.3.1. Linearisation of the non-linear terms.*

In (3.26), the non-linear terms depending of one or several unknowns ($T_1$, $T_v$, $T_{av}$, $q_{av}$ and $h_1$) are the $T_v^4$, $T_1^4$, $q_{sat}(T_v)$, $q_1$ and the products $L_v(T_1)E_g$, $L_v(T_{av})E$, $L_v(T_v)E_v$ because the dependence of the latent heat of vaporisation on temperature is taken into account (in this case second order terms of the linearised expressions are neglected). Values of the variables at time *t* and *t-1* will be denoted by subscripts $^{i}$ and $^{i-1}$ respectively. The linearisation of the various terms mentioned above is given below.

$$(T_1^4)^i = \left(T_1^4\right)^{i-1} + 4\left(T_1^3\right)^{i-1}\left(T_1^i - T_1^{i-1}\right) \tag{3.56}$$

$$(T_v^4)^i = \left(T_v^4\right)^{i-1} + 4\left(T_v^3\right)^{i-1}\left(T_v^i - T_v^{i-1}\right) \tag{3.57}$$

$$(q_{sat}(T_v))^i = \left(q_{sat}(T_v)\right)^{i-1} + \left(\frac{\partial q_{sat}}{\partial T_v}(T_v)\right)^{i-1}\left(T_v^i - T_v^{i-1}\right) \tag{3.58a}$$

with

$$q_{sat}(T_v) = 0.622 e_{sat}(T_v)\frac{1}{p_{atm} - 0.378 e_{sat}(T_v)} \tag{3.58b}$$

$$e_{sat}(T_v) = 618.78 \exp\left(17.269\frac{T_v - 273.16}{T_v - 35.86}\right) \tag{3.58c}$$

$$\frac{\partial q_{sat}}{\partial T_v}(T_v) = 0.622\, p_{atm}\frac{\partial e_{sat}}{\partial T_v}(T_v)\frac{1}{\left(p_{atm} - 0.378 e_{sat}(T_v)\right)^2} \tag{3.58d}$$

$$\frac{\partial e_{sat}}{\partial T_v}(T_v) = \frac{4097.93 e_{sat}(T_v)}{\left(T_v - 35.86\right)^2} \tag{3.58e}$$

$$(q_1)^i = (q_1)^{i-1} + \left(\frac{\partial q_1}{\partial T_1}(T_1, h_1)\right)^{i-1}\left(T_1^i - T_1^{i-1}\right) + \left(\frac{\partial q_1}{\partial h_1}(T_1, h_1)\right)^{i-1}\left(h_1^i - h_1^{i-1}\right) \tag{3.59a}$$

with $$q_1 = \frac{0.622 \exp\left(\frac{gh_1}{RT_1}\right) e_{sat}(T_1)}{p_{atm} - 0.378 \exp\left(\frac{gh_1}{RT_1}\right) e_{sat}(T_1)} \quad (3.59b)$$

$$\frac{\partial q_1}{\partial T_1}(T_1, h_1) = 0.622\, p_{atm} \frac{-\frac{gh_1}{RT_1^2} \exp\left(\frac{gh_1}{RT_1}\right) e_{sat}(T_1) + \exp\left(\frac{gh_1}{RT_1}\right) \frac{\partial e_{sat}}{\partial T_1}(T_1)}{\left(p_{atm} - 0.378 \exp\left(\frac{gh_1}{RT_1}\right) e_{sat}(T_1)\right)^2} \quad (3.59c)$$

$$\frac{\partial q_1}{\partial h_1}(T_1, h_1) = q_1 p_{atm} \frac{\frac{g}{RT_1}}{\left(p_{atm} - 0.378 \exp\left(\frac{gh_1}{RT_1}\right) e_{sat}(T_1)\right)} \quad (3.59d)$$

$$\left(L_v(T_1) E_g\right)^i = \frac{\rho_a}{R_{gV}} \left( \left(L_v(T_1)\right)^{i-1} \left(q_1^i - q_{av}^i\right) + B\left(T_1^i - T_1^{i-1}\right)\left(q_1^{i-1} - q_{av}^{i-1}\right) \right) \quad (3.60)$$

$$\left(L_v(T_v) E_v\right)^i = \rho_a \left( \frac{\delta}{R_{vV}} + \frac{(1-\delta)}{R_{vV} + R_{sto}} \right) \begin{pmatrix} \left(L_v(T_v)\right)^{i-1} \left( q_{sat}(T_v)\right)^i - q_{av}^i \\ + B\left(T_v^i - T_v^{i-1}\right)\left( q_{sat}(T_v)\right)^{i-1} - q_{av}^{i-1} \end{pmatrix} \quad (3.61)$$

$$\left(L_v(T_{av}) E\right)^i = \frac{\rho_a}{R_{aV}} \left( \left(L_v(T_{av})\right)^{i-1} \left(q_{av}^i - q_a\right) + B\left(T_{av}^i - T_{av}^{i-1}\right)\left(q_{av}^{i-1} - q_a\right) \right) \quad (3.62c)$$

where $$L_v(T) = A + BT \quad (3.62d)$$

with $A$=3.148735 $10^6$ Jkg$^{-1}$ and $B$=-2372 Jkg$^{-1}$ K$^{-1}$.

*3.3.2. Final linear system obtained (vegetation case).*

The non-linear system (3.26) can be rewritten in the following matrix form:

$$[C][Y] = [D] \quad (3.63)$$

where the vector of the unknowns is $Y = \begin{bmatrix} T_1 \\ T_v \\ T_{av} \\ q_{av} \\ h_1 \end{bmatrix}$ and the equations are listed in the following order:

energy budget over the bare soil, energy budget over the canopy, continuity of the heat and water vapor fluxes through the canopy and mass conservation at the surface (see 3.64);

$$Rn_g - H_g - L_v E_g - G = 0 \quad (3.64a)$$

$$Rn_v - H_v - L_v E_v = 0 \quad (3.64b)$$

$$H - H_g - H_v = 0 \quad (3.64c)$$

$$E - E_g - E_v = 0 \tag{3.64d}$$

$$E_g + Q_{mg} - P_g \rho_w = 0 \tag{3.64e}$$

The coefficients of the $[C]$ and $[D]$ matrices are listed below. Subscripts $^{i-1}$ have been omitted for all the variables, but it is implicit below that the coefficients of those matrices are calculated at the previous time step (explicit linearisation). There are however two exceptions: the values of $h_2$ and $T_2$, the values of the matric potential and temperature at node 2 are the values at time $t^i$ (see also chapter 5) and of course the values of the forcing variable are also taken at time $t^i$.

$$c_{11} = 4c_{ng}\sigma T_1^3 - \frac{\rho_a c_p}{R_{gH}} - \frac{\rho_a}{R_{gV}} L_v(T_1)\frac{\partial q_1}{\partial T_1}(T_1, h_1) - \frac{\rho_a}{R_{gV}} B(q_1 - q_{av}) - \frac{D_{cT1+1/2}}{dz_1} - \frac{C_{T1}\Delta z_1}{\Delta t} \tag{3.65a}$$

$$c_{12} = 4b_{ng}\sigma T_v^3 \tag{3.65b}$$

$$c_{13} = \frac{\rho_a c_p}{R_{gH}} \tag{3.65c}$$

$$c_{14} = \frac{\rho_a}{R_{gV}} L_v(T_1) \tag{3.65d}$$

$$c_{15} = -\frac{\rho_a}{R_{gV}} L_v(T_1)\frac{\partial q_1}{\partial h_1}(T_1, h_{11}) - \frac{D_{ch1+1/2}}{dz_1} \tag{3.65e}$$

$$\begin{aligned} d_1 = {} & -a_{ng} + 3b_{ng}\sigma T_v^4 + 3c_{ng}\sigma T_1^4 - \frac{D_{cT1+1/2}}{dz_1} T_2 - \frac{C_{T1}\Delta z_1}{\Delta t} T_1 - \frac{D_{ch1+1/2}}{dz_1} h_2 \\ & + \frac{\rho_a}{R_{gV}}\left[ L_v(T_1)\left( q_1 - \frac{\partial q_1}{\partial T_1}(T_1, h_1) T_1 - \frac{\partial q_1}{\partial h_1}(T_1, h_1) h_1 \right) - B T_1 (q_1 - q_{av}) \right] \end{aligned} \tag{3.65f}$$

where

$$a\begin{cases} {}_{ng} = \dfrac{RG(1-\alpha_g)(1-\sigma_f)}{1-\sigma_f \alpha_g \alpha_v} + \dfrac{(1-\sigma_f)\varepsilon_g RA}{1-\sigma_f(1-\varepsilon_v)(1-\varepsilon_g)} \\ b_{ng} = \dfrac{\varepsilon_v \varepsilon_g \sigma_f}{1-\sigma_f(1-\varepsilon_v)(1-\varepsilon_g)} \\ c_{ng} = -\dfrac{(1-\sigma_f)\varepsilon_g + \varepsilon_v \varepsilon_g \sigma_f}{1-\sigma_f(1-\varepsilon_v)(1-\varepsilon_g)} \end{cases} \tag{3.66a}$$

with

$$Rn_g = a_{ng} + b_{ng}\sigma T_v^4 + c_{ng}\sigma T_1^4 \tag{3.66b}$$

$$c_{21} = 4\sigma c_{nv} T_1^3 \tag{3.67a}$$

$$c_{22} = 4b_{nv}\sigma T_v^3 - \frac{\rho_a c_p}{R_{vH}} - \rho_a\left[\frac{\delta}{R_{vV}} + \frac{1-\delta}{R_{vV}+R_{sto}}\right]\left[B\left(q_{sat}(T_v) - q_{av}\right) + L_v(T_v)\frac{\partial q_{sat}}{\partial T_v}(T_v)\right] \quad (3.67b)$$

$$c_{23} = \frac{\rho_a c_p}{R_{vH}} \quad (3.67c)$$

$$c_{24} = \rho_a\left[\frac{\delta}{R_{vV}} + \frac{1-\delta}{R_{vV}+R_{sto}}\right]L_v(T_v) \quad (3.67d)$$

$$c_{25} = 0 \quad (3.67e)$$

$$d_2 = -a_{nv} + 3b_{nv}\sigma T_v^4 + 3c_{nv}\sigma T_1^4$$
$$+\rho_a\left[\frac{\delta}{R_{vV}} + \frac{1-\delta}{R_{vV}+R_{sto}}\right]\left[L_v(T_v)\left(q_{sat}(T_v) - T_v\frac{\partial q_{sat}}{\partial T_v}(T_v)\right) - BT_v\left(q_{sat}(T_v) - q_{av}\right)\right] \quad (3.67f)$$

where

$$\begin{cases} a_{ng} = RG\sigma_f(1-\alpha_v)\left[1 + \dfrac{(1-\sigma_f)\alpha_g}{1-\sigma_f\alpha_g\alpha_v}\right] + \sigma_f\left[\varepsilon_v RA + \dfrac{(1-\sigma_f)\varepsilon_v(1-\varepsilon_g)RA}{1-\sigma_f(1-\varepsilon_v)(1-\varepsilon_g)}\right] \\ b_{ng} = -\sigma_f\left[\varepsilon_v + \dfrac{(1-\sigma_f)(1-\varepsilon_g)\varepsilon_v + \varepsilon_v\varepsilon_g}{1-\sigma_f(1-\varepsilon_v)(1-\varepsilon_g)}\right] \\ c_{ng} = \dfrac{\varepsilon_v\varepsilon_g\sigma_f}{1-\sigma_f(1-\varepsilon_v)(1-\varepsilon_g)} \end{cases} \quad (3.68a)$$

with $$Rn_v = a_{nv} + b_{nv}\sigma T_v^4 + c_{nv}\sigma T_1^4 \quad (3.68b)$$

$$c_{31} = -\frac{c_p}{R_{gH}} \quad (3.69a)$$

$$c_{32} = -\frac{c_p}{R_{vH}} \quad (3.69b)$$

$$c_{33} = c_p\left[\frac{1}{R_{aH}} + \frac{1}{R_{gH}} + \frac{1}{R_{vH}}\right] \quad (3.69c)$$

$$c_{34} = 0 \quad (3.69d)$$

$$c_{35} = 0 \quad (3.69e)$$

$$d_3 = \frac{c_p}{R_{aH}}T_a \quad (3.69f)$$

$$c_{41} = -\frac{L_{vo}}{R_{gV}}\frac{\partial q_1}{\partial T_1}(T_1, h_1) \quad (3.70a)$$

$$c_{42} = -L_{vo}\left[\frac{\delta}{R_{vV}} + \frac{1-\delta}{R_{vV}+R_{sto}}\right]\frac{\partial q_{sat}}{\partial T_v}(T_v) \quad (3.70b)$$

$$c_{43} = 0 \tag{3.70c}$$

$$c_{44} = L_{vo}\left[\frac{1}{R_{aV}} + \frac{1}{R_{gV}} + \frac{\delta}{R_{vV}} + \frac{1-\delta}{R_{vV} + R_{sto}}\right] \tag{3.70d}$$

$$c_{45} = -\frac{L_{vo}}{R_{gV}}\frac{\partial q_1}{\partial h_1}(T_1, h_1) \tag{3.70e}$$

$$\begin{aligned} d_4 = {} & \frac{L_{vo}}{R_{aV}} q_a + \frac{L_{vo}}{R_{gV}}\left(q_1 - T_1\frac{\partial q_1}{\partial T_1}(T_1, h_1) - h_1\frac{\partial q_1}{\partial h_1}(T_1, h_1)\right) \\ & + L_{vo}\left[\frac{\delta}{R_{vV}} + \frac{1-\delta}{R_{vV} + R_{sto}}\right]\left(q_{sat}(T_v) - T_v\frac{\partial q_{sat}}{\partial T_v}(T_v)\right) \end{aligned} \tag{3.70f}$$

with $L_{vo}$=2.5 $10^6$ Jkg$^{-1}$.

$$c_{51} = \frac{\rho_a}{\rho_w R_{gV}}\frac{\partial q_1}{\partial T_1}(T_1, h_1) + \frac{D_{mT1+1/2}}{dz_1} \tag{3.71a}$$

$$c_{52} = 0 \tag{3.71b}$$

$$c_{53} = 0 \tag{3.71c}$$

$$c_{54} = -\frac{\rho_a}{\rho_w R_{gV}} \tag{3.71d}$$

$$c_{55} = \frac{\rho_a}{\rho_w R_{gV}}\frac{\partial q_1}{\partial h_1}(T_1, h_1) + \frac{D_{mh1+1/2}}{dz_1} + \frac{C_{h1}\Delta z_1}{\Delta t} \tag{3.71e}$$

$$\begin{aligned} d_5 = {} & -\frac{\rho_a}{\rho_w R_{gV}}\left[q_1 - T_1\frac{\partial q_1}{\partial T_1}(T_1, h_1) - h_1\frac{\partial q_1}{\partial h_1}(T_1, h_1)\right] + \frac{D_{mh1+1/2}}{dz_1} h_2 \\ & + \frac{C_{h1}\Delta z_1}{\Delta t} h_1 + \frac{D_{mT1+1/2}}{dz_1} T_2 - K_{1+1/2} - S_1\Delta z_1 + P_g \end{aligned} \tag{3.71f}$$

When $h_1$ is known either because $h_1$=0 (saturation of the surface) or $h_1=h_{1min}$ (very dry case), this system is reduced to four unknowns and four equations (the last equation disappears). In this case, the terms containing $h_1$ on the left-hand side of the system are moved to the right-hand side.

The matrix system $[C][Y]=[D]$ is solved using the Gauss elimination with a computation of the pivot for each line.

*3.3.3. Final linear system obtained (bare soil case).*

In the bare soil case, the non-linear system (3.26) is reduced to two equations: energy balance of the bare soil and continuity of the mass balance equation at the surface which reads:

$$Rn - H - L_v E - G = 0 \tag{3.72a}$$

$$E + Q_{mg} - P_g \rho_w = 0 \tag{3.72b}$$

In a matrix form, the system can be written:

$$[E][Y_b] = [F] \tag{3.73}$$

where the vector of the unknowns is $Y_b = \begin{bmatrix} T_1 \\ h_1 \end{bmatrix}$.

The coefficients of the $[E]$ and $[F]$ matrices are listed below.

$$e_{11} = 4c_{ng}\sigma T_1^3 - \frac{\rho_a c_p}{R_{aH}} - \frac{\rho_a}{R_{aV}} L_v(T_1)\frac{\partial q_1}{\partial T_1}(T_1, h_1) - \frac{\rho_a}{R_{aV}} B(q_1 - q_a) - \frac{D_{cT1+1/2}}{dz_1} - \frac{C_{T1}\Delta z_1}{\Delta t} \tag{3.74a}$$

$$e_{12} = -\frac{\rho_a}{R_{aV}} L_v(T_1)\frac{\partial q_1}{\partial h_1}(T_1, h_{1_1}) - \frac{D_{ch1+1/2}}{dz_1} \tag{3.74b}$$

$$f_1 = -a_{ng} + 3c_{ng}\sigma T_1^4 - \frac{D_{cT1+1/2}}{dz_1} T_2 - \frac{C_{T1}\Delta z_1}{\Delta t} T_1 - \frac{D_{ch1+1/2}}{dz_1} h_2$$
$$+ \frac{\rho_a}{R_{aV}} \left[ L_v(T_1) \left( q_1 - \frac{\partial q_1}{\partial T_1}(T_1, h_1) T_1 - \frac{\partial q_1}{\partial h_1}(T_1, h_1) h_1 \right) - B T_1 (q_1 - q_a) \right] \tag{3.74c}$$
$$- \frac{\rho_a c_p T_a}{R_{aH}} - \frac{\rho_a L_v(T_1) q_a}{R_{aV}}$$

where
$$a_{ng} = RG(1 - \alpha_g) + \varepsilon_g RA$$
$$c_{ng} = -\varepsilon_g \tag{3.75a}$$

with
$$Rn_g = a_{ng} + c_{ng}\sigma T_1^4 \tag{3.75b}$$

$$e_{21} = \frac{\rho_a}{\rho_w R_{aV}} \frac{\partial q_1}{\partial T_1}(T_1, h_1) + \frac{D_{mT1+1/2}}{dz_1} \tag{3.76a}$$

$$e_{22} = \frac{\rho_a}{\rho_w R_{aV}} \frac{\partial q_1}{\partial h_1}(T_1, h_1) + \frac{D_{mh1+1/2}}{dz_1} + \frac{C_{h1}\Delta z_1}{\Delta t} \tag{3.76b}$$

$$f_2 = -\frac{\rho_a}{\rho_w R_{aV}} \left[ q_1 - T_1 \frac{\partial q_1}{\partial T_1}(T_1, h_1) - h_1 \frac{\partial q_1}{\partial h_1}(T_1, h_1) \right] + \frac{D_{mh1+1/2}}{dz_1} h_2$$
$$+ \frac{C_{h1}\Delta z_1}{\Delta t} h_1 + \frac{D_{mT1+1/2}}{dz_1} T_2 - K_{1+1/2} - S_1 \Delta z_1 + P_g + \frac{\rho_a q_a}{\rho_w R_{aV}} \tag{3.76c}$$

## 3.4 List of subroutines used in the soil-plant-atmosphere interface module.

The full description of the subroutines, including input and output arguments is given in the Fortran code (Fortran 77). Here are only listed the names of the subroutines and what they are supposed to do.

| | |
|---|---|
| subroutine **albsol** | : Computation of the bare soil albedo as a function of surface soil moisture. The correction from the position of the sun is also taken into account. |
| subroutine **anglzenith** | : Computation of the correction applied to the albedo as a function of the solar angle. |
| subroutine **coefmat22** | : Computation of the **[E]** and **[F]** matrices in the case of a bare soil. |
| subroutine **coefmat55** | : Computation of the **[C]** and **[D]** matrices in the case of a canopy. |
| subroutine **coefrn** | : Computation of the coefficients $a_{ng}$, $b_{ng,}$ $c_{ng,}$ $a_{nv,}$ $b_{nv,}$ $c_{nv}$ . |
| function **emiss** | : Computation of the bare soil emissivity as a function of surface soil moisture. |
| subroutines **gauss** and **pivot** | : Resolution of the linear system $[C][Y]=[D]$ with the Gauss elimination. The pivot of each line is calculated. |
| subroutine **raynet** | : Computation of the net radiation over the bare soil and the canopy. |
| subroutine **resaero** | : Computation of aerodynamic and canopy resistances using the Thom (1972) and Taconet et al. (1986) approach. |
| subroutine **resaerosw** | : Computation of aerodynamic and canopy resistances using the Shuttleworth and Wallace (1985) approach. |
| subroutine **resaeronu** | : Computation of aerodynamic resistances in the case of a bare soil. |
| subroutine **resolinterfacelin** | : Computation of soil surface temperature, leaf temperature, canopy temperature and specific humidity, soil surface matric potential by solving the linearised soil-plant-atmosphere interface. Computation of associated turbulent fluxes and of the root extraction from the various soil layers. |
| subroutine **resolinterfacenu** | : The same as resolinterfacelin in the case of a bare soil. |
| subroutine **ressto** | : Computation of the stomatal resistance. |
| subroutine **xinterpcli** | : Linear interpolation of the climatic forcing data at the time step of the model. |

| | |
|---|---|
| subroutine **xinterpveg** | : Daily linear interpolation of *LAI*, vegetation height (and possibly of total albedo). The displacement height, roughness length for momentum and shielding factor are also computed in this routine. |
| function **fdv** | : Computation of the weighting function of the stomatal resistance depending on the vapour pressure deficit. |
| function **frg** | : Computation of the weighting function of the stomatal resistance depending on the incoming solar radiation. |
| function **fsigmaf** | : Function giving the shielding factor as a function of *LAI*. |
| function **fsigmaa** | : Function giving the partition factor of momentum as a function of *LAI*. |
| functions **psim** and **psih** | : Computation of the Paulson (1970) stability functions. |

# 4. SOIL-PLANT INTERFACE MODULE: CALCULATION OF LEAF WATER POTENTIAL AND ROOT EXTRACTION.

## 4.1. Introduction.

In this chapter, the coupling between the soil and the plant will be described. This includes the modelling of the root density profile within the soil, the water extraction by roots, which uses a model based on a resistance network to water transfer from the soil to the roots and within the plant proposed by Federer (1979). Then it will be shown how the assumption that the plant transpiration is equal to the total root extraction is used to compute the leaf water potential, which appears in the water stress function of the stomatal resistance.

## 4.2. Modelling of the root density profile.

A typical shape for the root density profile has been retained. It is defined by five characteristic depths and a parameter (Fig. 7):

- $z_{ri}$: : depth of the first root.
- $z_{rm1}$ and $z_{rm2}$ : depths between which the root density is equal to its maximum value $M_{rd}$.
- $z_{rpm}$: depth at which a percentage $p_{mr}$ of the maximum root density is affected
- $z_{rt}$: total root depth
- $p_{mr}$: percentage of the maximum root density affected at depth $z_{rpm}$.

The root density profile is finally completely determined by giving the maximum root length density $M_{rd}$ expressed in m of root per $m^3$ of soil and is given by:

$$\begin{cases} RDF(z) = 0 \quad z \le z_{ri} \; and \; z \ge z_{rt} \\ RDF(z) = M_{rd} \dfrac{z - z_{ri}}{z_{zm1} - z_{ri}} \quad z_{ri} \le z \le z_{rm1} \\ RDF(z) = M_{rd} \quad z_{rm1} \le z \le z_{rm2} \\ RDF(z) = M_{rd} \left[ 1 - (1 - p_{mr}) \dfrac{z - z_{rm2}}{z_{zpm} - z_{rm2}} \right] z_{rm2} \le z \le z_{rpm} \\ RDF(z) = M_{rd} \, p_{mr} \dfrac{z_{rt} - z}{z_{rt} - z_{rpm}} \quad z_{rpm} \le z \le z_{rt} \end{cases} \qquad (4.1)$$

*RDF(z)* is in m root per $m^3$ soil. The value of the root density for layer *j* $RDF_j$ (in m root per $m^2$ soil) is obtained by assuming that the value at depth $z_j$ is constant over the whole layer:

$$RDF_j = RDF(z_j)\Delta z_j \qquad (4.2)$$

In practice, the characteristic lengths of the root density profile do not match the depths of the layers as defined by the discretisation of the soil module. Therefore, they are adapted to it as follows (the example is given for $z_{ri}$ but can be generalised to the other characteristic depths). First, the layer to which $z_{ri}$ belongs to is determined. Let assumed that it is layer $k$. Then the numerical value used in the model for $z_{ri}$ is defined as follows (it corresponds to the depth of the top or bottom of a layer):

$$\begin{aligned} z_{ri} &= \sum_{l=1}^{k-1} dz_l \qquad if \quad z_{ri} \le z_k \\ z_{ri} &= \sum_{l=1}^{k} dz_l \qquad if \quad z_{ri} > z_k \end{aligned} \qquad (4.3)$$

where $z_k$ is the depth of node $k$.

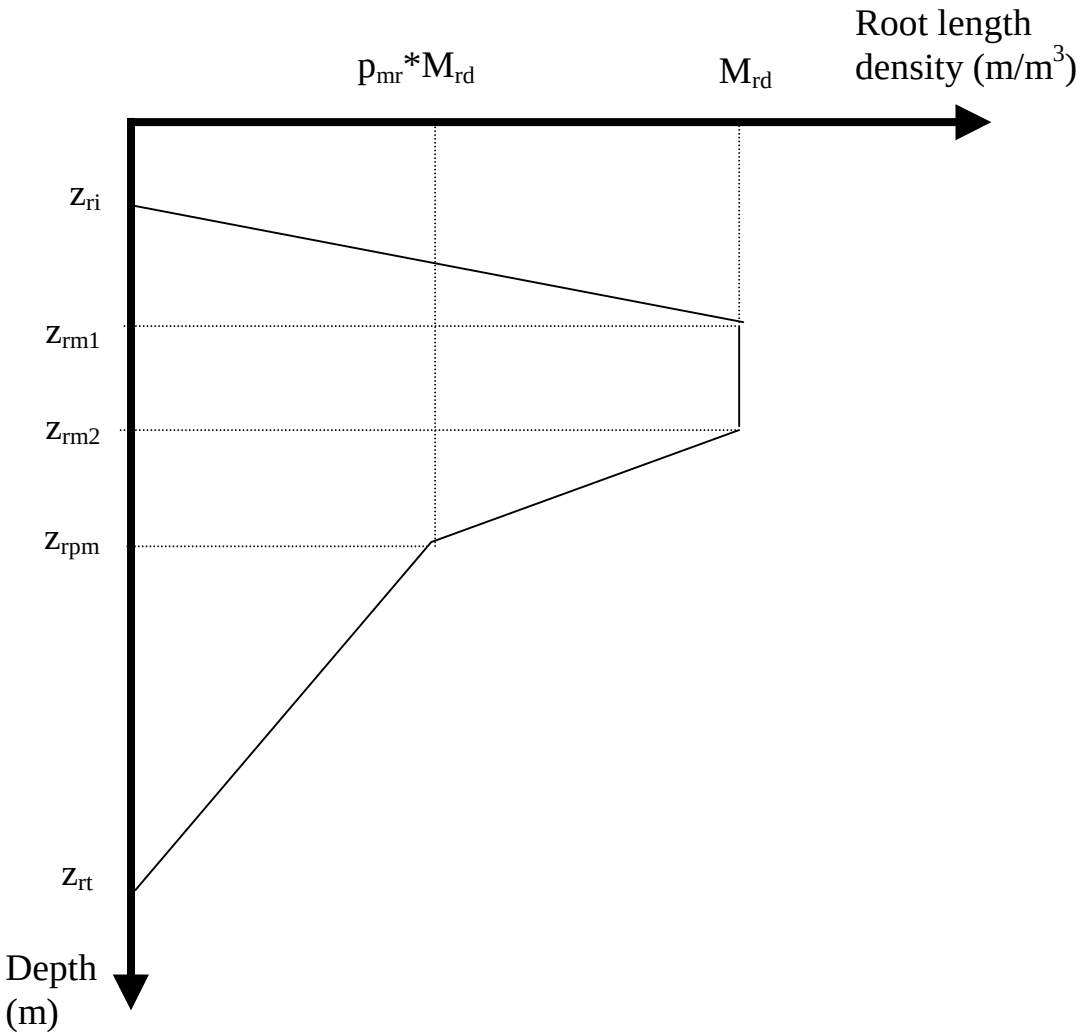


*<u>Fig. 7</u>: Typical shape of the root length density profile used in the SiSPAT model*

## 4.3. Modelling the root extraction.

The model proposed by Federer (1979) is used. The circulation of the water from the soil to the leaves is schematised as in Fig. 8: in the soil, for each layer *j*, two resistances are put in parallel: a resistance to the water path from the soil to the root $R_{sj}$ and a resistance to the water path through the plant $R_{rj}$.. The total water extraction by the roots is then given by:

$$Q_r = \rho_w \sum_{j,h_j>h_f} \frac{h_j - h_f - z_v}{R_{sj} + R_{rj}} \qquad (4.4)$$

The soil resistance of layer *j* is supposed to be inversely proportional to the hydraulic conductivity of that layer and to the density of roots within it (Federer, 1979):

$$R_{sj} = \frac{V_r - 3 - 2Log\left(\frac{V_r}{1-V_r}\right)}{8\pi RDF_j K_j} \qquad (4.5a)$$

where $V_r$ is the root volume per unit volume of soil given by:

$$V_r = \frac{\pi r_{rac}^2 RDF_j}{\Delta z_j} \qquad (4.5b)$$

$r_{rac}$ is the mean root radius, taken as 0.35 mm (Federer, 1979).

The plant resistance of layer *j* is simply obtained as the total plant resistance $R_r$, assumed to be constant on the whole soil profile, divided by the root density of this layer:

$$R_{rj} = \frac{R_r}{RDF_j} \qquad (4.6)$$

Note that, in Eq. (4.4), excretion of water from the plant to the soil is not allowed, even if Van Bavel et al. (1984) have shown evidence of the existence of such a phenomenon.

The root uptake *S* (see Eq. (2.1)) from layer *j* is obtained from (4.4) (written for one layer) by:

$$\begin{aligned} S_j &= 0 && \text{if } h_j < h_f \\ S_j &= \rho_w \frac{h_j - h_f - z_v}{R_{sj} + R_{rj}} \frac{1}{\Delta z_j} && \text{if } h_j \geq h_f \end{aligned} \qquad (4.7)$$

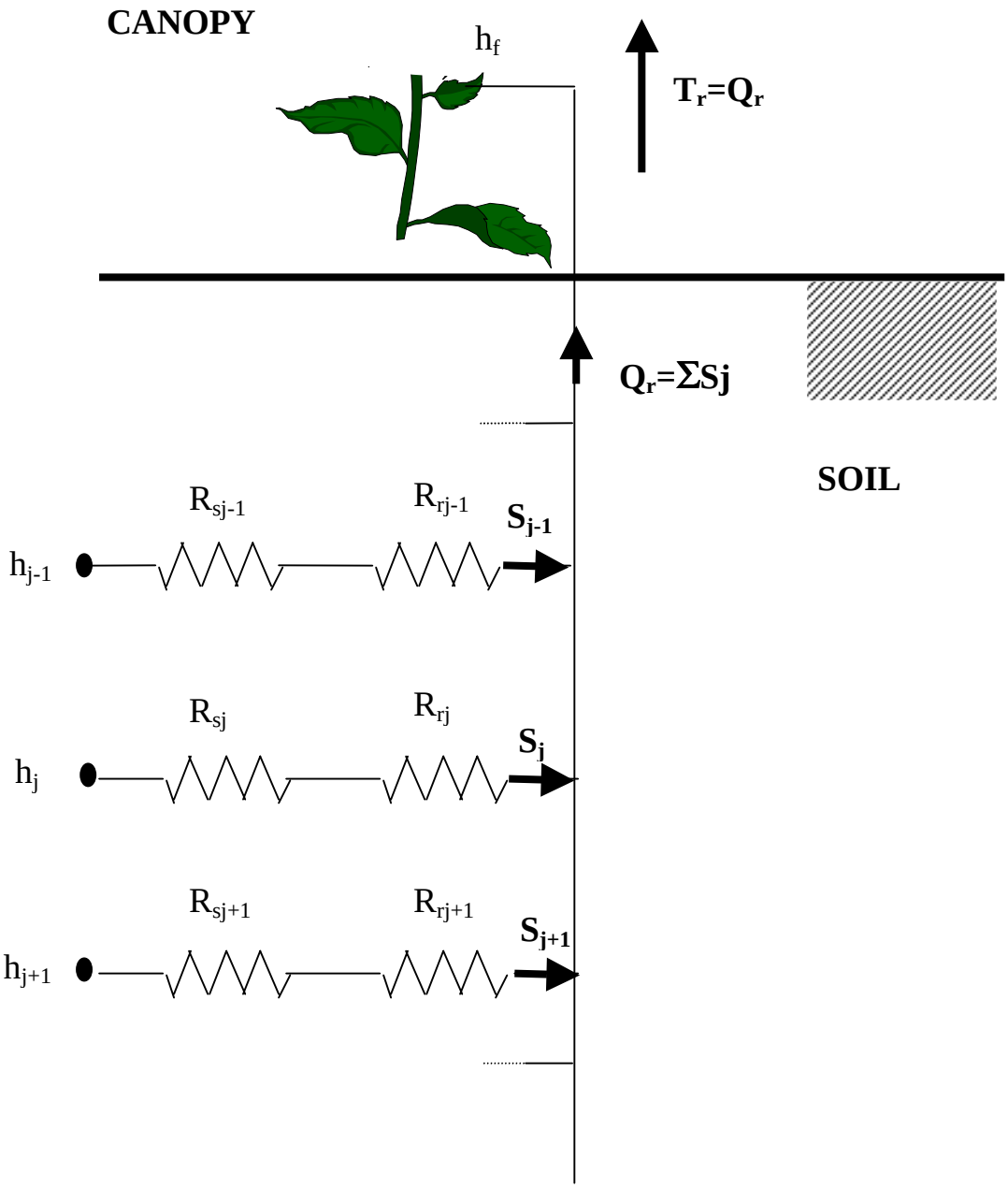


*Fig. 8: Modelling of the root water extraction*

## 4.4. Computation of the leaf water potential.

The leaf water potential is calculated from the equation $T_r=Q_r$, where it is assumed that the transpiration of the canopy is equal to the total water extracted by the roots. According to Carlson and Lynn (1991), time variation of water storage within the plant can be neglected for small vegetation, but must be taken into account for tall vegetation such as trees. This aspect is neglected here. Therefore, one non-linear equation with one unknown, the leaf water potential, is obtained and can be written as:

$$F\left(h_f\right) = h_f + z_v - \frac{a_1}{a_2} + \frac{T_r}{\rho_w a_2} = 0 \tag{4.8}$$

where

$$a_1 = \sum_{\substack{j=iraci \\ h_j \geq h_f}}^{iract} \frac{h_j}{R_{sj} + R_{rj}} \qquad a_2 = \sum_{\substack{j=iraci \\ h_j \geq h_f}}^{iract} \frac{1}{R_{sj} + R_{rj}} \tag{4.9}$$

In (4.9) *iraci* and *iract* are the indices of the layers of the first (resp. the last) layer with roots.

The non-linear equation (4.8) is solved iteratively using the Newton-Raphson algorithm. If subscripts $^{k-1}$ and $^{k}$ denotes iteration *k* and *k-1* respectively, $h_f$ is calulated until convergence is reached by:

$$h_f^k = h_f^{k-1} - \frac{F\left(h_f^{k-1}\right)}{\frac{\partial F}{\partial h_f}\left(h_f^{k-1}\right)} \tag{4.10}$$

with

$$\frac{\partial F}{\partial h_f}\left(h_f\right) = 1 - \frac{T_r}{\rho_w a_2 \left(R_{vf} + R_{sto}\right)} \frac{\partial R_{sto}}{\partial h_f} \tag{4.11}$$

and

$$\frac{\partial R_{sto}}{\partial h_f}\left(h_f\right) = R_{st\,\min} \frac{f_{RG}(RG) f_{VPD}(VPD)}{LAI} \left[ \frac{5.5}{h_{fc}} \left( \frac{h_f}{h_{fc}} \right)^{4.5} \right] \tag{4.12}$$

with the model chosen for the stomatal resistance.

## 4.5. List of subroutines used in the soil-plant interface module.

| | |
|---|---|
| subroutine **a1a2** | : Computation of the coefficients $a_1$ and $a_2$. |
| subroutine **bilanhf** | : Iterative computation of the leaf water potential by using the Newton-Raphson algorithm. |
| subroutine **distrac** | : Computation of the root density for the various layers. |
| subroutine **prof** | : Subroutine which computes the depth of the model layer which is the nearest of a given depth z. |
| subroutine **profrac** | : Computation of the characteristic depths of the root density profile corresponding with the soil discretisation. |
| subroutine **resissolrac** | : Computation of the soil and root resistances of the various soil layers. |
| subroutine **xinterprac** | : Linear interpolation in time of the characteristics of the root density profile. |

# 5. COUPLING BETWEEN THE VARIOUS MODULES AND ORGANISATION OF THE CODE.

## 5.1. Description of the coupling between the various modules.

At each time step, the main difficulty in linking the various modules is related to the interactions between all of them: the upper boundary condition of the soil module is provided by the resolution of the soil-plant-atmosphere interface which provides in particular the soil surface matric potential and temperature (and also the surface heat and mass fluxes) (see Eq. (3.26)). But, for this system of five equations with five unknowns to be solved, the matric potential and temperature at the second node are needed, but are a priori unknown. In the same way, the values of the root extraction of each soil layer is needed for the soil module to be solved. But their value depends on the transpiration flux calculated in the soil-plant-atmosphere module, which itself depends on the leaf water potential, used to compute the stomatal resistance.

The solution which has been retained here is a mixture of iterative procedures, which ensure the full implicit resolution of the system and of explicit linearisation to achieve computational efficiency. Indeed, the leaf water potential at the previous time step is used for the computation of the stomatal resistance and, as mentioned in section 3.3 the values of the state variables (surface temperature and matric potential, canopy temperature and specific humidity, leaf temperature) at the previous time step are used to compute the **[C]** and **[D]** matrices of the linearised interface. On the other hand, the values of the matric potential and temperature at the second node are taken at the present time step and an iterative procedure has been adopted: the soil-plant-atmosphere interface is solved first with the values at the previous time step. This provides one set of values for the upper boundary of the soil module and for the root extraction terms, used to solve the soil module. This resolution provides new value for the matric potential and temperature of the second node, which are compared to the one used in the resolution of the soil-plant-atmosphere. If the difference is greater than a specified thereshold, the procedure is iterated until convergence is reached. If convergence is not reached within a prescribed number of iterations, the time step is divided by two and the resolution performed at this new time step. The choice of the threshold for the convergence test on the matric potential and temperature at the second node mainly conditions the degree of accuracy reached on the mass balance at the end of the whole simulation. Indeed, a compromise must be adopted between a very accurate convergence and the computing time. The threshold retained in the code ensures (on the data sets tested) an accuracy of the mass balance of 4 to 5% of the rainfall amount, which is acceptable given the uncertainties on the inputs and on the parameters of the model.

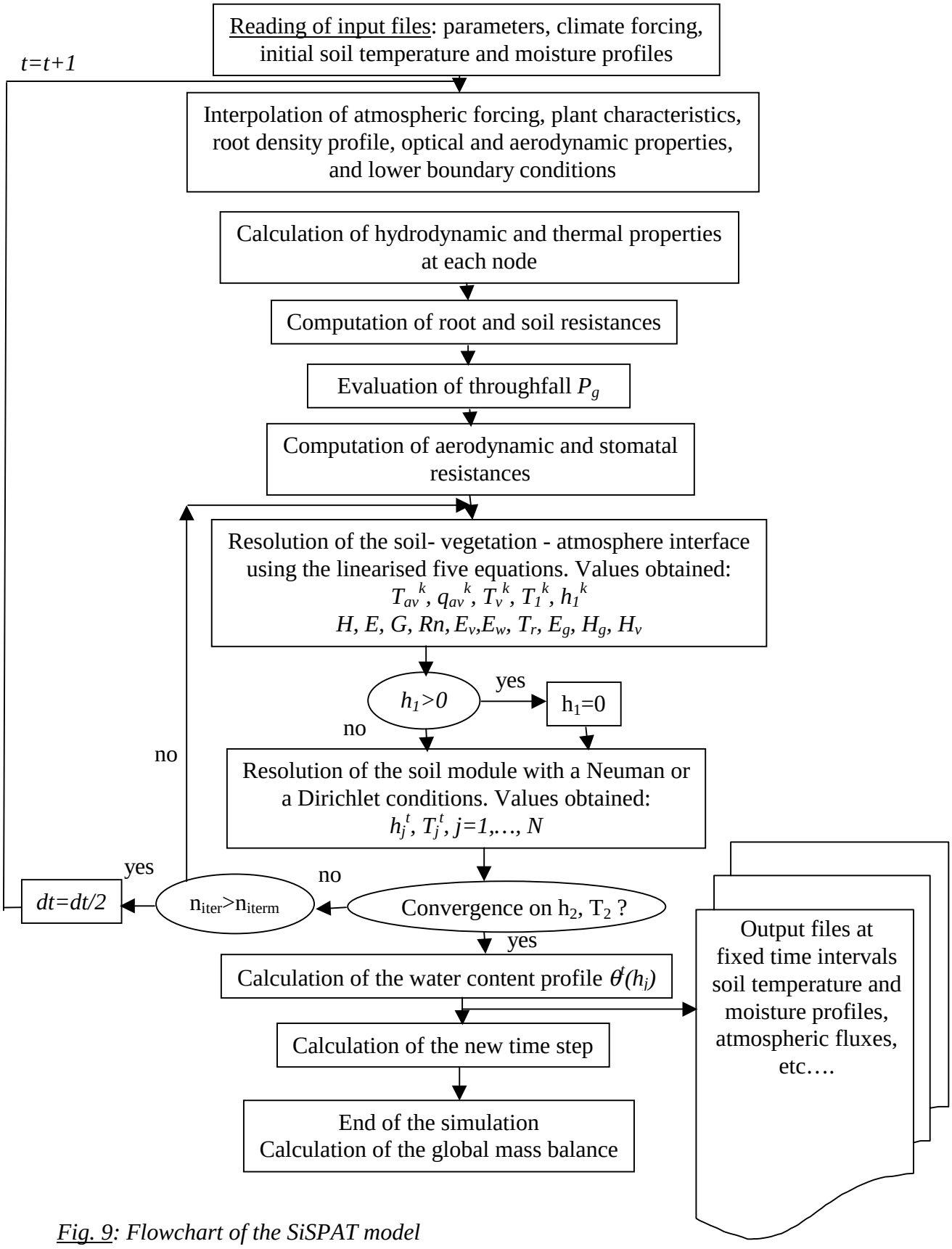


*Fig. 9: Flowchart of the SiSPAT model*

## 5.2. Flowchart of the model.

The main code can be divided into three parts:

1. Reading of input parameters and input data. Initialisation of the various variables.
2. Computation of the various output variables at each time step.
3. Writing of output variables at the time step chosen by the user.

A flowchart of the model is shown on Fig. 9.

The time step of the model is automatically adapted to the variation of soil matric potential and temperature gradients. The new time step is calculated as described by Passerat (1986).

$$\Delta t^i = \Delta t^{i-1} \frac{1}{Max\left(\frac{dh}{\varepsilon_h}, \frac{dT}{\varepsilon_T}\right)} \tag{5.1}$$

where

$$dh = Max\left(\frac{h_j^i - h_j^{i-1}}{h_j^{i-1}}, h_j^{i-1} \neq 0, j = 1, \ldots, N\right)$$
$$dT = Max\left(\frac{T_j^i - T_j^{i-1}}{T_j^{i-1}}, j = 1, \ldots, N\right) \tag{5.2}$$

and $\varepsilon_h$ and $\varepsilon_T$ are prescribed thresholds for the gradients. The following values are used: $\varepsilon_h = 0.01$ and $\varepsilon_T = 0.015$.

In practice, the time step is very small in case of rainfall and can be increased when it is not raining. However, due to the linearisation of the soil-plant-atmosphere interface, it is recommanded to limit the maximum time step to 100-200 s when it is not raining and 50 s when it is raining. A minimum value of the time step is also imposed in the routine of automatic calculation (typically 1 s when it is raining and 10 s when it is not) to increase the computational efficiency. However, no limit is imposed when the time step is divided by two because the convergence on the second node of the soil module is not reached.

For the output files, the user defines the time step at which the output variables are calculated. Linear interpolation between the values of the variables at the two time step before and after the desired output time is used. These routines can be modified by the user if he/she wants to add or modify the output variables.

## 5.3. List of general subroutines not specifically associated to a module.

| | |
|---|---|
| subroutine **calcdt** | : Automatic computation of the time step of the model |
| subroutine **xinterpsortieatm** | : Linear interpolation of output variables, for which the time series are wished. The time step is chosen by the user. Instantaneous values are obtained. |
| Subroutine **xinteratmmoy** | : Output of a selection of variables for which average values over the time step are calculated |
| subroutine **xinterpsortiesol** | : Linear interpolation of output soil variables (soil temperatue, matric potential and volumetric water content) for which soil profiles are wished, with a time step specified by the user. Instantaneous values are obtained. |

# 6. HOW TO RUN SISPAT: INPUTS AND OUTPUTS OF THE MODEL.

## 6.1. Name of the input and output files.

A file called ***nomfich*** is read first and contains all the names of the input and output files used in the simulation.

***nomfich***

| | |
|---|---|
| *Soil.dat* | Soil profiles output file or average fluxes output file |
| *Atm.dat* | Atmospheric output file |
| *Parameter.dat* | Parameters input file |
| *List.dat* | Listing output file |
| *Icbc.dat* | Initial and boundary conditions input file |
| *Climate.dat* | Atmospheric forcing input file |
| *Hbottom.dat* | Input file of matric potential at the bottom of the profile |
| *Tpbottom.dat* | Input file of temperature at the bottom of the profile |

## 6.2. Parameters file.

This file contains all the input parameters needed to run the model. This includes

1. The description of the soil profile discretization
2. Soil parameters describing soil hydrodynamic and thermal properties
3. Vegetation characteristics and rooting depth and their evolution if any

4. Vegetation parameters

5. Surface properties (albedo, emissivity, roughness length, etc..)

6. Information dealing with the time step of the climate forcing, the duration of the simulation and the date and time of beginning and ending of the simulation, the minimum and maximum time steps allowed in the model, the time step of output files.

In the description below, the names of the variables correspond to the names used in the code (and are not exactly the same as the description given in the previous chapters).

***Parameter.dat***

Number of soil horizons *ncouch*
4 définition du domaine spatial
Number of nodes for each horizon (*nntot(i), i=1,..ncouch*)
22 21 25 32
Total number of nodes *n*
100
Thicknesses between nodes (m) (*dz(i),i=1,...n-1*)
1.1746429E-03 1.4683036E-03 1.8353796E-03 2.2942245E-03 2.8677806E-03
3.5847258E-03 4.4809072E-03 5.6011342E-03 7.0014177E-03 8.7517714E-03
1.0939714E-02 1.0939714E-02 8.7517714E-03 7.0014177E-03 5.6011342E-03
4.4809072E-03 3.5847258E-03 2.8677806E-03 2.2942245E-03 1.8353796E-03
1.4683036E-03 1.1746429E-03 5.0398507E-03 6.2998133E-03 7.8747664E-03
9.8434584E-03 1.2304323E-02 1.5380404E-02 1.9225504E-02 2.4031881E-02
2.0000001E-02 2.0000001E-02 2.0000001E-02 2.0000001E-02 2.0000001E-02
2.4031881E-02 1.9225504E-02 1.5380404E-02 1.2304323E-02 9.8434584E-03
7.8747664E-03 6.2998133E-03 5.0398507E-03 1.2184674E-02 1.5230842E-02
1.9038552E-02 2.3798192E-02 2.9747739E-02 2.0000001E-02 2.0000001E-02
2.0000001E-02 2.0000001E-02 2.0000001E-02 2.0000001E-02 2.0000001E-02
2.0000001E-02 2.0000001E-02 2.0000001E-02 2.0000001E-02 2.0000001E-02
2.0000001E-02 2.0000001E-02 2.0000001E-02 2.9747739E-02 2.3798192E-02
1.9038552E-02 1.5230842E-02 1.2184674E-02 1.2184674E-02 1.5230842E-02
1.9038552E-02 2.3798192E-02 2.9747739E-02 5.0000001E-02 5.0000001E-02
5.0000001E-02 5.0000001E-02 5.0000001E-02 5.0000001E-02 5.0000001E-02
5.0000001E-02 5.0000001E-02 5.0000001E-02 5.0000001E-02 5.0000001E-02
5.0000001E-02 5.0000001E-02 5.0000001E-02 5.0000001E-02 5.0000001E-02
5.0000001E-02 2.4031881E-02 1.9225504E-02 1.5380404E-02 1.2304323E-02
9.8434584E-03 7.8747664E-03 6.2998133E-03 5.0398507E-03
Depth of the cracks *zfiss* (m) (*zfiss*=0. If no crack)
0.
Fraction of the surface flux infiltrated within the cracks *fiss*
0.
Type of *h(θ)* curve *imodh=0* for Van Genuchten (VG) *=1* for Brooks and Corey (BC) =2 if VG + extension in the dry domain =3 if VG Mualem hypothesis (*imodh(i), i=1,.., ncouch*)
2 2 2 2
If Brooks and Corey *icurve=0* for MWC and *icurve=1* for MDC (*icurve(i), i=1,.., ncouch*)
0 0 0 0
Type *K(θ) ikh*=0 if *K(θ)* Brooks and Corey *ikh*=1 if *K(θ)* Van Genuchten Mualem
0 0 0 0
Porosity (*por(i), i=1,.., ncouch*)
0.509 0.49 0.396 0.366
Scale parameter $h_g$ of VG or $h_{ae}$ of BC (m) (*hgvg(i), i=1,.., ncouch*)
-0.4 -0.8 -3.0 -2.0
Shape parameter *n* of VG or $\gamma$ of BC (*qvg(i),i=1,.., ncouch*)
2.133 2.136 2.1103 2.131
Saturated water content $\theta_{sat}$ ($m^3m^{-3}$) (*wsat(i), i=1,.., ncouch*)

0.43 0.41 0.383 0.366
Shape parameter $n_2$ of the Van Genuchten model for dry domain extension (*qvg2(i),i=1,.., ncouch*)
2.1138 2.1287 2.208 2.1643
Scale parameter $h_{g2}$ of VG for the dry domain extension (m) (*hgvg2(i), i=1,.., ncouch*)
-84.53 -86.42 -125.69 -99.34
Soil water pressure $h_c$ at which continuity between the wet and dry domain of the VG model are imposed (m) (*hc2(i), i=1,.., ncouch*)
-100. -100. -100. -100.
Soil water pressure $h_o$ at which water content is zero (m) *ho2*
-60000.
Wilting point ($\theta(h$=-150m) ($m^3\ m^{-3}$) (must be greater than $\theta_k$) (*wwilt(i), i=1,.. , ncouch*)
0.195 0.201 0.249 0.208
$K_{sat}$ of the BC model for the soil matric (m $s^{-1}$) (*xksat1(i), i=1,.., ncouch*)
5.e-9 1.8e-9 5.e-9 6.4e-9
$\eta$ of BC model (*beta1(i), i=1,.., ncouch*)
18.97 18.67 22.30 19.27
Macropores content $\theta_{macro}$ ($m^3\ m^{-3}$) (*wmacro(i), i=1,.. , ncouch*)
0.013 0.013 0.013 0.0
Saturated hydraulic conductivity $K_{sat}$ (m $s^{-1}$) including macropores if any (*xksat2(i), i=1,.., ncouch*)
7.e-6 2.4e-6 2.0e-6 2.75e-6
Residual volumetric water content $\theta_r$ ($m^3 m^{-3}$) (*wresid(i), i=1, .., ncouch*)
0. 0. 0. 0.
Water content $\theta_k$ at which the liquid phase is no more continuous ($m^3 m^{-3}$) (*wk(i), i=1, .., ncouch*)
0.015 .015 .015 0.015 0.015
Quartz content ($m^3 m^{-3}$ of soil matter) (*wqtz(i), i=1, .., ncouch*)
0.60 0.60 0.60 0.60
Other minerals content ($m^3 m^{-3}$ of soil matter) (*wmin(i), i=1, .., ncouch*)
0.39 0.39 0.39 0.39
Organic matter content ($m^3 m^{-3}$ of soil matter) (*worg(i), i=1, .., ncouch*)
0.01 0.01 0.01 0.01
Volumetric heat capacity at zero water content ($Jm^{-3}\ K^{-1}$) (*csec(i), i=1, .., ncouch*)
0.982e6 1.02e6 1.21e6 1.27e6
Code for the choice of the thermal conductivity model *icth=0* for De Vries *icth=1* for constant value *icth=1* if Laurent's model *icth=3* if Van de Griend model
2 2 2 2
Thermal conductivity (in the case of a constant value) ($Wm^{-1}\ K^{-1}$) (*xxlambda(i), i=1, .., ncouch*)
0.5 0.7 1.0 1.3
Coefficients *aj, bj, cj, dj, ej* of the Laurent's model if *icth=2* $\lambda(\theta) = ej + aj\frac{\theta}{\theta_{sat}} + bj\left(1 - \exp\left(cj\left(\frac{\theta}{\theta_{sat}}\right)^{dj}\right)\right)$
0.734d0 0.303d0 34.54d0 3.82d0 0.492d0
Thermal inertia at saturation $\Lambda_s$ ($J\ m^{-2}\ K^{-1}\ s^{-1/2}$) for the van de Griend and O'Neill model if icth=3(*xlambdas(i), i=1, .., ncouch*)
2440. 2440. 2440. 2440.
Reference temperature for the calculation of *h(θ)* curves (K) (not relevant in this version) *tpo*
298.15
Coefficient *vch* of the dependence on the *h(θ)* curve on temperature ($K^{-1}$) (not relevant in this version)
0.
Number of days with vegetation measurements *nveg*
158
DOY, *LAI*, height of vegetation $z_v$, total albedo $\alpha_t$ *(jveg(j), xxlai(j), xzf(j), xalphat(j)*

| | | | | |
|---|---|---|---|---|
| 386 | 0.1309 | 0.12141138 | 0.2 | |
| 387 | 0.1386 | 0.12341789 | 0.2 | *nveg* lines |
| 388 | 0.1466 | 0.12542439 | 0.2 | |
| 389 | 0.1551 | 0.12743089 | 0.2 | |
| 390 | 0.164 | 0.1294374 | 0.2 | |

.
.

.
542 0.000149 0.68807692 0.2
543 0.000149 0.68807692 0.2
Critical leaf water potential $h_{fc}$ (m) *hfc*
-140.
Minimum stomal resistance $R_{stmin}$ (s $m^{-1}$) *rstmin*
50.
Maximum stomatal resitance $R_{stmax}$ (s $m^{-1}$) *rstmax*
5000.
Total plant resistance $R_r$ (s per m root ) *rplante*
3.e12
Parameter $\mu$ of the *VPD* function for the stomatal resistance ($Pa^{-1}$) *gfdv*
2.5e-4
Type of land use *veg=0* for bare soil *veg=1* for vegetated surface
1
Number of days with measurements of the root density profile *nrac*
11
*DOY jrac(i) ,x zri(i), xzrm1(i), xzrm2(i), xzrpm(i), xzrt(i), xprm(i)* (m) *xdrmax(j)* (m of root per $m^{-3}$ of soil)
387 0.03 0.050 0.07 0.10 0.10 0.20 10000
408 0.03 0.050 0.10 0.15 0.15 0.20 10000
417 0.03 0.050 0.15 0.25 0.25 0.20 10000
422 0.03 0.050 0.15 0.30 0.35 0.20 10000 *nrac* lines
432 0.03 0.050 0.15 0.35 0.40 0.23 10000
436 0.03 0.050 0.15 0.40 0.65 0.26 10000
443 0.03 0.050 0.15 0.45 0.75 0.30 10000
450 0.03 0.050 0.15 0.50 0.85 0.35 10000
460 0.03 0.050 0.15 0.55 1.10 0.40 10000
464 0.03 0.050 0.15 0.60 1.35 0.52 10000
527 0.03 0.050 0.15 0.70 1.65 0.64 10000
Total number of observations in the atmospheric forcing file *nobs*
11161
Time step of forcing data (s) *dtobs*
1200.
Measurement height for air temperature (m) *zat*
2.0
Measurement height of wind speed (m) *zav*
2.0
Surface atmospheric pressure $p_{atm}$ (Pa) *patm*
100700.
Choice of the function for *d* and $z_{om}$ (m) calculation *idzom=0* constant values =1 Brutsaert =2 Shaw and Pereira =*f(LAI, $z_v$)*
1
Displacement heigth *d* (m) (needed in case of a constant value) *d0*
0.
Roughness length for momentum $z_{om}$ (m) (needed in case of a constant value) *zom0*
.001
Code for roughness length for heat *izoh=0* if $z_{oh}=z_{om}$/*rapzoh izoh=1* if $z_{oh}=f(u^*)$
0
Ratio $z_{om}/zoh$(if constant) *rapzoh*
54.6
Code for the choice of aerodynamic resistances *iresaero=0* (Taconet et al.) *iresaero=1* (Shuttle. and Wall.)
1
Vegetation albedo $\alpha_v$ *alphaf0*
.22
Vegetation emisisvity $\varepsilon_v$ *emisv0*
.98
Code for the choice of soil albedo *ialphas=0* constant value =1 function of the surface humidity =2 to match total albédo
1

Bare soil albedo $\alpha_g$ (if constant) *alphas0*
.20
Coefficients of the function of surface humidity for albedo *coef1, coef2, coef3, wlimo*
0.43 -0.079 0.14 0.20
Code for the choice of bare soil emissivity *iemiss=0* constant value =1 function of surface humidity
0
Bare soil emissivity (if constant) $\varepsilon_g$ *emiss0*
.96
Extinction coefficient $a_b l$ of the formula $\sigma_s = 1 - \exp(-a_{bl} LAI)$ *abl*
0.5
Initial time step (s) *dt*
5.
Minimum time step when it is raining (s) *dtminpl*
2.
Minimum time step when it is not raining (s) *dtminsec*
5.
Maximum time step when it is raining (s) *dtmaxpl*
10.
Maximum time step when it is not raining (s) *dtmaxsec*
30.
Time step of soil output file (s) or average flux outputs *tsors*
3600.
Time step of atmospheric output file (s) *tsora*
1200.
Number of nodes used for the calculation of surface humidity over 0-0.05, 0-2,..etc cm *n005, n02, n05, n010, n015*
6 8 10 12 82
Depth of the layer over which this humidity is calculated (m) *prof005, prof02, prof05, prof010, prof015*
0.00964 0.01771 0.03031 0.05 1.40
Number of soil temperature output time series (9 maxi) *ntp*
8
Number of the corresponding nodes (*numtp(i), i=1,..,ntp*)
4 6 9 15 29 33 49 74
Number of volumetric soil moisture output time series (9 maxi) *ntheta*
8
Number of the corresponding nodes (*numtheta(i), i=1,..,ntheta*)
9 15 27 30 33 44 56 74
Number of volumetric soil moisture output time series (9 maxi) *npot*
7
Number of the corresponding nodes (*numpot(i), i=1,..,npot*)
23 31 36 49 64 76 80
Year Month Day of the beginning of the simulation *naa, nmm, njj*
1997 01 21
Day Hour Minute of the beginning of the simulation *xjini, heurini, xminini*
387 0 00
Day Hour Minute of the end of the simulation *xjfin, heurfin, xminfin*
542 0 00
Longitude (°) *xlongi*
4.75
Latitude (°) *xlati*
43.783

### 6.3. Atmospheric forcing file.

It contains the atmospheric forcing.

Each line is composed of the following records which are read in a * format:

1. Julian day
2. Hour
3. Minute
4. Incoming solar radiation (W $m^{-2}$)
5.Incoming long wave radiation (W $m^{-2}$)
6. Air temperature (K)
7. Air specific humidity (kg $kg^{-1}$)
8. Wind speed (m $s^{-1}$)
9. Rainfall (mm per time step)

***climate.dat***

```
245 13.00   .00  758.000  431.790  303.310 .17532E-01  4.020   .000
245 13.00 20.00  744.000  431.700  303.250 .17213E-01  4.310   .000
245 13.00 40.00  793.800  432.500  303.320 .17307E-01  3.740   .000
245 14.00   .00  893.500  431.700  303.570 .17681E-01  4.270   .000
245 14.00 20.00  795.000  433.840  303.730 .17349E-01  4.280   .000
245 14.00 40.00  629.850  432.680  303.870 .17411E-01  3.680   .000
.                                                              nobs lines
.
.
263  8.00 40.00  683.400  410.810  300.300 .16339E-01  1.970   .000
263  9.00   .00  745.000  415.160  300.890 .16377E-01  2.050   .000
263  9.00 20.00  827.500  421.190  301.680 .17101E-01  1.780   .000
263  9.00 40.00  804.500  425.800  302.560 .17551E-01  1.430   .000
263 10.00   .00  935.000  425.660  302.930 .17302E-01  1.700   .000
263 10.00 20.00  972.500  426.350  303.480 .15750E-01  1.930   .000
263 10.00 40.00  978.000  428.820  304.020 .15226E-01  1.400   .000
```

**6.4. Soil module initial and boundary conditions file.**

This file contains first the specification of the type of upper and lower boundary condition retained for the soil module and if needed the values of the constant values used.

First line: which BC at top and bottom

*itypsup=1* : $h_1$ and $T_1$ imposed at the surface (Dirichlet condition)
*itypsup=2* : heat and mass fluxes imposed at the surface (Neumann condition)
*itypsup=3* : mass flux and temperature imposed at the surface
*itypinf=1* : *h* and *T* imposed at the bottom of the profile
*itypinf=2* : constant mass flux and sinusoidal temperature at the bottom
*itypinf=3* : gravitational mass flux and sinusoidal temperature at the bottom
*itypinf=4* : *h* and *T* evolution at the bottom of the soil profile is given in a file
*itypinf=5* : *h* evolution at the bottom of the soil profile is given in a file and the temperature is sinusoidal

Second and/or third line:

- $h_1$ and $T_1$ if prescribed or surface fluxes if prescribed
- *h* and *T* at the bottom of the soil profile or bottom mass flux *fluxn* plus parameters of the temperature sinusoidal function *tpnmean, tmnamp, tpnphase*

Then the file contains the initial soil temperature and matric potential profiles.

***ibc.dat***

| | |
|---|---|
| 2 5 | *itypsup itypinf* |
| 140. 2. 130. | $T_{mean}(z_N)$, $T_{amp}(z_N)$,*phase*$(z_N)$, |
| 39.4 | |
| 39.03278 | |
| 38.57377 | |
| . | *n* values for the initial soil temperature profile |
| 33.93941 | |
| 33.97307 | |
| 34.0 | |
| -.906368 | |
| -.906368 | |
| -.906368 | |
| . | *n* values for the initial soil matric potential profile |
| -1.58734 | |
| -1.58734 | |
| -1.58734 | |

### 6.5. Output file of soil variables profiles.

This file contains profiles of soil temperature, matric potential and volumetric water content, with a time step specified in the parameter file (*tsors*). The structure of the file is the following:

line 1 : number of soil profiles contained in the file *iss* and number of nodes per profile *n*

line 2 : format for reading the profiles (*formatsol*)

line 3 : Day, hour minute of the following profile

line 4 to n+3 : *n* lines containing the following records:

depth (m) , soil temperature (°C), matric potential (m) and volumetric water content ($cm^3cm^{-3}$) (*z(i), tp(i), h(i), w(i))*

line 4 to n+3 : repeated for the following profiles

***soil.dat***

| | |
|---|---|
| 17 88 | *iss n* |
| (4f10.3) | *formatsol* |
| 246 13 0 | DOY, hour, minute of the first profile |
| .000 -8107.492 309.944 .000 | *z(i), tp(i), h(i), w(i)* |
| .003 -43.090 309.638 .000 | |
| .006 -1.339 309.611 .029 | |
| .010 -1.141 309.542 .037 | |
| . | *n* lines for the first profile |
| 3.694 -1.129 306.836 .081 | |
| 3.797 -1.129 306.941 .081 | |
| 3.900 -1.129 307.047 .081 | |
| 3.941 -1.129 307.089 .081 | |
| 3.974 -1.130 307.123 .081 | |
| 4.000 -1.130 307.150 .081 | |

| | |
|---|---|
| 247 13 0 | DOY, hour, minute of the second profile |
| .000-22366.762 322.886 .000 | |
| .003-14686.488 322.125 .000 | |
| . | *n* lines for the second profile |

**6.6. Output file of time evolution of selected output variables (or of the average of selected output variables) .**

This file contains the time evolution of a set of selected variables (instantaneous values or averaged values over the time step) with a time step defined in the parameter file (*tsora*). A maximum of five time series of the mean surface humidity calculated over chosen depths can be written (see parameter file). A maximum of 9 temperature series defined in the parameter file can be written.

The user is of course free to modify the output variables according to the application considered and processes he is interested in.

The structure of the file is the following:

line 1 : number of time steps written *isa* number of variables written *nvar*

line 2 : format used to write and read each line of the time series *formatatm*

line 3 to 2+nvar/6 (+1) : names of the variables (*nomvar(j), j=1,.., nvar*) written in the following format

(6(1x, a8))

line .. : *isa* lines with DOY, heure, minute and the *nvar* variables written with the *formatatm* format

***atm.dat***

| | | | | | | | | |
|---|---|---|---|---|---|---|---|---|
| 1290 48 | | | | | | | | *isa, nvar* |
| (3i3,27f12.3,17f12.3,4f12.3) | | | | | | | | *formatatm* |
| HEURE RN SOL RN VEG RN TOT H SOL H VEG | | | | | | | | |
| H TOT LE SOL LE FEUIL LE VEG LE TOT G | | | | | | | | *(nomvar(j), j=1,..nvar)* |
| ETR/ETP TF HF IR NET TS TAF | | | | | | | | |
| QAF EV TOT ETR EV SOL EV FEUIL RUIS SUR | | | | | | | | |
| PERCOL PLUIE STOCK RHF RHS RAH | | | | | | | | |
| RSTO ETP ETPRAD TS 0.5CM TS 1CM TS 2 CM | | | | | | | | |
| TS 3CM TS 5 CM TS 10CM TS 15CM TS 25CM TS 50CM | | | | | | | | |
| TET0-0.5 TET 0-2 TET 0-5 TET 0-10 TET 0-15 TETA MOY | | | | | | | | |
| 245 13 0 | .333 | 378.440 | 98.868 | 477.308 | 17.940 | 34.859 | 52.799 | 470.069 |
| .000 | 64.011 | 534.239 | -109.730 | 990.035 | 19.976 | -25.595 | 505.578 | 33.873 |
| 18.206 | .016 | .288 | .032 | .257 | .000 | .000 | .001 | .000 | 367.970 |
| 31.472 | 8.024 | 85.302 | 66.925 | 539.616 | 462.028 | 34.544 | 34.936 | 35.675 |
| 35.942 | 36.152 | 35.108 | 33.139 | 30.981 | 30.255 | 12.032 | 12.844 | 13.301 | 13.600 |
| 13.603 | 9.199 | | | | | | | |
| 245 13 20 | .333 | 378.440 | 98.868 | 477.308 | 17.940 | 34.859 | 52.799 | 470.069 |
| .000 | 64.011 | 534.239 | -109.730 | 990.035 | 19.976 | -25.595 | 505.578 | 33.873 |
| 18.206 | .016 | .288 | .032 | .257 | .000 | .000 | .001 | .000 | 367.970 |
| 31.472 | 8.024 | 85.302 | 66.925 | 539.616 | 462.028 | 34.544 | 34.936 | 35.675 |

```
35.942    36.152    35.108    33.139    30.981    30.255    12.032    12.844    13.301    13.600
13.603    9.199
245 13 40      .667    394.598    105.481    500.078    15.163    35.217    50.380    409.783
.000    70.258    480.268    -30.570    985.009    20.378    -27.724    507.937    34.139    18.356
.017    .536    .066    .471    .000    .000    .003    .000    367.726    35.577    9.072
94.709    66.688    487.578    417.962    34.318    34.461    34.780    34.921    35.087
34.593    33.243    31.279    30.280    10.830    12.055    12.765    13.284    13.348    9.193
...
```

### 6.7. Listing output file.

This file contains the values of the parameters, the type of initial and boundary conditions chosen, the initial soil profiles and the final water balance.

### 6.8. Matric potential and temperature at the bottom of the soil profile.

Both files are constructed with the same scheme: the first line contains the number of observation available and the other lines the Day of the Year and corresponding value.

```
25                    njhn
378 0.98                    DoY    Matric potential
380 1.00
390 1.24
391 1.19
393 1.16
.
.                     njhn lines
.
452 -0.64
457 -1.99
464 -6.41
```

```
15                    njtpn
378 25.0                    DoY    Temperature
380 25.0
390 25.0
391 25.3
393 25.5
.
.                     njtpn lines
.
452 27.0
457 27.1
464 27.9
```

# 7. SUMMARY OF THE SISPAT MODEL APPLICATIONS. ADDITIONAL VERSIONS AVAILABLE.

Our objective in this chapter is not to give a detailed description of all the studies conducted up to now with the SiSPAT model but rather to give an overview of the type of work conducted with it. For more information, the reader is invited to refer to the relevant publications cited below.

A first class of the studies conducted with the SiSPAT model was devoted to a tentative validation of the model. Given the number of parameters used in the model, measurements for all of them are seldom (if not never) available. A calibration phase of the model is therefore necessary with a portion of the data set. Then, a validation with the remaining data set can be performed and enables to test the robustness of the model and of the calibration. This validation is performed using as much as possible variables of different nature (time evolution of soil temperature, moisture content and water potential profiles, surface energy fluxes, radiative temperature, leaf water potential), in order to test the consistency of model results and restrain the problem of equifinality of parameters (Franks et al., 1997), i.e. various sets of parameters leading to the same solution for a given output variable.

The following criteria were in general calculated in order to quantify model and observations agreement:

- the bias *B* measuring the average difference between model and observation:

$$B = \frac{1}{n}\sum_{i=1}^{n}\left(Y_{i\,\mathrm{mod}} - Y_{iobs}\right) \qquad (7.1)$$

- the root mean square error *RMSE* measuring the dispersion between model and observation

$$RMSE = \sqrt{\frac{1}{n}\sum_{i=1}^{n}\left(Y_{i\,\mathrm{mod}} - Y_{iobs}\right)^2} \qquad (7.2)$$

- the efficiency *E* or Nash coefficient (Nash and Stucliffe, 1970) which must be as close as possible to one, for a good agreement between model and measure. If the efficiency becomes negative, it means that model prediction is performing worse than if the average of the observations had been used as a predictor:

$$E = 1 - \frac{\sum_{i=1}^{n}\left(Y_{i\,\mathrm{mod}} - Y_{iobs}\right)^2}{\sum_{i=1}^{n}\left(Y_{i\,\mathrm{mod}} - \overline{Y}_{obs}\right)^2} \qquad (7.3)$$

- the regression line between model and observation, characterised by its slope *Pente*, the offset *Origine* and the determination coefficient $R^2$.

$$Y_{i\,\mathrm{mod}} = Pente * Y_{iobs} + Origine \qquad (7.4)$$

where $n$ is the number of values, $Y_{imod}$ et $Y_{iobs}$ are the calculated and observed values and $\overline{Y}_{obs}$ is the average of the observations.

A second class of research studies was devoted to the study of surface fluxes response to spatial variability of parameters. Finally in order to study specified processes more in detail, additional versions of the model were developed. The main characteristics of these versions is also briefly summarised below.

## 7.1. Applications of the SiSPAT model.

7.1.1. *Application to a soybean field located in Montpellier (France) (7 days).*

It was the first application of the model. The data set was quite complete (atmospheric forcing, surface fluxes and soil temperature at a time step of 30 min, soil matric potential and water content profile every day, soil hydraulic and thermal properties, the evolution of the Leaf Area Index and a few days of diurnal cycles of leaf water potential ). Its main drawback was its shortness: only 7 days and it was not raining during this week. However, the study showed that the model was performing quite well after a calibration phase (Fig. 10) (Dantas-Antonino, 1992; Braud et al., 1995b).

In this first application, the sensitivity of surface variables to the soil hydraulic properties was conducted using the stochastic approach for the Miller and Miller scaling factor (see 7.2.2). The difference between bare soil and vegetation was investigated, showing that a relatively dense vegetation was smoothing the spatial variability of soil properties, allowing for the definition of ″average parameters″ (Braud et al., 1995a).

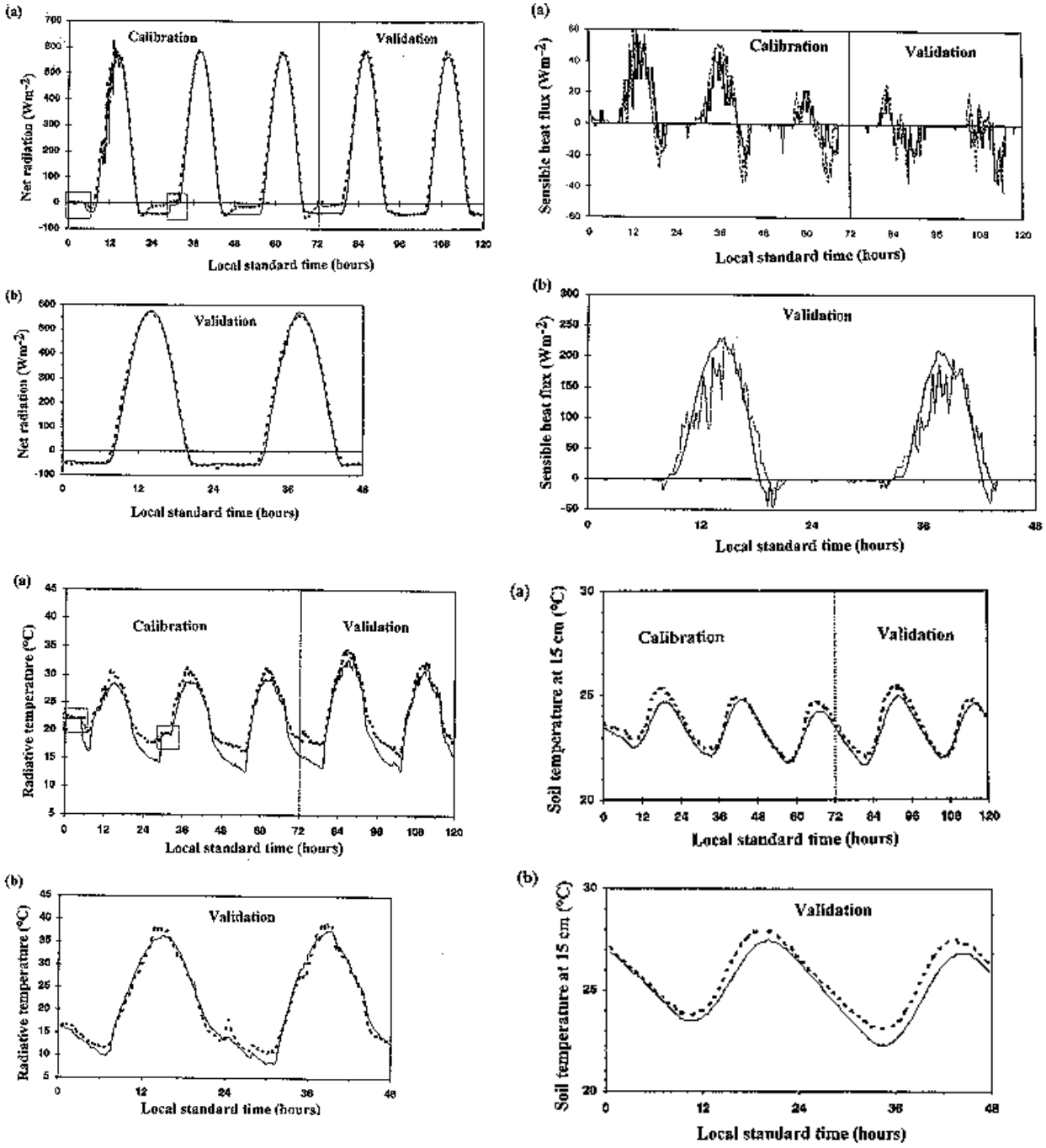


*<u>Figure 10a</u>: Comparison of calculated (solid lines) and observed (dotted lines) values of net radiation (top left), sensible heat flux (top right, radiative temperature (bottom left), soil temperature at 15 cm depth (bottom right) on the soybean field in Montpellier (from Braud et al., 1995b).*

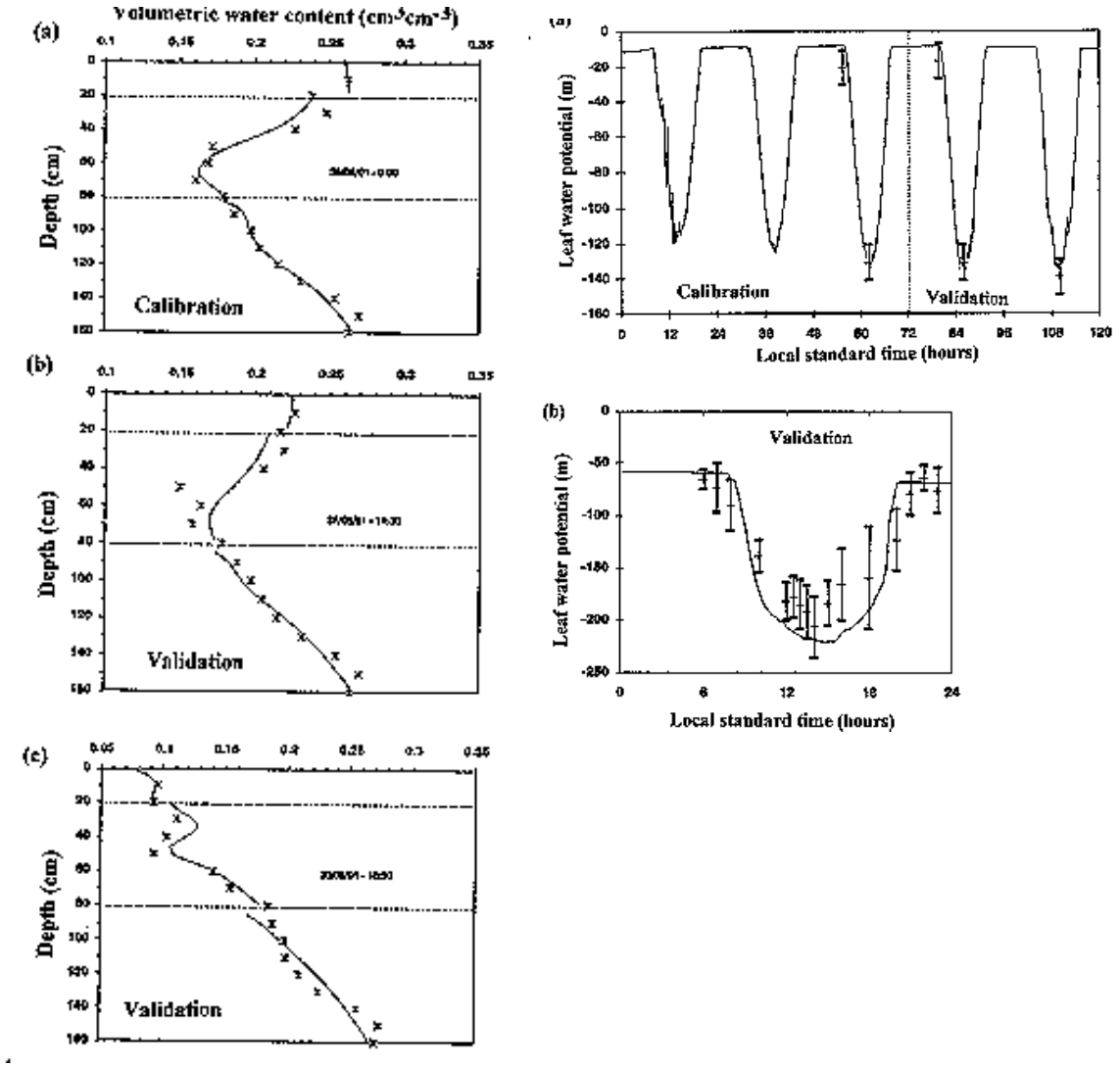


*Figure 10b: Comparison of calculated (solid lines) and observed (points) values of soil moisture profiles (left) and leaf water potential (right) on the soybean field in Montpellier (from Braud et al., 1995b).*

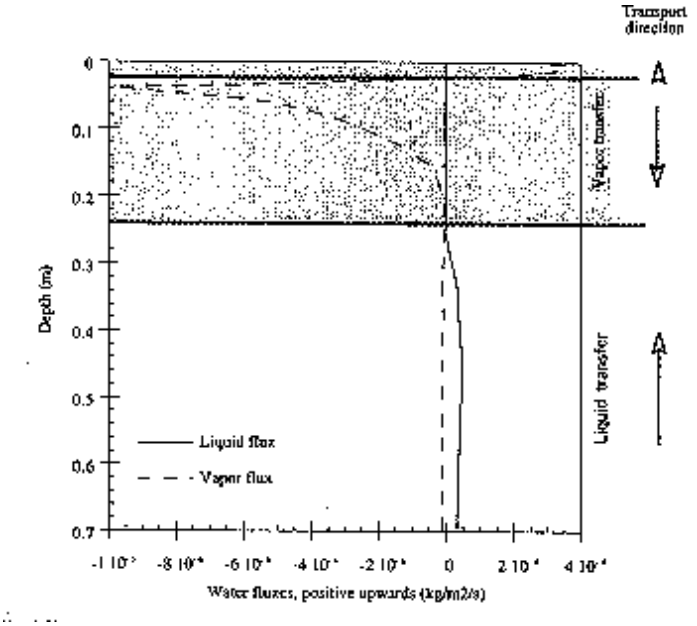


*Figure 11: Profiles of liquid and vapour fluxes in the soil (fallow land in Barrax) (from Boulet et al., 1997).*

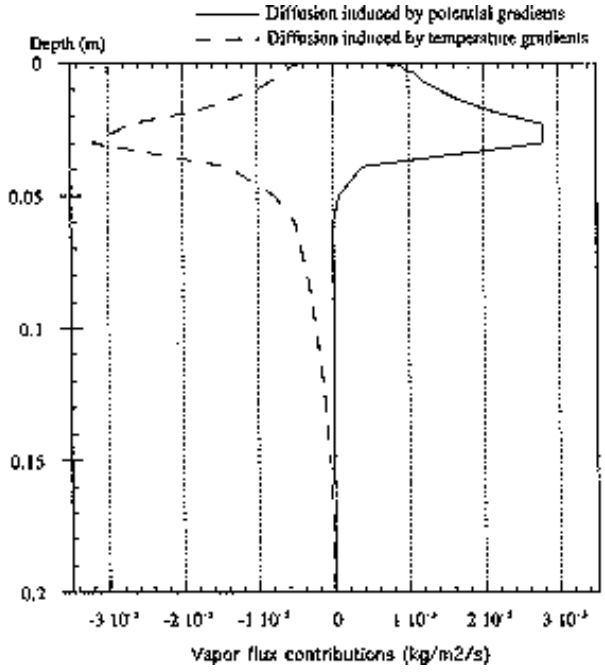


*Figure 12: Profiles of vapour fluxes induced by matric potential and temperature gradients in the soil surface layer for a fallow land (Barrax, Spain) (from Boulet et al., 1997)*

7.1.2. *Application to the EFEDA experiment*.

The EFEDA (Echieval Field Experiment in a Desertification Threatened Area) took place in June 1991 in the Castilla-La Mancha region (Spain). A second measurement phase was performed in June and July 1994. The experiment was dedicated to the understanding of the interactions between the soil, the biosphere and the atmosphere at the scale of the mesh of a General Circulation Model (Bolle et al., 1993). Only data of 1991 were used in the study conducted with SiSPAT (except on the vineyard). At the field scale, several types of land use were instrumented: fallow land (11 days), vineyard (1 month), natural vegetation (bushland) (8 and 15 days) and irrigated maize (1 month). Atmospheric forcing and surface fluxes every 30 min, evolution of Leaf Area Index and vegetation height, soil moisture content and matric potential (one profile every day) and soil hydraulic properties (the last two only for the fallow and the irrigated maize) were available. An intercomparison of the surface schemes used by the various participants was undertaken with those 4 data sets. Results of the SiSPAT model are summarized in Braud (1995) and the conclusions of the intercomparison in Linder et al. (1996). The main conclusions were that:

i) the minimum achievable error for the turbulent fluxes on the time scale of one week is around 20 $Wm^{-2}$, independently of the complexity of the surface scheme.

ii) some reasonable agreement arises between the various surface schemes for the sensible heat flux, but significant difference for the latent heat flux is observed, especially on the partition of latent heat flux between the bare soil and the vegetation. Measurements of both components is needed to discriminate between the various schemes.

iii) a large variability on the computation of the surface resistance is also found, advocated for more measurements of these quantities.

More specific studies were conducted to characterize heat and water transfer under such a semi-arid climate.

i) On the fallow land, it was shown that, near the surface, vapor phase transfer were dominant (Fig. 11) and that thermal gradients were greatly reducing the evaporation flux (Fig. 12) (Boulet, 1994; Boulet et al., 1997). This study was performed by using a more complete version of the soil module as described by Milly (1982) and detailed in Boulet et al. (1997) (see also 7.2.1).

ii) The vineyard was very sparse (1 plant every 2.5 m) and was growing on a very special soil: an arable layer was overlying a calcacerous crust, for which hydraulic and thermal properties were determined (Haverkamp et al., 1996). It was shown that vine roots were able to penetrate the crust and reach larger depths. This land use was modelled during one month by using a 3 m depth soil profile and the soil properties determined in-situ. It was shown that the crust was acting as a water reservoir and that the vineyard was not water stressed. A large sensitivity of the stomatal resistance to the Vapour Pressure Deficit was found but the model was not able to reproduce the decrease of

evapotranspiration observed during the afternoon. The model showed that the vineyard was very well adapted to its environment (Braud et al., 1995c).

iii) During the field campaign in 1994, soil hydraulic properties were sampled every 1 km on a 10x10 $km^2$ area. The retention and hydraulic conductivity curves were fully determined for 78 locations (Braud et al., 2000). These properties were used to study the influence of the spatial variability of soil properties on surface fluxes and their aggregation on the 100 $km^2$ area. A one-year data set of atmospheric forcing generated using a 1-D atmospheric model for the SLAPS project (see 7.1.5) was used and the model run for the 78 columns, having different surface soil properties but the same forcing and vegetation characteristics (typical of a vineyard, dominant in the area) (Braud et al., 2000). The stochastic version of the SiSPAT model described in 7.2.2 was used for this purpose.

It was found that for such a long term study the choice of the lower boundary condition was greatly conditioning the results. The highest variability was obtained for transpiration under water stress conditions. Aggregation rules of soil parameters were also tested and the use of the geometric mean was found to provide the closest result to the average of the 78 simulations. The use of parameters derived from textural classes was found to led to a serious bias, especially under water stress (Braud et al., 2000).

### 7.1.3. *Application to the HAPEX-SAHEL experiment.*

The aim of the HAPEX-SAHEL experiment was very similar to that of EFEDA. The set up of the experiment is described in Goutorbe et al. (1994). Three main land uses were instrumented: tiger bush, fallow savannah and crop (mainly millet crop). Only millet and fallow savannah were modelled using the SiSPAT model.

i) A first study was conducted on a well developed fallow savannah for which atmospheric forcing, surface fluxes and soil temperatures profiles were available at a 20 min time step, the evolution of leaf area index and vegetation height was followed regularly and soil moisture profiles sampled throughout a period of 54 days situated during the rainy season of 1992. Surface soil hydraulic properties, including the characterisation of surface crusts encountered in the region were also estimated using the Triple Ring Infiltrometer at Multiple Succion (Vandervaere, 1995, Vandervaere et al., 1997). The model was shown to perform quite well for surface fluxes and soil temperature, except just after a rainfall event (Fig. 13) (Braud et al., 1997, Goutorbe et al., 1997). The variability of soil moisture was large in the field, due to the co-existence of crusted and non-crusted zones. Therefore the 1-D approach was not performing well to reproduce the water movement within the soil (Fig. 14) (Braud et al., 1997).

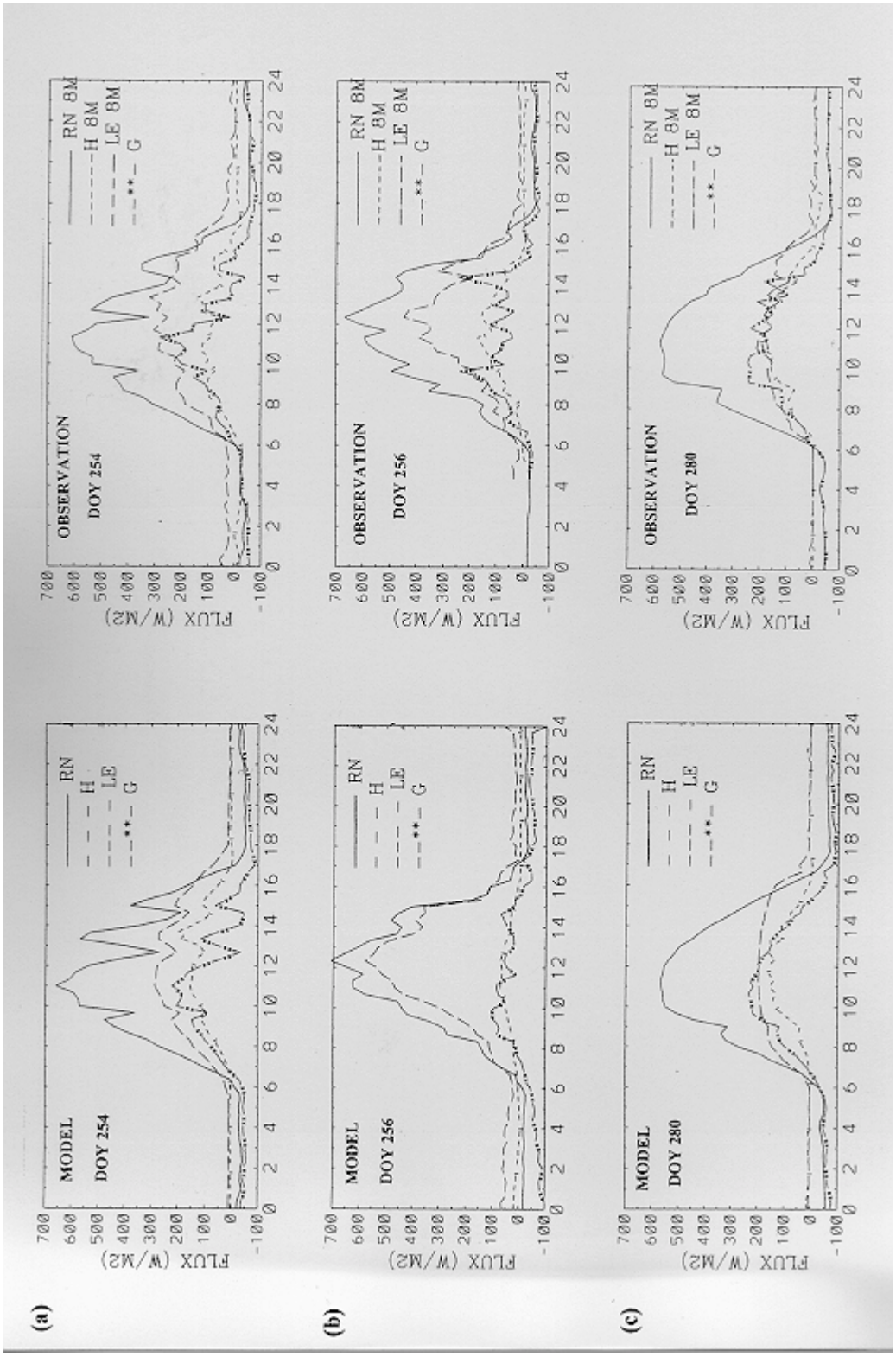


*<u>Figure 13</u>: Examples of observed (right) and modelled (left) surface energy budgets of a fallow savannah of the Hapex-Sahel experiment in 1992 for (a) DOY 254 (3 days after a rainfall of 27.6 mm), (b) DOY 256 (the day following an intense rainfall of 28.7 mm), (c) DOY 280 (21 days after the last rainfall) (from Braud et al., 1997)*

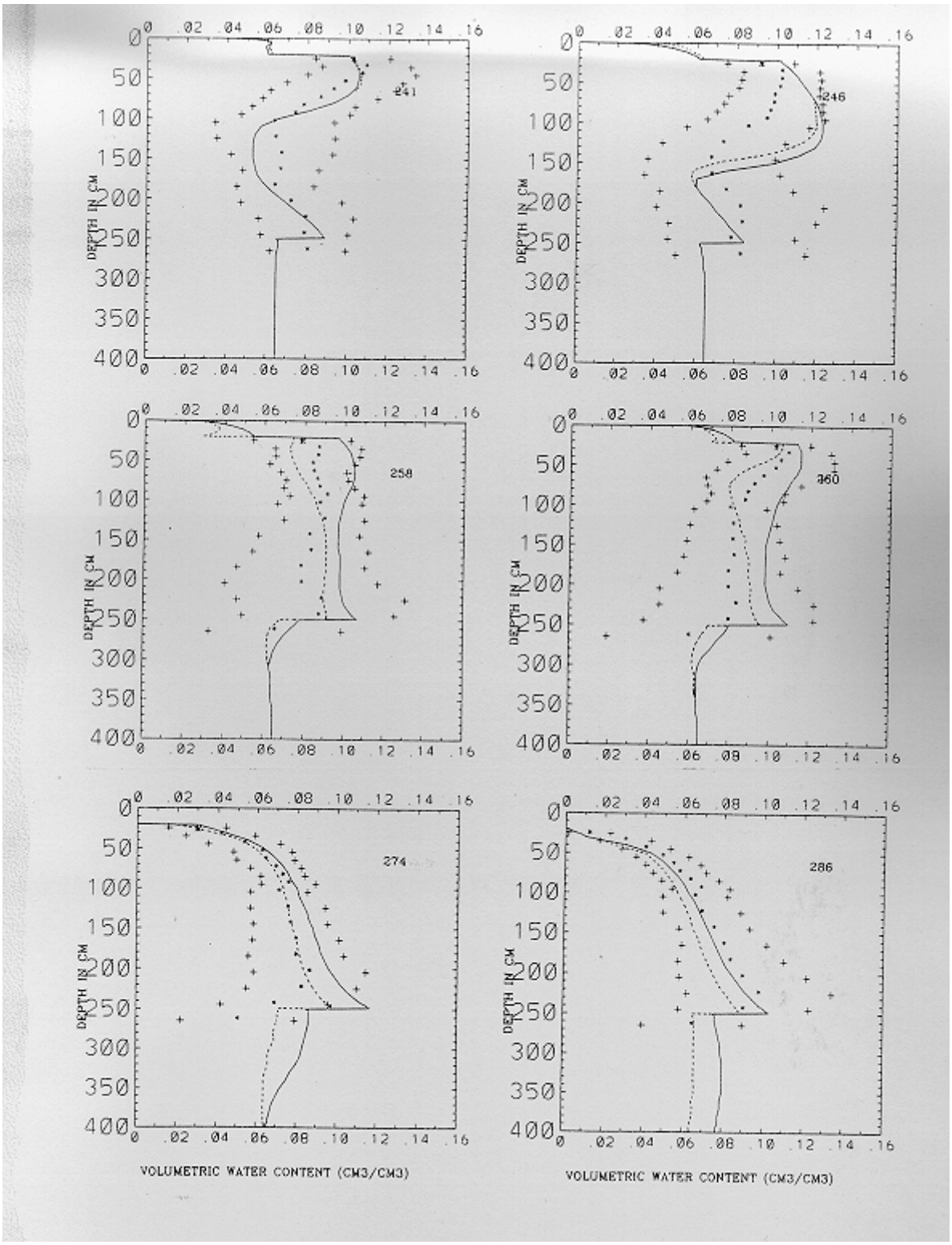


*<u>Figure 14</u>: Comparison of observed mean (*) ± one standard deviation (+) soil water content profiles with predicted profiles without crust (full line) and with a crust of 2 cm at the surface with $K_{sat}$(crust)=2.67 $10^{-6}$ $m^{s-1}$ (dotted line). Rainfall occurred between DOY 241 and 246 (63.6 mm) , 246 and 258 (55,0 mm), 258 and 260 (22.1 mm) (from Braud et al., 1997).*

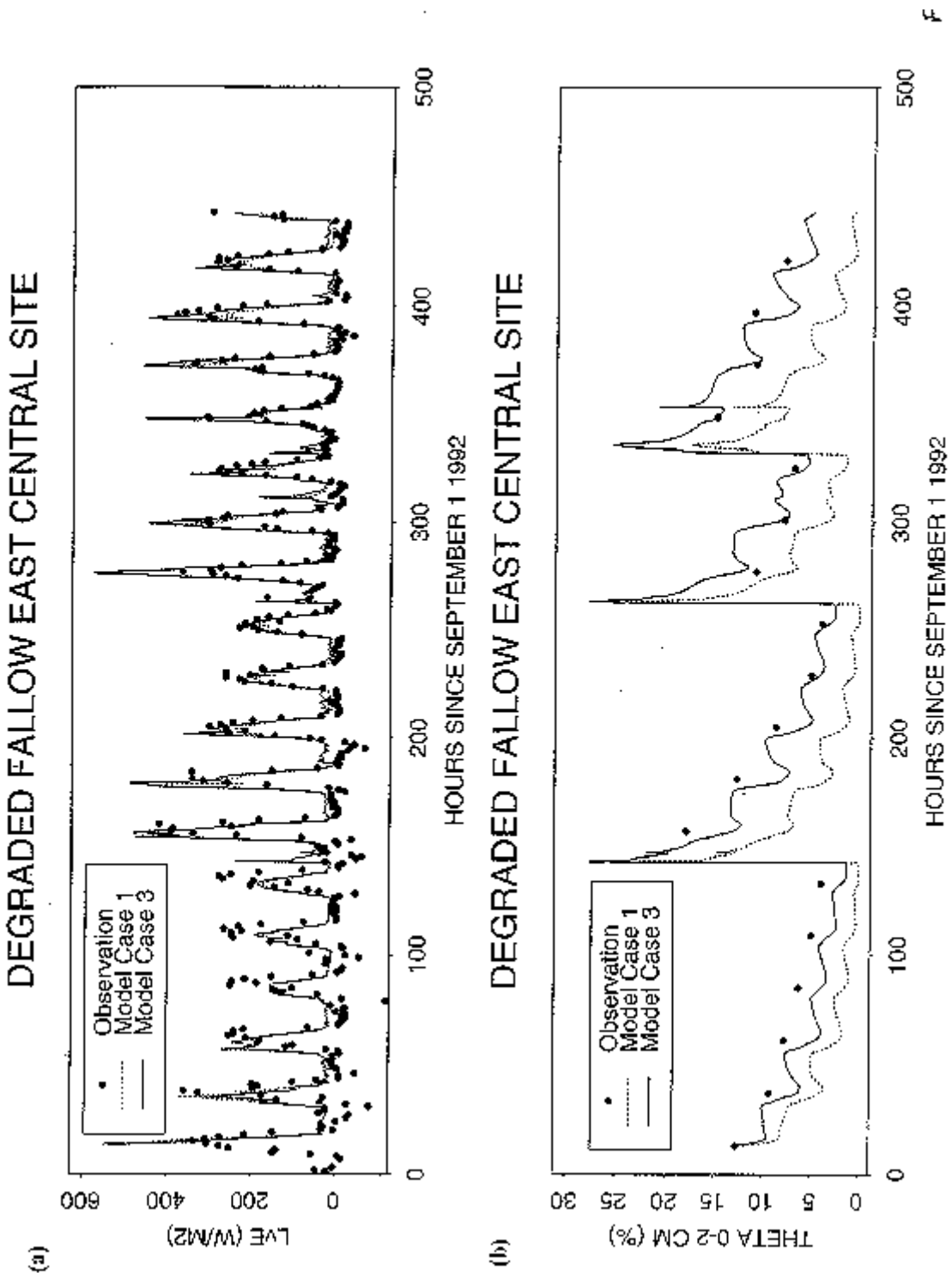


*Fig. 15: Time evolution of (a) latent heat flux and (b) surface (0-2 cm) soil moisture. Dotted line: model with soil surface properties derived from in situ infiltration measurements. Full line: model with surface retention curve fitted using laboratory measurements obtained during drying of the soil and a fitted saturated hydraulic conductivity. Black points: observations (from Braud, 1998).*

ii) A second study was performed on a degraded fallow savannah. 18 days of measurements were available (the same as for the full developed fallow savannah). In addition surface soil moisture data. were available. The aim was to use the model as a tool for the interpretation of micro-wave retrieved surface soil moisture and the prediction of the evolution of the actual evapotranspiration (ETR) as a function of surface soil moisture. For this application, the model had to predict perfectly both the surface soil moisture and the evapotranspiration. A lot of work was needed to achieve this first goal (Fig. 15) (Braud, 1998). Once this was done, the model was used to test the sensitivity of the curves relating the ratio *ETR/ETP* (actual evapotranspiration over potential one) to surface soil moisture to the variation of wind speed, leaf area index, length of the drying periods between rainfall events, etc.. It was shown that the leaf area index was mainly controling the value of the *ETR/ETP* ratio for a zero value of the soil moisture, i.e. the ordinate at the origin (this type of curves passes through the originin in the case of a bare soil). This value is shown to decrease when the *LAI* decreases. Wind speed also influences the slope of these curves, which is found to be insensitive to the length of the drying period (Chanzy et al., 1996).

In addition, a sensitivity study was conducted using a stochastic approach. It showed the large sensitivity of the model to the specification of the soil surface hydraulic properties (Table 3) (Braud, 1998). The robustness of the results obtained with such a model is shown to depend strongly on the accuracy reached in the characterisation of soil properties.

*Table 3: Components of the soil water balance from DOY 245 13h GMT to DOY 263 10h40 for ten soil columns run with the Miller and Miller scaling factor $\alpha$ drawn from a log-normal distribution. All quantities of the water budget are in mm. Rainfall is equal to 78.1 mm (from Braud, 1998).*

| $\alpha$ | Runoff | Deep drainage | Change in water storage | Total evapotran-piration | Bare soil evaporation | Transpira-tion |
|---|---|---|---|---|---|---|
| 0.18 | 33.1 | 1.5 | -34.4 | 78.7 | 58.4 | 20.5 |
| 0.30 | 25.4 | 1.5 | -26.0 | 77.3 | 57.2 | 20.5 |
| 0.40 | 20.5 | 1.5 | -19.2 | 75.4 | 54.8 | 20.9 |
| 0.51 | 17.3 | 1.5 | -13.7 | 73.4 | 52.3 | 21.3 |
| 0.64 | 14.4 | 1.5 | -8.4 | 70.9 | 49.2 | 21.9 |
| 0.78 | 11.3 | 1.5 | -2.6 | 68.4 | 46.2 | 22.3 |
| 0.97 | 7.7 | 1.5 | 4.0 | 65.7 | 42.9 | 22.9 |
| 1.24 | 3.2 | 1.5 | 11.7 | 62.5 | 39.1 | 23.6 |
| 1.68 | 1.1 | 1.5 | 19.3 | 58.4 | 34.1 | 24.3 |
| 2.78 | 0.0 | 1.5 | 25.8 | 52.4 | 26.8 | 25.6 |

7.1.4. *Application to the LOCKERSLEIGH catchment (Australia).*

The LOCKERSLEIGH catchment (27 $km^2$) is situated in a semi-arid region of the Goulburn-Marulan region of new-South-Wales (Australia). Climate there shows large seasonal variations, and can be defined as semi-arid in terms of the ratio between actual and potential evaporation (mostly related to the high incoming solar radiation). The catchment is gently ondulating (altitude ranges from 600 to 720 m above mean see level). It has been largely cleared and is used for mixed-grazing. The catchment is covered by grassland (around 70%) and open woodland. Soils are duplex soils, constituted by a sandy layer overlaying a less impervious layer mainly composed of clay.

The aim of the study was to assess the impact of the spatial and temporal variability of soil physical properties and land-surface descriptors on the components of the energy and water budget at the catchment-scale. One year of atmospheric forcing, measured continuously with a time step of 30 min, was available at one location, considered as representative of the whole catchment. In particular, rainfall was assumed to be uniform over the whole catchment, because no significant difference was observed between the three raingages situated within the catchment. Data available for the soil properties include soil water budget measurement at 35 locations organized along 3 latitudinal transects, a detailed soil survey around one of the transects and a regional soil survey describing 100 selected sites in the tablelands. Spatial variability of the land-surface (aerodynamic fluxes, albedo and normalized vegetation index (NDVI)) was accessible through a 1-day aircraft survey of the catchment.

The SiSPAT model was used in a stochastic approach: heat and water transfers were assumed to be vertical. In this catchment, it seemed a reasonable assumption because groundwater flow was very small, and runoff was mostly generated by an Horton scheme. The catchment was modelled as the juxtaposition of independant soil columns (10 to 114 according to the simulations).

Three different temporal scales have been selected to study this impact of surface properties on the components of the water balance (Boulet, 1999):

i) the daily time scale. One dimensional simulations of the energy balance components have been carried out at 114 locations and compared with 114 estimations of the same components by the aircraft (correction of the aircraft surface fluxes had to be applied because the soil heat flux was obviously overestimated). The results show that a point-to-point intercomparison is not feasable because of advection effects on the fluxes. However, there is a good agreement in terms of statistical descriptors (mean, standard deviation, minimum and maximum values) between simulated and observed fluxes and surface temperatures (Boulet et al., 1995b).

ii) the monthly time scale. Two versions of the SiSPAT model were developped. The first one used a stochastic approach where the model was run for each column with the same atmospheric forcing but one or several parameters were drawn from appropriate statistical distributions. An alternative solution of this approach was to use the measured distribution of the relevant parameters. In this case, runoff was assumed to reach instantaneously the outlet of the

catchment. The second approach was more deterministic: the catchment was divided into homogeneous units, and the runoff of the highest units was allowed to reinfiltrate in the lowest adjacent units. The runoff at the outlet was in this case directly accessible. The outputs of those two versions of the SiSPAT model have been compared, on a 2-months simulation basis, with observed runoff and the outputs from their hydrological modelling equivalents, a Variable Infiltration Capacity model, PATCHY (Wood et al., 1992; Sivapalan and Wood, 1995; Kalma et al., 1995) and a deterministic eco-hydrological model, TOPOG-IRM (Dawes et al., 1993). Results show that both versions of SiSPAT (stochastic and deterministic), uncalibrated, give very similar results and compare better with observations than the simplified representation of the calibrated PATCHY and the uncalibrated TOPOG-IRM (Boulet et al., 1995a, Boulet and Kalma, 1997a, b).

iii) the annual time scale. At this scale, the aggregation of surface fluxes and the quantification of their variability as a result of the variability of surface processes was investigated. The Statistical-Dynamical method of Avissar (1992) was applied to a one-year forcing in order to derive the aggregated water budget components when observed or estimated distributions of the main physical properties and land-surface descriptors were considered. Results show that the difference between the components of the water budget obtained by averaging the outputs of simulations run over a set of parameters representative of their statistical distribution and the 1-D simulation run with the mean value of that parameter is in general small for runoff and total evapotranspiration, but bias can be large for bare soil evaporation. The non-linearities of the processes themselves are smoothed by the major dependence on atmospheric forcing. However, the range of variations of the components of the water balance, due to parameter variability is quite large, especially for bare soil evaporation and runoff (Fig. 16). Runoff is not very sensitive to plant parameters but reacts mainly to change in soil hydraulic properties. Transpiration is mostly sensitive to plant parameters and bare soil evaporation to all of the parameters. However, the effects on bare soil and vegetation are opposite and the final sensitivity of total evapotranspiration is reduced (Fig. 16) The results are summarised in Boulet et al. (1999a).

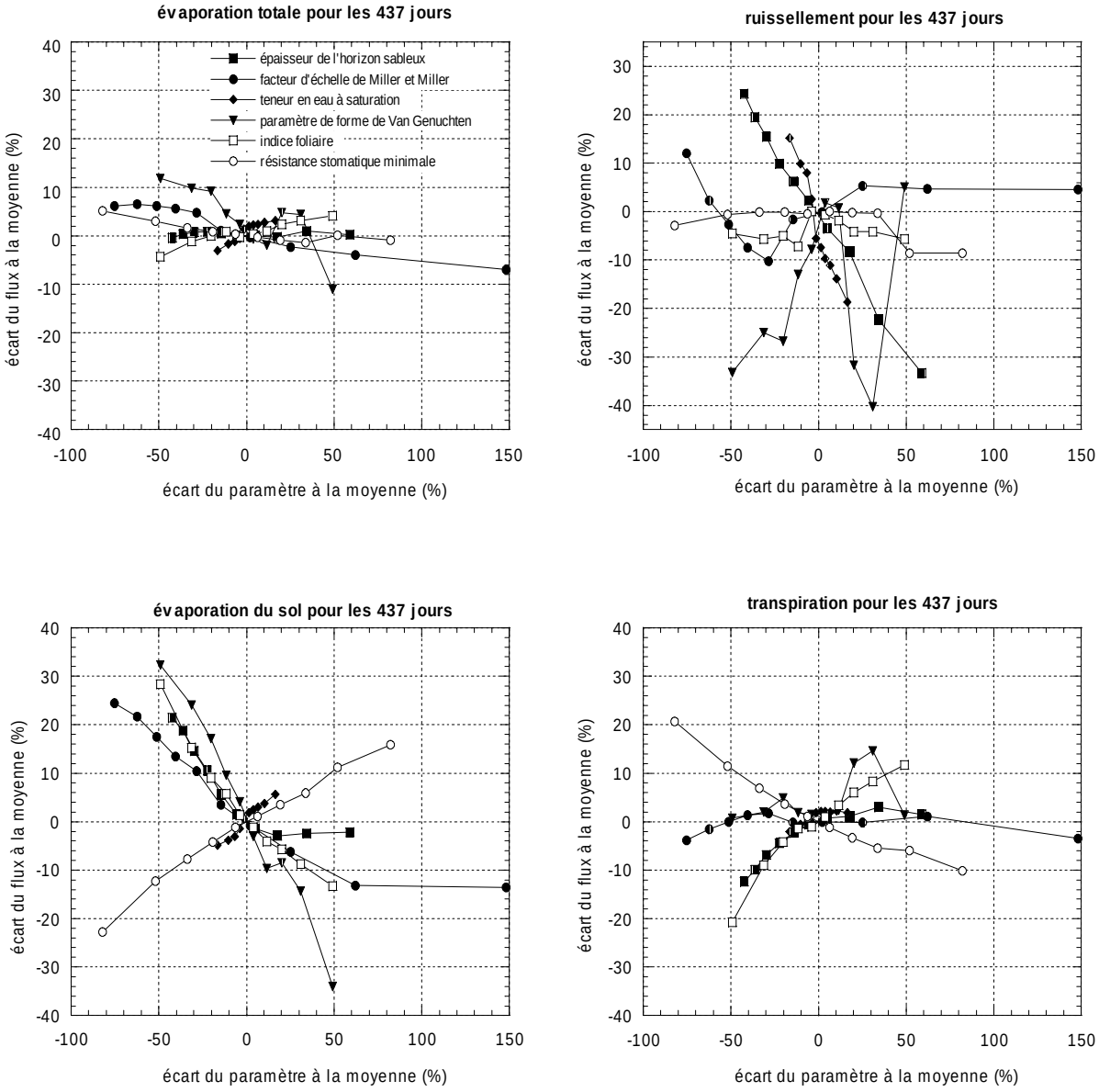


*<u>Fig. 16</u>: Sensitivity diagrams for cumulative (437 days) total evaporation (top left), runoff (top right), bare soil evaporation (bottom left), transpiration (bottom right). For each parameter respectively sandy layer depth (black squares), Miller and Miller scale coefficient (black diamonds), saturated water content (black points), Van Genuchten retention curve shape parameter (black triangles), Leaf Area Index (white squares) and minimum stomatal resistance (white points), ten values were drawn into appropriate distributions and output of the model calculated for each value. The percentage of variation of one of the parameter value relatively to the mean value is plotted in abscissa and the ordinate corresponds to the percentage of variation of one output relatively to the reference value of this output (calculated with the mean value of the parameter) from (Boulet et al.,1999a)*

7.1.5. *Application in the framework of the SLAPS (Spatial Variability of Land-Surface Processes) project.*

The aim of this project was to quantify the influence of the variability of surface processes on the components of the water and energy budgets. An intercomparison of the soil-plant-atmosphere transfer models used by the various participants (both meteorologists and hydrologists) was undertaken in an off-line test (the atmospheric forcing was imposed at a reference level and no feedback between the atmosphere and the surface was allowed). Eight data sets of atmospheric forcing, one year long, were generated with the 1-D version of the British Meteorological Office climatic model (with interactions between the atmosphere and the surface in this case) and distributed to the participants who forced their own model with those files. A common set of parameters was also used and the simulation was repeated until equilibrium has been reached (initial and final water content profiles were identical) in order to obtain results not influenced by the initial condition. The eight data sets were resulting from the combination of two climates: typical climate of England and Spain, two soil types: sand and silt, two vegetation types: full covered pasture and bare soil. The results of the project are detailed in Dooge et al. (1994a) and summarised in Dooge et al. (1994b).

The SiSPAT model was only applied for the pasture case. Table 3 shows the components of the water budget on an annual basis. The partition of rainfall between runoff and deep drainage is the most affected by the soil type, whereas evapotranspiration is less affected.

*Table 3: Annual values of rainfall amount, evapotranspiration, runoff and deep drainage for the last year of the simulation. E=England, S=Spain, 1=sand, 2=silt, 5=full cover pasture.*

| | Rainfall (mm) | Evapotranspiration (mm) | Runoff (mm) | Deep drainage (mm) | Runoff + deep drainage (mm) |
|---|---|---|---|---|---|
| E15 | 696.5 | 382.4 | 0. | 309.2 | 309.2 |
| S15 | 366.9 | 333.6 | 0. | 26.9 | 26.9 |
| E25 | 692.9 | 375.2 | 99.3 | 212.6 | 311.9 |
| S25 | 352.1 | 343.6 | 21.1 | 16.0 | 37.1 |

*7.1.6. Application to a mountainous area situated in the Vosges (North-East of France)*

A mountainous area situated in the Vosges (North-East of France) was instrumented since 1994 in order to measure the water and energy budget of a small catchment. A simulation over three months was conducted. Results of the SiSPAT model on soil moisture evolution were compared to observation and to results of two other model EARTH (Choisnel, 1985) and ISBA (Noilhan and Planton, 1989; Noilhan and Mahfouf, 1996), showing satisfactory results without calibration of the model (use of measured parameters and literature values for unmeasured ones) (Fouché-Roguiez et al., 1996; Fouche-Roguiez, 1998). Unfortunately, no surface fluxes data were available to validate more in detail the model.

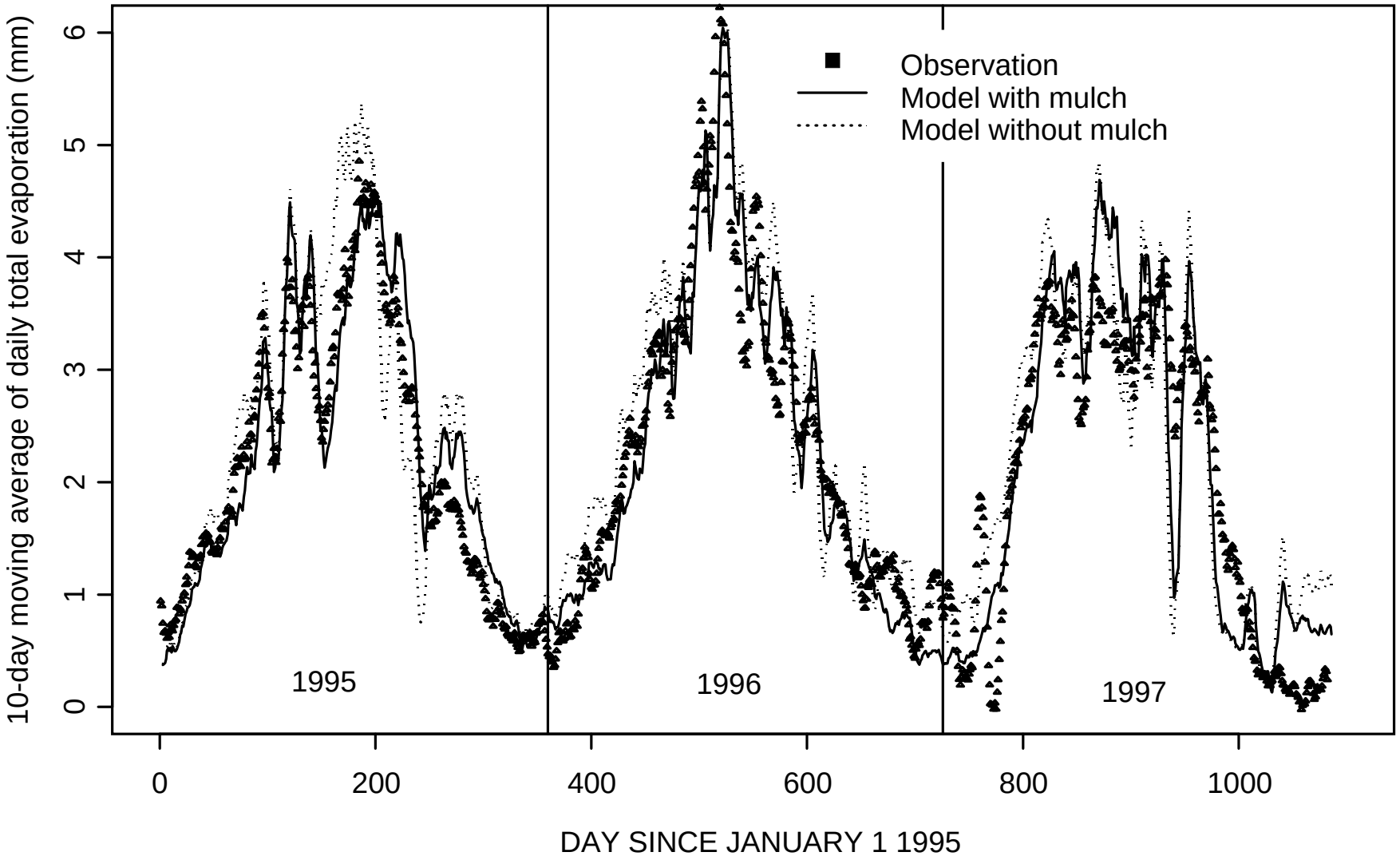


*Figure 17: Comparison of observed 10-day moving average of daily total evaporation (mm) with calculated values with (solid line) and without mulch (dotted line) (Gonzalez et al., 2000a).*

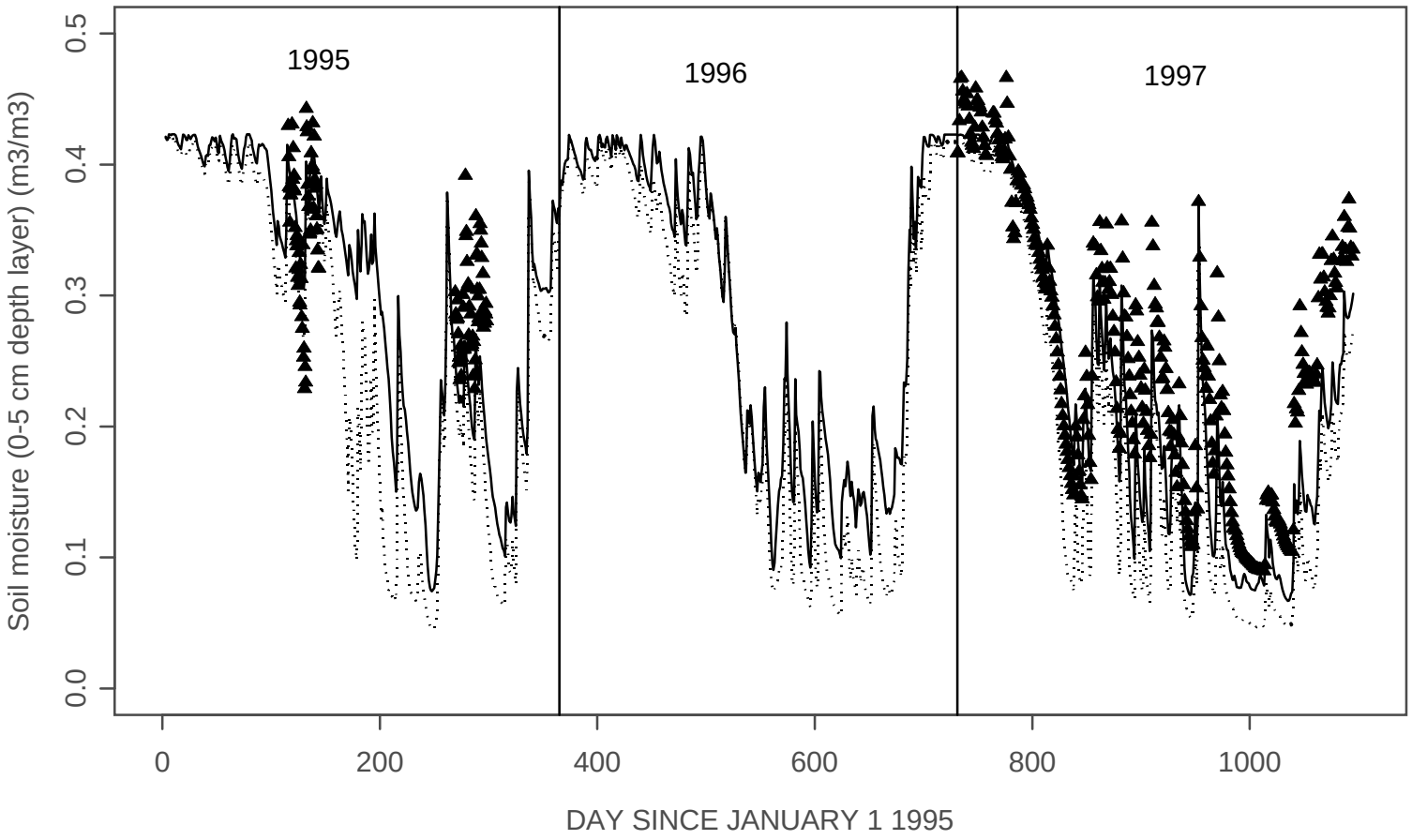


*Figure 18:Comparison of observed 0-5 cm depth soil moisture (triangles) with calculated values with (solid line) and without (dotted line) mulch (Gonzalez et al., 2000a).*

*7.1.7. Application to the MUREX experiment.*

A fallow land situated in an agricultural region of the South-West of France (near the city of Toulouse) was instrumented during years 1995-1996 and 1997. Atmospheric forcing, surface fluxes, soil temperature profiles were measured continuously. Matric potential profiles and water content profiles were sampled every week at three locations. The evolution of leaf area index, biomass (both above and below the soil surface) and of plant species was also measured regularly. The soil hydraulic and thermal properties were estimated using in-situ and laboratory techniques. The experimental set up was described in Calvet et al. (1998, 1999), as well as a first data analysis.

Such a data set was used to validate the long term behaviour of the SiSPAT model. Despite the large amount of data, some parameters mostly related to hydraulic properties of the deepest horizons and root extraction were lacking. A calibration of the model was therefore necessary. However, with the original model, it was not possible to find parameters values allowing for a correct prediction of soil temperature amplitude, surface soil moisture and evaporation fluxes. A large amount of dead biomass was present at the soil surface. It was assumed that this mulch layer might be responsible for this discrepancies. The hypothesis could only be tested using model results, due to a lack of a proper characterisation of the mulch layer. A modified version of the SiSPAT model, called SiSPAT-mulch (see 7.2.4) was built. It was found that when transfer within the mulch were taken into account, measured variable long term evolution was better simulated (Fig. 17 and 18). The physical processes responsible for this better agreement was a decrease of bare soil evaporation induced by the mulch layer, leading to more water available to sustain transpiration (Gonzalez-Sosa et al., 2000a). The decrease of soil evaporation was furthermore confirmed by a laboratory experiment comparing a mulched and a non-mulched sample (Gonzalez-Sosa et al., 2000b).

7.1.8. *Applications in progress*.

Validation of the model is still going on. The SiSPAT model is currently applied on data from two experiments:

- the ALPILLES-ReSEDA experiment (Olioso et al., 2000a) conducted in an agricultural region situated in the South-East of France near Avignon. Various crop fields were instrumented leading to a large amount of data (the same variables as in the MUREX experiment). A intercomparison of various SVAT model is going on (Olioso et al., 2000b). In the framework of this project, SiSPAT was coupled with a radiative transfer model (Visbile, Near Infra-red and hyperfrequences) for feasibility studies of assimilation of remote sensing data
- the AVIGNON99 project aiming at better understanding of root extraction. The partition of total evaporation between transpiration and evaporation of the soil was measured using isotopic methods. This would allow to validate the partition of theses quantities as

calculated by SiSPAT. A coupling between SiSPAT and a isotopic geochemistry module is also planned

## 7.2. Additional versions of the SiSPAT model available.

In this paragraph, a quick overview of additional versions of the SiSPAT model, developed for more specific applications is given. They can be summarised as follows.

### 7.2.1. *Full heat and water transfer equations within the soil.*

The original SiSPAT model was modified to include the full heat and mass transfer equations into the soil as proposed by Milly (1982). Additional terms to (2.1) are taken into account, mainly change in moisture storage due to temperature variations, change in heat content due to matric potential variations and a term accounting for transport of heat through convection (see 7.5) (Additional notations can be found in the Table of notations). The dependance of the retention and hydraulic conductivity curves on temperature is also taken into account (see Boulet et al., 1997 for more details).

$$C_{mh}\frac{\partial h}{\partial t}+C_{mT}\frac{\partial T}{\partial t}=\frac{\partial}{\partial z}\left(D_{mh}\frac{\partial h}{\partial z}+D_{mT}\frac{\partial T}{\partial z}-K\right)-\frac{S}{\rho_w} \tag{7.5a}$$

$$C_{ch}+\frac{\partial h}{\partial t}C_{cT}\frac{\partial T}{\partial t}=\frac{\partial}{\partial z}\left(D_{ch}\frac{\partial h}{\partial z}+D_{cT}\frac{\partial T}{\partial z}-c_l\left(T-T_o\right)Q_m\right) \tag{7.5b}$$

Convection was found to be negligible as well as the change in heat content due to matric potential variations. On the other hand, moisture storage due to temperature variations was found to be of the same order of magnitude as that due to matric potential variations on a bare soil under semi-arid conditions (Boulet et al., 1997). However, even with a sparse vegetation (fallow savannah of the Hapex-sahel experiment), those terms could be neglected. With this more complete set of equations, computing times are greatly increased, therefore, its use is only recommended for bare soil under quite dry conditions.

### 7.2.2. *Stochastic version*.

The stochastic approach is based on the assumption that, the area under study can be divided into *N* homogeneous surfaces, for which heat and water transfers are supposed to be vertical. Therefore, the various soil columns are independent with each other and no lateral transfer between them is allowed. For each column, one or several parameters are drawn from appropriate probability density functions, the other ones and the forcing being the same for all the columns. The method is described in Braud (1998) and Boulet et al. (1999a)

In this version, the basic model is the one described in this user's manual. The only difference is that some input parameters can be treated as stochastic variables. This includes:

- saturated water content of the soil surface horizon
- shape parameter $m$ of the retention curve of the surface horizon
- scale parameter $h_g$ of the retention curve of the surface horizon
- saturated hydraulic conductivity of the surface horizon
- scale parameter $\chi$ of the Miller and Miller (1955, 1956) similarity theory of porous media which enable to link $h_g$ and $K_{sat}$ for the surface layer through:

$$K_{sat\ j} = \chi_j^2 K_{sat\ ref} \tag{7.6a}$$

$$h_{g\ j} = \frac{h_{g\ ref}}{\chi_j} \tag{7.6b}$$

where $\chi_j$ is the scaling factor relating hydraulic properties of location $j$ to a reference soil, characterised by $K_{sat\ ref}$ and $h_{g\ ref}$. For a given field, the normalized scaling factors are such that $\frac{1}{N}\sum_{i=1}^{N} \chi_j = 1$, where $N$ is the number of soil columns.

- leaf area index
- minimum stomatal resistance.

Four statistical distributions are presently available in the code. For each of them, the mean and standard deviation must be specified:

- uniform
- normal
- lognormal
- gamma.

Note that the stochastic simulation is not performed by using the classical Monte-Carlo approach where the stochastic variable is randomly drawn into the distribution. In this case, more than 100-500 hundred simulations are needed to get statistically representative results. The approach retained here is to draw equiprobabilistic values (i.e. with the same probability of occurrence) in their distribution. The enables to get a set of parameters representative of the whole distribution and to decrease the number of simulations needed to get a representative set (10 to 50) (Boulier and Vauclin, 1987).

The program computes, at each time step of the atmospheric output file, the following statistics: mean, standard deviation, minimum and maximum of the values obtained for the $N$ soil columns. The influence of the spatial variability of surface parameters on surface fluxes can therefore be quantified.

7.2.3. *Mosaic approach for two land uses*.

On the degraded fallow savannah presented in 7.1.3., the SiSPAT representation of radiative transfer was not giving satisfactory results in terms of soil temperature, which was underestimated. It was assumed that this could be due to the representation of the field as an homogeneous vegetation layer, intercepting radiation. Indeed, the proportion of pure bare soil had been estimated to 45% (Chanzy, pers. com.) and this bare soil was receiving the incoming radiation without interception. In order to take into account this heterogeneity of the land use, the following ″mosaic″ approach was tested. Two simulations, consisting of a pure bare soil (PBS) and a vegetated + bare soil (VBS) (two source model of Fig. 4) components were run in parallel. Then the fluxes were averaged, with weighting factors being the percentage coverage of each type ((*1-f*) for PBS and *f* for VBS) (see Fig. 19). The *LAI* of the VBS is the *LAI* of the initial two source model divided by *f*. In this case the PBS and VBS components are independent (no interaction between them). This is of course a rough simplification because in reality the bare soil is spread throughout the sparse vegetation. However, the assumption proved to improve the simulated fluxes, especially because the net radiation was no more overestimated (the bare soil was experiencing higher temperatures) (Braud, 1998).

The version was most completely tested by Boulet et al. (1999b), showing that it was giving more accurate surface temperature when the heterogeneity of the surface was due to large patches of bare soil. When the heterogeneity of the soil /vegetation components is defined with smaller scales, the original SiSPAT model was performing better.

*7.2.4. SiSPAT-mulch.*

As mentioned in section 7.1.7, this version was developed in the framework of the MUREX experiment (Calvet et al., 1999). It is fully described in Gonzalez-Sosa, (1999) and Gonzalez-Sosa et al. (1999, 2000). Transfer within the mulch are modelled using equations very similar to that used for the soil, expect that water transfer is only allowed in the vapour phase and can be enhanced by convective transport within the mulch. Interception of rainfall by the mulch is also considered, the stored water acting as a source term for water vapour production.

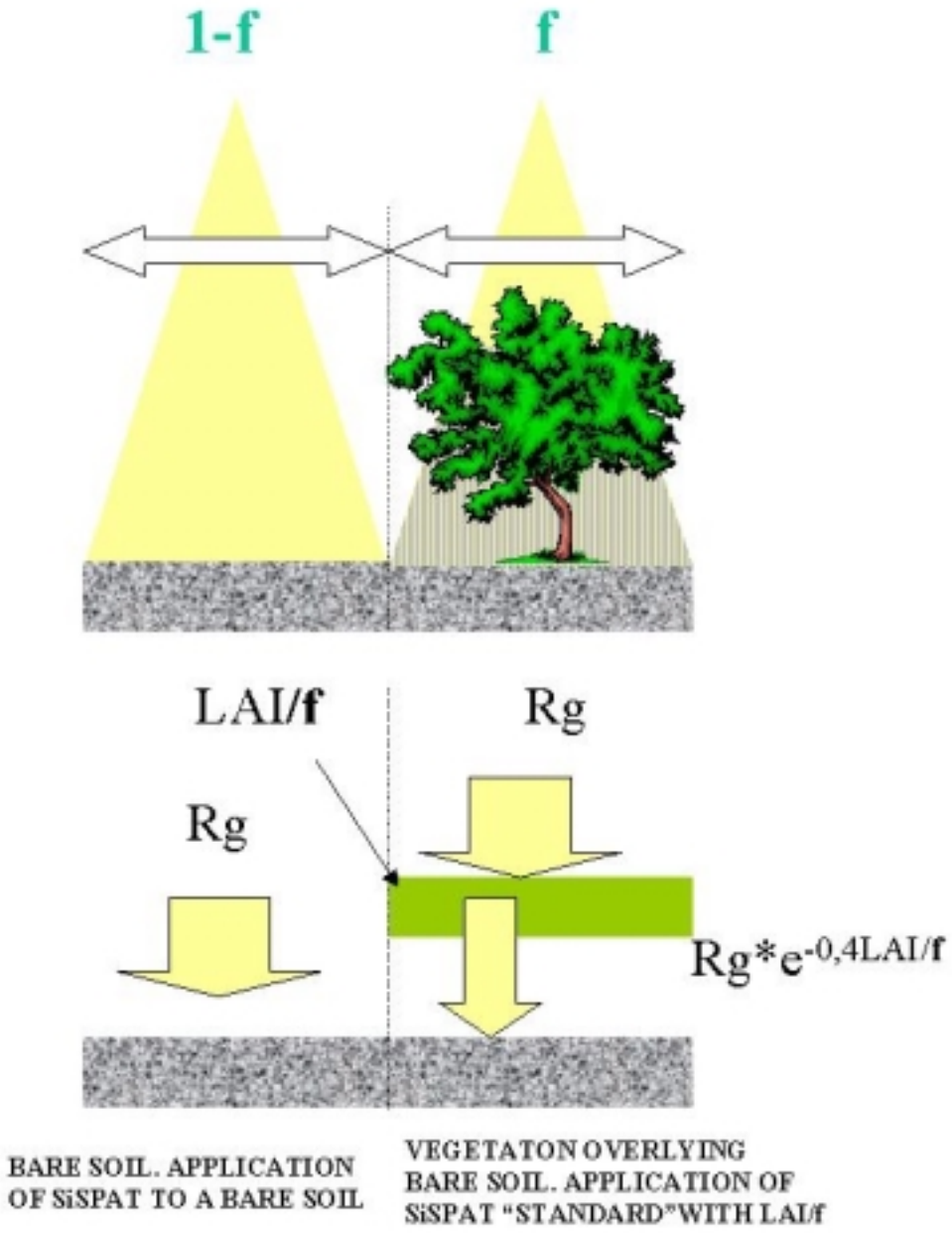


*Figure 19: Scheme of the two components model used to model sparse vegetation. (1-f) is the bare soil fraction of the surface receiving the whole incoming radiation. f is the fraction of the surface covered with vegetation overlying bare soil. Fluxes are then obtained as weighed average of individual fluxes.*

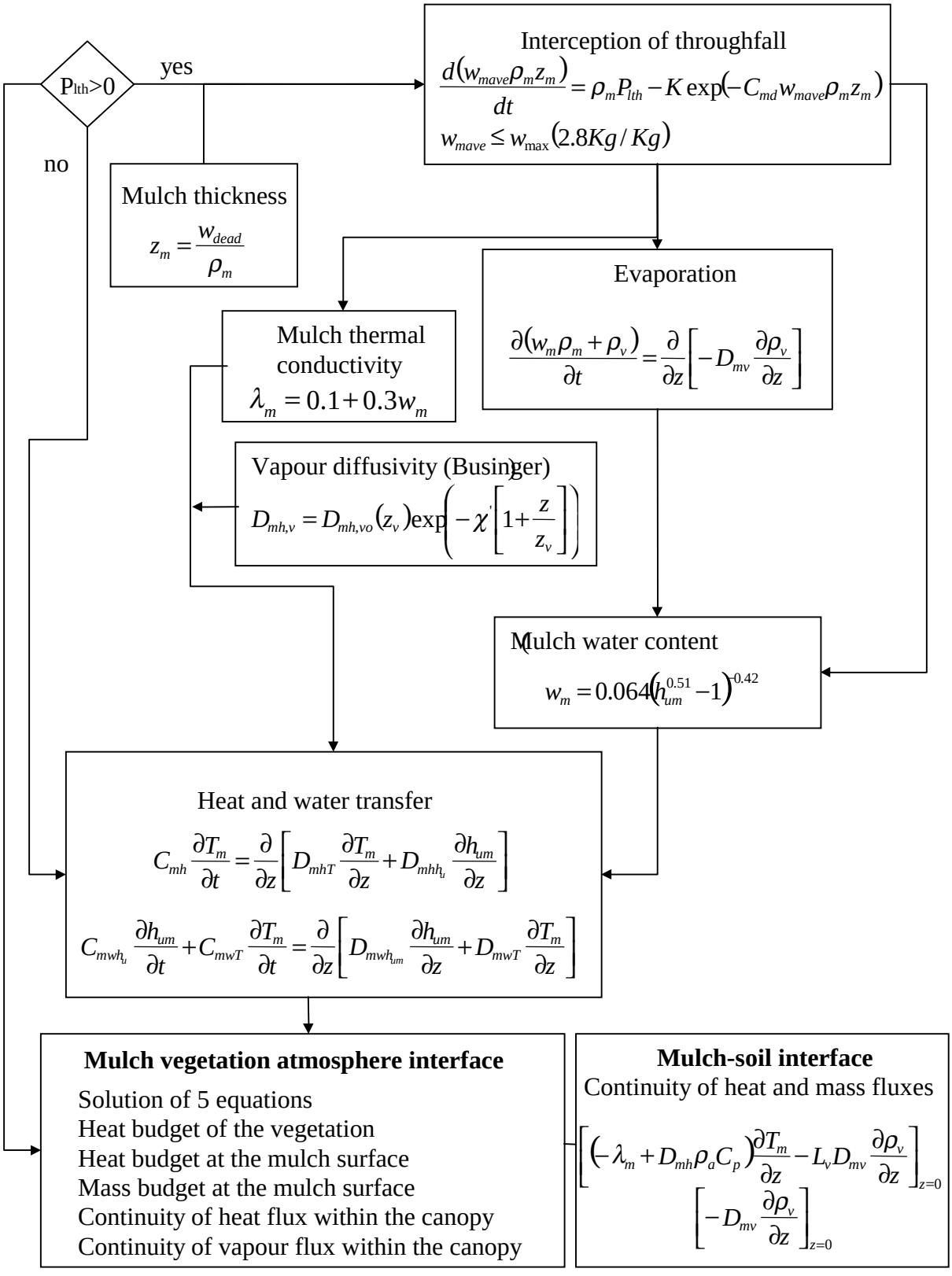


*Figure 20:: Flow diagram of the SiSPAT-mulch model (Gonzalez, 1999; Gonzalez et al., 1999)*

# 8. REFERENCES.


Abramopoulos, F., Rosenzweig, C. and Choudhury, B.J., 1988. Improved ground hydrology *calculations for global climate models (GCMs): soil water movement and evapotranspiration,* J. Clim., 1: 921-941.

Avissar, R., 1992. Conceptual aspects of a statistical-dynamical approach to represent landscape subgrid-scale heterogeneities in atmospheric models, *J. Geophys. Res*., 97: 2729-2742.

Bégué, A., Hanan, N.P. and Prince, S.D., 1994. Modélisation de la conductance stomatique de couverts végétaux sahéliens- Site Central Ouest, Hapex-Sahel, 1992, Comptes-rendus des Xèmes Journées Hydrologiques de l'ORSTOM, 13-14 Septembre 1994, Montpellier, France, 10pp.

Beljaars, A.C. and Holtstag, A.M., 1991. Flux parameterization over land surfaces for atmospheric models, *J. Appl. Meteorol.*, 30: 327-341.

Belmans, C., Wesseling, J.G. and Feddes, R.A., 1983. Simulation model of the water balance of a cropped soil: SWATRE, *J. Hydrol*., 63: 271-286.

Bolle, H.J. and 29 co-authors, 1993. EFEDA: European Field Experiment in a Desertification Threatened Area, *Ann. Geophysicae*, 11: 173-189.

Boulet G., 1994: Modélisation des transferts de masse et d'énergie à l'interface sol nu-atmosphère dans des conditions arides. Application à un sol nu de l'expérience EFEDA 1991. Rapport de DEA Mécanique des Milieux Géophysiques et Environnement, Septembre 1994, 54 pp.

Boulet, G., Kalma, J.D. and Guerra, L., 1995a. Estimation of the catchment-scale water balance: comparison of a Soil-Vegetation-Atmosphere Transfer (SVAT) model and two hydrologicalmodels, Proceedings of the congress on Modelling and Simulation (MODSIM95), 27-30 November 1995, Newcastle, Australia: 208-213.

Boulet, G., Kalma, J.D. and Hacker, J.M., 1995b. Short-term modeling of regional-scale energy and mass exchange at the land surface and comparison with aircraft measurement, Proceedings of the congress on Modelling and Simulation (MODSIM95), 27-30 November 1995, Newcastle, Australia: 202-207.

Boulet, G., Braud, I. and Vauclin, M., 1997. Study of the mechanisms of evaporation under arid conditions using a detailed model of the soil-atmosphere continuum, *J. Hydrol*., 193 : 114-141.

Boulet, G. and Kalma, J.D., 1997a. Impact of spatial variability in land surface characteristics on regional-scale evapotranspiration and runoff, Proc. International Congress on Modelling and simulation,December 1997, Hobart, Australia : 210-215.

Boulet, G. and Kalma, J.D., 1997b. Estimation of catchment-scale water balance with a Soil-Vegetation-Atmosphere Transfer model, *Env. Modelling and Software*, 12(4) : 323-328.

Boulet, G., Chehbouni, A. and Braud, I., 1998. Mosaic versus dual source approach for modeling the surface energy balance of a semi-arid land, Special Symposium on Hydrology, American Meteorological Society, Phoenix, January 1998 : 24-26.

Boulet G., 1999. Modélisation des changements d'échelle et prise en compte des hétérogénéités de surface et de leur variabilité spatiale dans les interactions sol-végétation-atmosphère, Thèse de l'Université Joseph Fourier, Grenoble I, 22 Mars 1999, 211 pp.

Boulet, G., Chehbouni, A. and Braud, I., 1999b. Mosaic versus dual source approach for modeling the surface energy balance of a semi-arid land, *Hydrology and Earth System Sciences*, 3(2): 247-258.

Boulet, G., Kalma, J.D., Braud, I. and Vauclin, M., 1999a. An assessment of effective parameterization of soil physical and land surface properties in regional-scale water balance studies, *J. Hydrol*., 217: 225-238.

Boulier, J.F. and Vauclin, M., 1987. Régimes permanents bidimensionnels d'infiltration dans un sol cultivé et microirrigué. II Comparaison de la théorie avec des mesures in-situ, *J. Hydrol*., 94: 371-394.

Braud I., 1995. Application of the SiSPAT model to four data sets of the 1991 EFEDA experiment for the intercomparison of surface schemes conducted in the framework of the modelling group activity, Rapport Interne LTHE, 18 pp., Mai 1995.

Braud I., A.C. Dantas-Antonino, M. Vauclin, J.L. Thony and P. Ruelle, 1995b: A Simple Soil Plant Atmosphere Transfer model (SiSPAT), Development and field verification, *J. Hydrol.*, 166: 213-250.

Braud I., A.C. Dantas-Antonino and M. Vauclin, 1995a: A stochastic approach to study the influenceof the spatial variability of soil hydraulic properties on surface fluxes, temperature and humidity, *J. Hydrol.*, 165: 283-310.

Braud, I., Angulo-Jaramillo, R., Haverkamp, R., Laurent, J.P., Noilhan, J. and Vandervaere, J.P., 1995c. Modélisation locale 1-D des transferts de masse et d'énergie d'une vigne à Tomelloso (EFEDA) incluant une croûte profonde de calcite, Atelier de Modélisation de l'Atmosphère, Toulouse, 28-29 Novembre 1995, Comptes-Rendus: 173-182.

Braud, I., 1996. SiSPAT user's manual, version 2.0, 83 pp.

Braud, I., Bessemoulin, P., Monteny, B., Sicot, M., Vandervaere, J.P. and Vauclin, M;, 1997 Unidimensional modelling of a fallow savannah during the Hapex-Sahel experiment using the SiSPAT model, *J. Hydrol*., 188-189: 912-945 (Hapex-Sahel special issue).

Braud. I., 1998. Spatial variability of surface fluxes versus spatial variability of surface properties. Application to a fallow savannah of the Hapex-Sahel experiment using the SiSPAT SVAT model, *Agric. For. Meteorol*., 89(1): 15-44.

Braud, I. and Chanzy, A., 2000. Soil properties, initial and boundary conditions for use within SVAT models in the framework of the intercomparison of SVAT models used in the ALPILLES-ReSEDA project, Alpilles-ReSeDA data base, 43 pp.

Braud, I., Haverkamp, R. and Arrué, J.L., 2000. Spatial variability of soil surface properties and consequences on the annual and monthly water balance of a semi-arid environment (EFEDA experiment), submitted to *J. Applied. Meteorl.*

Brooks, R.H. and Corey, A.T., 1964. Hydraulic properties of porous media, Hydrology paper, 3, Colorado State University, Fort Collins.

Brutsaert, W., 1982. *Evaporation into the atmosphere*, D. Reidel, 299 pp.

Burdine, N.T., 1953. Relative permeability calculation from size distribution data, Trans. AIME, 198: 71-78.

Calvet, J.C., Noilhan, J. and Bessemoulin, P., 1998. Retrieving the root-zone soil moisture form surface soil moisture or temperature estimates, *J. Appl. Meteorol*., 37(4): 371-386.

Calvet, J.C., Bessemoulin, P., Berne, C., Braud, I., Courault, D., Fritz, N., Gonzalez-Sosa, E., Goutorbe, J.P., Haverkamp, R., Jaubert, G., Kergoat, L., Lachaud, G., Laurent, J.P., Mordelet, P., Noilhan, J., Olioso, A., Péris, P., Roujean, J.L., Thony, J.L., Tosca, C., Vauclin, M., Vignes, D., 1999. MUREX : a land-surface field experiment to study the annual cycle of the energy and water budgets, *Annales Geophysicae*, 17(6): 838-854.

Camillo, P.J., Gurney, R.J. and Schmugge, T.J., 1983. A soil and atmospheric boundary layer model for evapotranspiration and soil moisture studies, *Water Resour. Res*., 19: 371-380.

Campbell, G.S., 1985. Soil physics with BASIC: transport models for soil-plant systems, Elsevier, Amsterdam, 150 pp.

Carlson, T.N., and Lynn, B., 1991. The effects of plant water storage on transpiration and radiometric surface temperature, *Agric. For. Meteorol*., 57: 171-186.

Cary, J.W., 1979. Soil heat trancuders and water vapour flow, *Soil Sci. Soc. Am. J*., 43: 835-839.

Chanzy, A., Schmugge, T. and Braud, I., 1996. Soil moisture and fluxes using microwave radiometry in the frame of Hapex-Sahel, 5th meeting on micro-wave radiometry and remote sensing of the environment, Boston, 4-6 November 1996.

Choisnel, E. , 1985. Un modèle agrométéorologique opérationnel de bilan hydrique utilisant les données climatiques. In Perrier, A. and Riou C. (Eds), *Les besoins en eau des cultures*, INRA : 115-132.

Choudhury, B.J. and Idso, S.B., 1985. An empirical model for stomatal resistance of field grown wheat, *Agric. For. Meteorol*., 36: 65-82.

Daamen, C. and Simmonds, L., 1994. SWEAT, A numerical model of water and energy fluxes in soil profiles and sparse canopies, Department of Soil Science, University of Reading, UK, 119 pp.

Dantas-Antonino, A.C., 1992. Modélisation des transferts de masse et de chaleur dans le système sol-plante-atmosphère.Influence de la variabilité spatiale des caractéristiques hydrodynamiques du sol, Thèse de l'Université Joseph Fourier Grenoble I, Grenoble, France, 195 pp.

Dawes, W. and Hatton, T.J., 1993. TOPOG-IRM: model description, CSIRO Division of Water Resources, Tech. Memo, 93/5.

Deardorff, J.W., 1977. A parameterization of ground surface moisture content for use in atmospheric prediction model, *J. Appl., Meteorol*., 16: 1182-1185.

Deardorff, J.W., 1978. Efficient prediction of ground surface temperature and moisture with inclusion of a layer of vegetation, *J. Geophys. Res*., 20: 1889-1903.

De Vries, D.A., 1963. Thermal properties of soils, Physics of plant environment, Van Wijik, North Holland, Amsterdam: 210-235.

De Vries, D.A., 1975. Heat transfer in soils, In: D.A. De Vries and N.H. Afgan (Editors), Heat and mass transfer in the biosphere, John Wiley and Sons: 5-28.

Dickinson, R.E., 1984. Modeling evapotranspiration for three dimensional global climate models, In: J.E. Hansen and K. Takahashi (Editors), Climate processes and climate sensitivity, Geophysical Monograph 29, Maurice Ewing, vol. 5, Amer. Geophys. Union, Washington D.C.: 58-72.

Dooge, J.C.I., Bruen, M., Dowley, A., 1994a. Research contract PL 890016 EPOCH, Spatial Variability of Land Surface Processes, Report LSP/94/19, Final Report, CWRR, University College Dublin, 140 pp.

Dooge, J.C.I., Rowntree, P.R., Vauclin, M., Todini, E., Dumenil, L., Laval, K., André, J.C., Stricker, H., 1994b. Spatial Variability of Land-Surface Processes (SLAPS II). Symposium ″Global change: climate change and climate change impacts″, Copenhaguen, (5-12 Sep; 1993). Proc. edited by the European Union (Ib Troen, editor).

Douglas, J., Peaceamn, D.W. and Rachford, H.H., 1959. A method for calculating multi-dimensional immiscible displacement, Petrol. Trans. AIME, 216: 297-308.

Entekhabi, D. and Eagleson, P.S., 1989. Land surface hydrology parameterization for atmospheric general circulation models including subgrid scale spatial variability, *J. Clim.*, 2: 816-831.

Federer, C.A., 1979. A soil-plant-atmosphere model for transpiration and availability of soil water, *Water Resour. Res*., 15: 555-562.

Flerchinger, G.N. and Pierson, F.B., 1991. Modeling plant canopy effects on variability of soil temperature and water, *Agric. For. Meteorol*., 56: 227-246.

Fouché-Roguiez, S., 1998. Modélisation spatialisée du cycle de l'eau en milieu de moyenne montagne tempérée: Application au petit bassin versant de recherches du Ringelbach (Hautes-Vosges), Thèse de l'Université Louis Pasteur, Strasbourg I, 286 pp.

Fouché-Roguiez S., Najjar, G., Braud, I., Noilhan, J. and Ambroise, B., 1996. Comparison between three Soil-Vegetation-Atmosphere Transfer Models (EARTH, ISBA, SiSPAT). Application to a middle mountain site (Vosges, France), Proceedings of the Conference on Ecohydrological Processes in Small Basins, September 24-26 1996, Strasbourg, 39-41.

Franks, S.W., Beven, K.J., Quinn, P.F. and Wright, I.R., 1997. On the sensitivity of the soil-vegetation-atmosphere transfer (SVAT) schemes: equifinality and the problem of robust calibration, *Agr. For. Meteorol*., 86: 63-75.

Fuentes, C., Haverkamp, R. and Parlange, J.Y., 1992. Parameter constraints on closed-form soil water relationships, J. Hydrol., 134: 117-142.

Gardner, W.A., 1958. Some steady-state solutions of the unsaturated moisture flow equation with application to evaporation from a water table. Soil Sci., 85:228-232.

Gonzalez-Sosa, E., 1999. Mesure et modélisation à long terme du bilan de masse et d'énergie d'une jachère du sud-ouest de la France. (Influence et rôle d'une couche naturelle de résidus végétaux, ou mulch), Thèse de l'Institut National Polytechnique de Grenoble, 04 Octobre 1999, 251 pp.

Gonzalez-Sosa, E., Braud, I., Thony, J.L., Vauclin, M., Bessemoulin, P. and Calvet, J.C., 1999. Modelling heat and water exchanges of fallow land covered with plant-residue mulch, *Agr. For. Meteorol*., 97: 151-169.

Gonzalez-Sosa, E., Braud, I., Thony, J.L. Vauclin, M. and Calvet, J.C., 2000a. Three years of observation and modelling of heat and water exchanges of a fallow land covered with a plant-residue mulch layer, *J. Hydrology*, submitted.

Gonzalez-Sosa, E., Thony, J.L., Braud, I. And Vauclin, M., 2000b. Laboratory evidence of plant residue mulch layer influence on soil evaporation, *Agr. Forest Meteorol*., submitted.

Goutorbe, J.P., Lebel, T., Tinga, A., Bessemoulin, P., Brouwer, J., Dolman, A.J., Engman, E.T., Gash, J.H.C., Hoepffner, M., Kabat, P., Kerr, Y.H., Monteny, B., Prince, S., Said, F., and Wallace, J.S., 1994. Hapex-Sahel: a large-scale study of land-atmosphere interactions in the semi-arid tropics. *Ann. Geophysicae,* 12: 53-64.

Goutorbe, J.P., Noilhan, J., Lacarrère, P. and Braud, I., 1996. Modeling of the atmospheric column over the central sites, *J. Hydrol*., 188-189: 1017-1039 (Hapex-Sahel special issue).

Haverkamp, R., Vauclin, M., Touma, J., Wierenga, P.J. and Vachaud, G., 1977. A comparison of numerical simulation models for one-dimensional infiltration, *Soil Sci. Soc. Am. J*., 41:285-294.

Haverkamp, R. and Parlange, J.Y., 1986. Predicting the water-retention curve from particle-size distribution: 1. Sandy soils without organic matter, *Soil Sci*., 142: 325-339.

Haverkamp, R., Arrue, J.L., Vandervaere, J.P., Braud, I., Boulet, G., Laurent, J.P., Taha, A., Ross, P., Angulo-Jaramillo, R., 1996. Hydrological and thermal behaviour of the vadoze zone in the area of Barrax and Tomelloso Spain, experimental study, analysis and modelling. Final integrated report EFEDA II Spain, Project UE n° EV5C-CT 92 00 90.

Haverkamp, R., Zammit, C. and Bouraoui, F., 1997. GRIZZLY: Grenoble soil catalogue. Soil survey field data and description of particle size, soil water retention and hydraulic conductivity functions for more than 700 soils.

Inclán, M.G., 1993. A simple soil-vegetation-atmosphere model intercomparison with data and sensitivity studies, *Ann. Geophysicae*, 11: 195-203.

Itier, B., 1980. Une méthode simplifiée pour la mesure du flux de chaleur sensible, *J. Rech. Atm*., 14: 17-34.

Jackson, R.D., 1988. Surface temperature and the surface energy balance, In: W.L. Steffen and O.J. Denmead (Editors), Flow and transport in the material environment: Advances and applications: 133-182.

Jarvis, P.G., 1976. The interpretation of the variations in leaf water potential and stomatal conductance found in canopies in the field, *Philos. Trans. R. Soc. London*, Ser. B, 273: 593-602.

Kalma, J.D., Bates, B.C. and Woods, R.A., 1995. Predicting catchment-scale soil moisture status with limited field measurements, *Hydrological Processes*, 9: 445-468.

Kanemasu, E.T., Rosenthal, U.D., Raney, R.J. and Stone, L.R., 1977. Evaluation of an evaporation model for corn, *Agron. J*., 69: 461-464.

Lascano, R.J., Van Bavel, C.H.M., Hatfield, J.L. and Upchurch, D.R., 1987. Energy and water balance of a sparse crop: simulated and measured soil and crop evaporation, *Soil Sci. Soc. Am. J*., 51: 1113-1121.

Laurent, J.P. and Guerre-Chaley, C., 1995. Influence de la teneur en eau et de la température sur la conductivité thermique du béton cellulaire autoclavé, Material and structures, 28: 464-472.

Linder, W., Noilhan, J., Berger, M., Bluemel, K.,, Blyth, E., Boulet, G., Braud, I., Dolman, A., Fiedler, F., Grunwald, J., Harding, R., vd Hurk, B., Jaubert, G. Mueller, A.. and Ogink, M., 1996.

Intercomparison of surface schemes using EFEDA flux data, Report n° 39. Groupe de Météorologie à Moyenne Echelle, Météo-France/CNRM, 105 pp.

Lynn, B., and Carlson, T.N., 1990. A stomatal resistance model illustrating plant versus external control of transpiration, *Agric. For. Meteorol*., 52: 5-43.

Miller, E.E. and Miller, R.D., 1955. Theory of capillary flow, I, Practical implications, *Soil Sci. Soc. Am. Proc*., 19: 267-271.

Miller, E.E. and Miller, R.D., 1956. Physical theory of capillary flow phenomena. *J. Appl. Phys*., 27: 324-332.

Milly, P.C.D., 1982. Moisture and heat transport in hysteretic inhomogeneous porous media: a matric head-based formulation and a numerical model, *Water Resour. Res*., 18: 489-498.

Monin, A.S. and Obukhov, A.M., 1954. Basic laws of turbulence mixing in the ground layer of the atmosphere, *Tr. Geofiz. Inst. Akad. Nauk*., SSSR, 24: 163-187.

Mualem, Y., 1976. A new model for predicting the hydraulic conductivity of unsaturated porous media, *Water Resour. Res*., 12: 513-522.

Nash, J.E. and Sutcliffe, J.V., 1970. River flow forecasting through conceptual models: 1. A discussion of principles, *J. Hydrol*., 10: 282-290.

Noilhan, J. and Mahfouf, J.F., 1996. The ISBA land surface parameterization scheme, *Global and Planetary Change*, 13: 145-159.

Noilhan, J. and Planton, S., 1989. A simple parameterization of land surface processes for meteorological models, *Month. Weath. Rev*., 117: 536-549.

Olioso, A., Autret, H., Bethenot, O., Bonnefond, J.M., Braud, I., Calvet, J.C., Chanzy, A., Courault, D., Demarty, J., Ducrot, Y., Gaudu, J.C., Gonzalez-Sosa, E., Gouget, R., Jongschaap, R., Kerr, Y., Lagouarde, J.P., Laurent, J.P., Lewan, L., Marloie, O., Mc Anneney, J., Moulin, S., Ottlé, C., Prévot, L., Thony, J.L., Wigneron, J.P., Zhao, W., 2000a. Compariosn of SVAT models over the Alpilles-ReSeDA experiment, I. Description of the framework and the data, submitted to *Physics Chem Earth*.

Olioso, A., Autret, H., Bethenot, O., Bonnefond, J.M., Braud, I., Calvet, J.C., Chanzy, A., Courault, D., Demarty, J., Ducrot, Y., Gaudu, J.C., Gonzalez-Sosa, E., Gouget, R., Jongschaap, R., Kerr, Y., Lagouarde, J.P., Laurent, J.P., Lewan, L., Marloie, O., Mc Anneney, J., Moulin, S., Ottlé, C., Prévot, L., Thony, J.L., Wigneron, J.P., Zhao, W., 2000b. Compariosn of SVAT models over the Alpilles-ReSeDA experiment, II. Models and results, submitted to *Physics Chem Earth*.

Passerat de Silans, A., 1986. Transferts de masse et de chaleur dans un sol stratifié soumis à une excitation atmosphérique naturelle. Comparaison modèle-expérience. Thèse de l'Institut National Polytechnique de Grenoble, Grenoble, France, 205 pp.

Passerat de Silans, A., Bruckler, L., Thony, J.L. and Vauclin, M., 1989. Numerical modelling of coupled heat and water flows during drying in a stratified bare soil. Comparison with field observations. *J. Hydrol*., 105: 109-138.

Paulson, C.A., 1970. The mathematical representation of windspeed and temperature profiles in the unstable atmospheric surface layer, *J. Appl. Meteorol*., 9: 857-861.

Philip, J.R. and De vries, D.A., 1957. Moisture movement in porous materials under temperature gradients, *Trans. Am. Geophys. Union*, 38: 222-232.

Ross, P.J., Williams, J., and Bristow, K.L., 1991. Equation for extending water-retention curves to dryness, *Soil Sci. Soc. Am. J*., 55(4): 923-927.

Sasamori, T., 1970. A numerical study of atmospheric and soil boundary layers, *J. Atm. Sci*., 27: 1122-1137.

Sellers, W.D., 1965: Physical climatology, University of Chicago Press, Chicago Ill., 272 pp.

Sellers, P.J., Mintz, Y., Sud, Y.C. and Dalcher, A., 1986. A Simple Biosphere model (SiB) for use within general circulation models, *J. Atm. Sci*., 43: 505-530.

Shaw, R.H. and Pereira, A.R., 1981. Aerodynamic roughness of vegetated surfaces. The effect of canopy structure and density, 15th Conference on Agriculture and Forest Meteorology and 5th Conference on Biometeorology, April 1-3, 1981, Anaheim, Calif., Amer. Meteorol. Soc.

Shuttleworth, W.J. and Wallace, J.S., 1985. Evaporation from sparse crops -an energy combination theory, *Quart. J. R. Met. Soc*., 111: 839-855.

Sivapalan, M. and Woods, R.A., 1995. Evaluation of the effects of GCM subgrid variability and patchiness of rainfall and soil moisture on land surface water balance fluxes, *Hydrological Processes*, 9: 697-718.

Taconet, O., Bernard, R. and Vidal-Madjar, D., 1986. Evapotranspiration over an agricultural region using a surface flux/temperature model based on NOAA-AVHRR data, *J. Clim. Appl. Meteorol*., 25: 284-307.

Taconet, O., 1987. Analyse de la thermographie infrarouge satellitaire pour la modélisation de l'évaporation sur une région agricole, Thèse de Doctorat d'Etat es-Sciences Physiques, Université de Paris-Sud, centre d'Orsay, 200 pp.

Thom, A.S., 1971: Momentum absorption by vegetation, *Quart. J. R. Met. Soc*., 97: 414-428.

Thom, A.S., 1972. Momentum, mass and heat exchange of vegetation, *Quart. J. R. Met. Soc*., 98: 124-134.

Touma, J., 1984. Etude critique de la caractérisation hydrodynamique des sols non saturés: rôle de l’air. Influence de l’écoulement multidimensionnel de l’eau. Thèse de Docteur ès Sciences Physiques, Université Scientifique et Technique de Grenoble, Grenoble, France;

Van Bavel, C.H.M., Lascano, R.J. and Stroosmijder, L., 1984. Test and analysis of a model of water use by sorghum, Soil Sci., 137: 443-456.

Van de Griend, A.A. and O'Neill, P.E., 1986. Discrimination of soil hydraulic properties by combined thermal infrared and microwave remote sensing, Proceedings of IGARSS'86 Symposium, Zürich, 8-11 Septemeber 1986, Ref ESA SP-254, Published by ESA Publications Division, 1986.

Van de Griend, A.A. and Van Boxel, J.H., 1989. Water and surface energy balance model with a multilayer canopy representation for remote sensing purposes, *Water Resour. Res*., 25: 949-971.

Vandervaere, J.P., 1995. Caractérisation hydrodynamique du sol in-situ par infiltrométrie à disques. Analyse critique des régimes pseudo-permanents. Méthodes transitoires et cas des sols encroûtés. Thèse de l'Université Joseph Fourier, Grenoble I, Grenoble, France.

Vandervaere, J.P., Peugeot, C., Vauclin, M., Angulo-Jaramillo, R. and Lebel, T., 1996. Estimating hydraulic conductivity of crusted soils using disc infiltrometers and minitensiometers, *J. Hydrol*., 188-189: 203-223 (Hapex-Sahel Special Issue).

Van Genuchten, M.T., 1980. A closed-form equation for predicting the hydraulic conductivity of unsaturated soils, *Soil Sci. Soc. Am. J*., 44: 892-898.

Vauclin, M., Haverkamp, R. and Vachaud, G., 1979. Résolution numérique d'une équation de diffusion non-linéaire. Application à l'infiltration de l'eau dans les sols non saturés, Presses Universitaires de Grenoble, Grenoble, 183 pp.

Verhoef, A., De Bruin, H.A.R. and Van den Hurk, B.J.M., 1997. Some practical notes on the parameter kB-1 for sparse vegetation, *J. Appl. Meteorol*., 36: 560-572.

Witono, H. and Bruckler, L., 1989. Use of remotely sensed soil-moisture content as boundary conditions in soil-atmosphere water transport modelling, 1. Field validation of a water flow model, *Water Resour. Res*., 25: 2423-2435.

Wood, E.F., Lettenmaier, D.P. and Zartarian, V.G., 1992. A land surface hydrology parameterisation with subgrid variability for general circulation models, *J. Geophys. Res*., 97: 2717-2728.

Zammit, C., 1999. Analyse et évaluation des paramètres hydrodynamiques des sols. Prédiction par un modèle analytique à base physique à partir de données texturales. Implications pour l'hydrologie de la zone non saturée, Thèse de l'Université Joseph Fourier, Grenoble I.

## APPENDIX I

# Estimation of retention parameters in the dry domain for the Van Genuchten model

In section 2, it was mentioned that the following choice was possible for the retention curve:

$$\begin{cases} \dfrac{\theta}{\theta_s} = \left[1+\left(\dfrac{h}{h_{g1}}\right)^{n1}\right]^{-1+\frac{2}{n1}} & h \geq h_c \\ \dfrac{\theta}{\theta_s} = \left[1+\left(\dfrac{h}{h_{g2}}\right)^{n2}\right]^{-1+\frac{2}{n2}} - \left[1+\left(\dfrac{h_o}{h_{g2}}\right)^{n2}\right]^{-1+\frac{2}{n2}} & h \leq h_c \end{cases} \tag{A1.1}$$

Parameters $n_2$ and $hg_2$ must be determined. They are calculated such that the curve and its first derivative is continuous for $h=h_c$ which leads to the following non-linear system:

$$\begin{cases} F_1\left(n_2, h_{g2}\right) = \left[1+\left(\dfrac{h_c}{h_{g2}}\right)^{n2}\right]^{-1+\frac{2}{n2}} - \left[1+\left(\dfrac{h_o}{h_{g2}}\right)^{n2}\right]^{-1+\frac{2}{n2}} - C_1 = 0 \\ F_2\left(n_2, h_{g2}\right) = \dfrac{n_2-2}{h_{g2}}\left[1+\left(\dfrac{h_c}{h_{g2}}\right)^{n2}\right]^{-2+\frac{2}{n2}}\left(\dfrac{h_c}{h_{g2}}\right)^{n2-1} - C_2 = 0 \end{cases} \tag{A1.2}$$

with:

$$\begin{cases} C_1 = \left[1+\left(\dfrac{h_c}{h_{g1}}\right)^{n1}\right]^{-1+\frac{2}{n1}} \\ C_2 = \dfrac{n_1-2}{h_{g1}}\left[1+\left(\dfrac{h_c}{h_{g1}}\right)^{n1}\right]^{-2+\frac{2}{n1}}\left(\dfrac{h_c}{h_{g1}}\right)^{n1-1} \end{cases} \tag{A1.3}$$

Eq. (A1.2) can be solved using the Newton-Raphson algorithm. For iteration $^k$, the various functions can be written:

$$F_i\left(n_2, h_{g2}\right)^k = F_i\left(n_2, h_{g2}\right)^{k-1} + \left(\frac{\partial F_i}{\partial n_2}\right)^{k-1}\left(n_2^k - n_2^{k-1}\right) + \left(\frac{\partial F_i}{\partial h_{g2}}\right)^{k-1}\left(h_{g2}^k - h_{g2}^{k-1}\right) = 0 \tag{A1.4}$$

$i = 1,2$

which leads to the following linear system, solved iteratively:

$$\begin{bmatrix} \frac{\partial F_1}{\partial n_2} & \frac{\partial F_1}{\partial h_{g2}} \\ \frac{\partial F_2}{\partial n_2} & \frac{\partial F_2}{\partial h_{g2}} \end{bmatrix}^{k-1} \begin{bmatrix} n_2^k - n_2^{k-1} \\ h_{g2}^k - h_{g2}^{k-1} \end{bmatrix} = \begin{bmatrix} -F_1\left(n_2, h_{g2}\right) \\ -F_2\left(n_2, h_{g2}\right) \end{bmatrix}^{k-1} \tag{A1.5}$$

where:

$$\begin{cases} \frac{\partial F_1}{\partial n_2} = \left[1+\left(\frac{h_c}{h_{g2}}\right)^{n2}\right]^{-1+\frac{2}{n2}} \left\{-\frac{2}{n_2^{\,2}} Log\left[1+\left(\frac{h_c}{h_{g2}}\right)^{n2}\right] + \left(\frac{2}{n_2}-1\right)\frac{\left(\frac{h_c}{h_{g2}}\right)^{n2} Log\left(\frac{h_c}{h_{g2}}\right)}{1+\left(\frac{h_c}{h_{g2}}\right)^{n2}}\right\} - \\ -\left[1+\left(\frac{h_o}{h_{g2}}\right)^{n2}\right]^{-1+\frac{2}{n2}} \left\{-\frac{2}{n_2^{\,2}} Log\left[1+\left(\frac{h_o}{h_{g2}}\right)^{n2}\right] + \left(\frac{2}{n_2}-1\right)\frac{\left(\frac{h_o}{h_{g2}}\right)^{n2} Log\left(\frac{h_o}{h_{g2}}\right)}{1+\left(\frac{h_o}{h_{g2}}\right)^{n2}}\right\} \\ \frac{\partial F_1}{\partial h_{g2}} = -\left[1+\left(\frac{h_c}{h_{g2}}\right)^{n2}\right]^{-2+\frac{2}{n2}} \frac{2-n_2}{h_{g2}}\left(\frac{h_c}{h_{g2}}\right)^{n2} + \left[1+\left(\frac{h_o}{h_{g2}}\right)^{n2}\right]^{-2+\frac{2}{n2}} \frac{2-n_2}{h_{g2}}\left(\frac{h_o}{h_{g2}}\right)^{n2} \\ \frac{\partial F_2}{\partial n_2} = \frac{1}{h_{g2}}\left[1+\left(\frac{h_c}{h_{g2}}\right)^{n2}\right]^{-2+\frac{2}{n2}} \left(\frac{h_c}{h_{g2}}\right)^{n2-1} \\ \left\{1+\left(n_2-2\right)\left[-\frac{2}{n_2^2} Log\left(1+\left(\frac{h_c}{h_{g2}}\right)^{n2}\right) + \frac{\left(\frac{2}{n_2}-2\right)\left(\frac{h_c}{h_{g2}}\right)^{n2} Log\left(\frac{h_c}{h_{g2}}\right)}{1+\left(\frac{h_c}{h_{g2}}\right)^{n2}} + Log\left(\frac{h_c}{h_{g2}}\right)\right]\right\} \\ \frac{\partial F_2}{\partial h_{g2}} = -\frac{\left(n_2-2\right)}{h_{g2}^{\,2}} n_2\left[1+\left(\frac{h_c}{h_{g2}}\right)^{n2}\right]^{-2+\frac{2}{n2}} \left(\frac{h_c}{h_{g2}}\right)^{n2-1} \left\{1+\left(\frac{2}{n_2}-2\right)\frac{\left(\frac{h_c}{h_{g2}}\right)^{n2}}{1+\left(\frac{h_c}{h_{g2}}\right)^{n2}}\right\} \end{cases} \tag{A1.6}$$

–